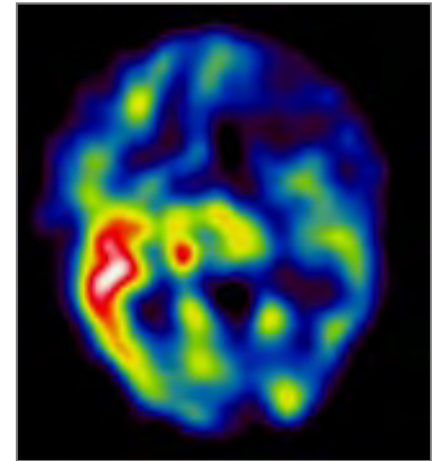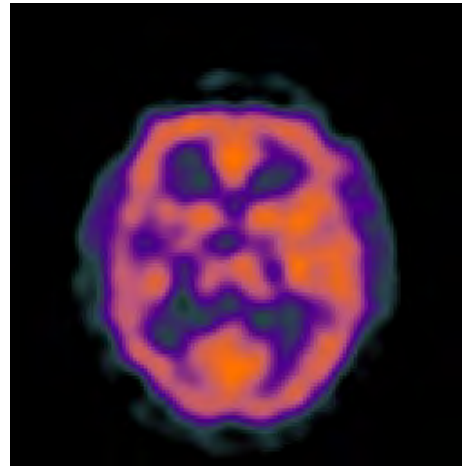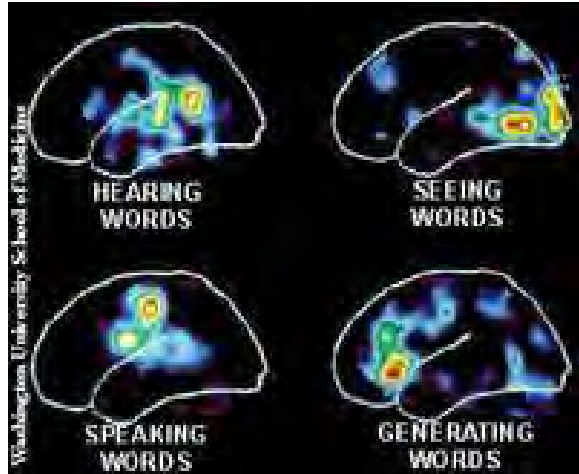# nuclear medical imaging techniques

nuclear medical imaging techniques

contents:

- historical overview

- physical basics

- generating radioactive isotopes

- recording technique

- imaging with radioactive isotopes

planar scintigraphy

Single-Photon-Emission-Computed-Tomography (SPECT)

Positron-Emission-Tomography (PET)

(images: Dössel, 2000; Morneburg, 1995; Siemens, Philips, Internet)

principle

- **active** imaging through exposure of energy (radioactive substances)

  and

- **passive** imaging through recording of "endogenous" signals (function and metabolism)

- characterize **intensity distributions** in body tissue depending on function and metabolism

nuclear medical imaging techniques

history

Antoine H. Becquerel (1852-1908)

discovery of naturally occurring radioisotopes
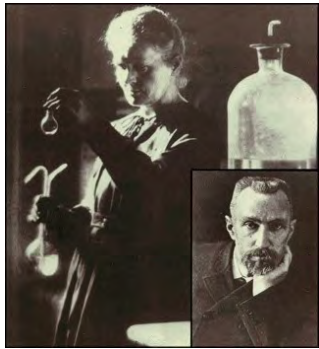
Marie Curie (1867-1934) and Pierre Curie (1859-1906)

generating synthetic radioisotopes
coining the term "radioactivity"

1903   Nobel Physics price awarded to Becquerel and the Curies

1911   Nobel Chemistry price awarded to M. Curie

1935   Georg von Hevesy

applied ^{32}P for metabolic studies using Geiger-Müller counter
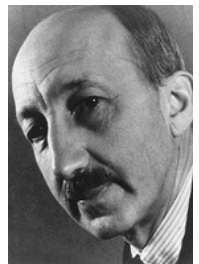
1943   Nobel Chemistry price awarded to von Hevesy

4

1949 B. Cassen et al.: first radionuclide-imaging
(^{131}J in thyroid gland)

1951-1953   first ideas to PET
W.H. SWEET, *The use of nuclear disintegration in the diagnosis and treatment of brain tumor*, **New England Journal of Medicine** *1951*; 245:875-878.
G.L. BROWNELL, W.H. SWEET, *Localization of brain tumors with positron emitters*, **Nucleonics** *1953*, 11:40-45.

1957 H.O. Anger
development of a scintillation camera (later named after Anger)
(planar imaging)

1960 D.E. Kuhl and R.Q. Edwards
construction of Mark IV-SPECT scanner with Anger camera
(~10 years prior to x-ray CT)

1962 S. Rankowitz and J.S. Robertson
tomographic imaging with positron emitter

1975   M.E. Phelps (Los Angeles); M.M Ter-Pogossian (St. Louis);
       T.F. Budinger (Berkeley)
       first PET scanner
       (innovation push due to CT reconstruction algorithms)

1977   W.I. Kayes and R.J. Jaszczak
       commercial development of SPECT

1978   first commercial PET
       (resolution: 1.5 - 2.0 cm)

1979   M.E. Phelps et al.; M. Reivich et al.
       first PET-based investigations of regional cerebral glucose metabolism
       in the living (!) human brain

1983   M. Singh and D. Doria
       use of Compton camera for SPECT

since the 1990s
       exponential growth of installations (infrastructure!)

nuclear medical imaging techniques

PET-installations in Germany

1988

1998

PET- Zentrum

1	Hannover
2	Heidelberg
3	Köln
4	Jülich

PET- Satellit

1	Aachen
2	Düsseldorf

PET- Zentrum (17)

1	Hannover
2	Heidelberg
3	Köln
4	Jülich
5	München
6	Ulm
7	Tübingen
8	Bad Oeynhausen
9	Essen
10	Hamburg
11	Berlin
12	Rossendorf
13	Freiburg
14	Bad Berka
15	Leipzig
16	Aachen
17	Düsseldorf

☆ Koinzidenz-Scanner (8)

1	Lübeck
2	Bremen
3	Frankfurt
4	Karlsruhe
5	München
6	Erfurt
7	Neu-Ulm
8	Bad Oeynhausen
9	Bad Berka

PET-Satellit (30)

1	Aachen
2	Düsseldorf
3	Frankfurt
4	Karlsruhe
5	München (2)
6	Mainz
7	Bonn
8	Koblenz
9	Münster (2)
10	Homburg
11	Kiel
12	Oberhausen
13	Freiburg
14	Siegen
15	Leipzig
16	Stuttgart
17	Jena
18	Gera
19	Trier
20	Regensburg
21	Erlangen
22	Lemgo
23	Dortmund
24	Dresden
25	Wuppertal
26	Marburg
27	Hamm
28	Rheine
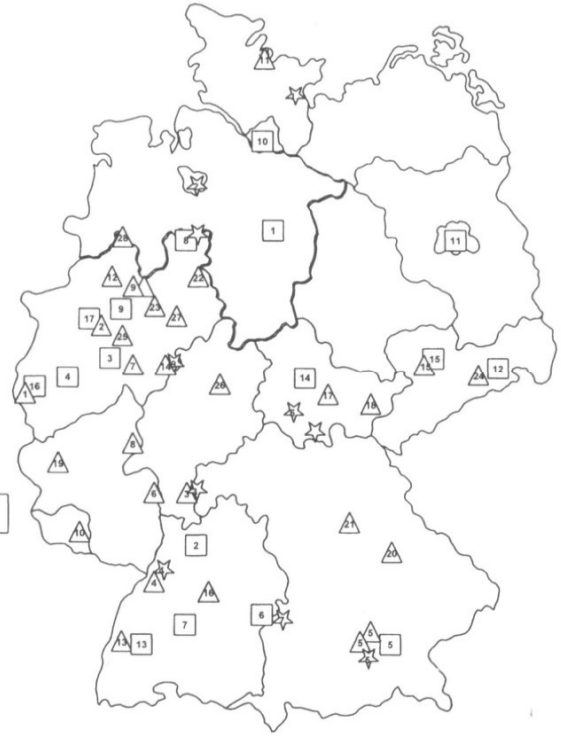
from: H.J. Wieler (ed):
PET in der klinischen Onkologie, Steinkopf, Darmstadt, 1999

7

nuclear medical imaging techniques

SPECT

radio-
pharmaceutical

detector

processing/
quantifying
tracer
distribution

- inject
- swallow
- inhale

PET
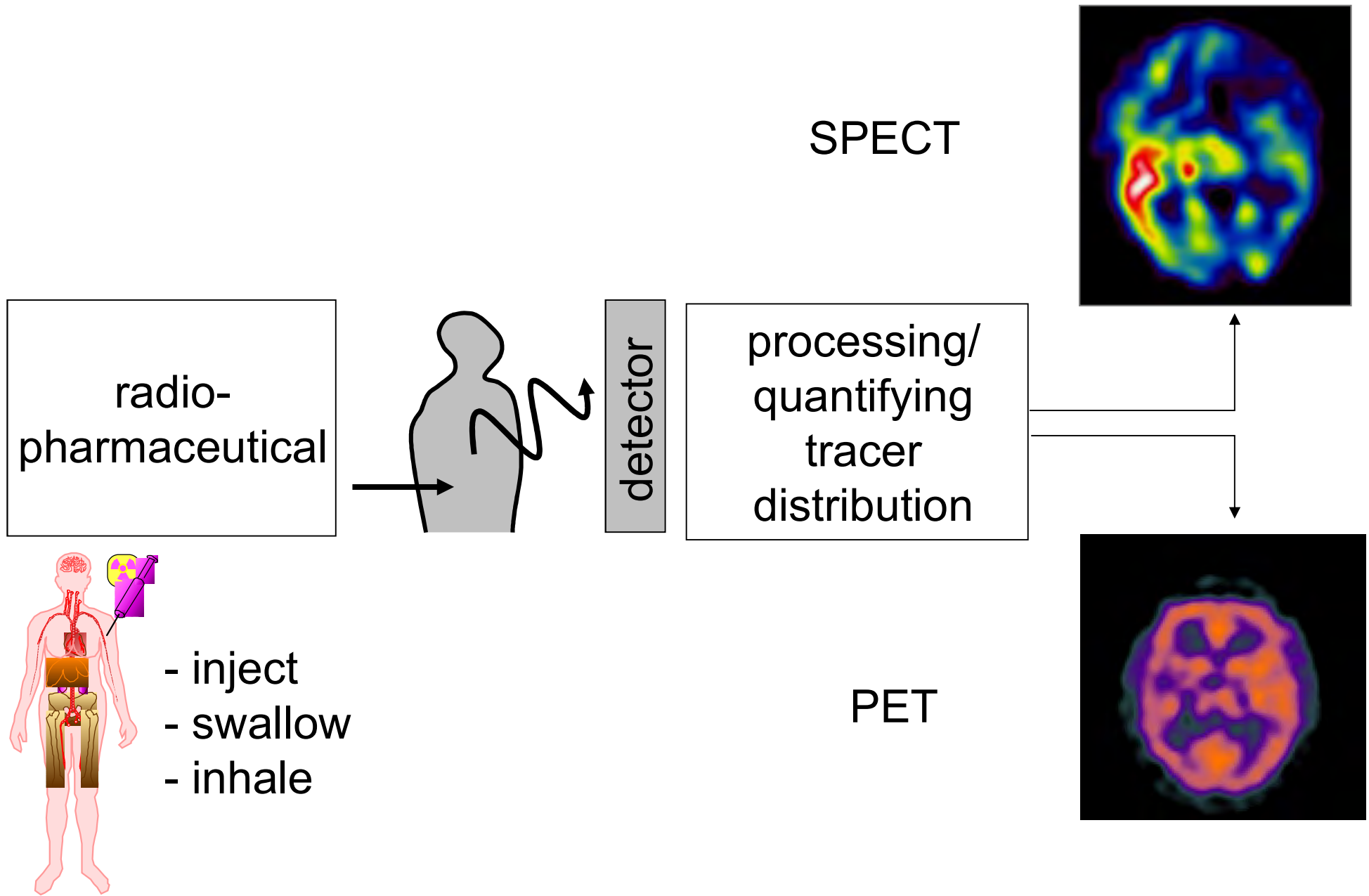
aim:
visualize (patho-)physiological and biochemical processes
(transport, metabolism, clearance, ...)

requirements for radiopharmaceuticals
- decay-related radiation easily detectable outside body
  (no or only very minor absorption)

- visualization of real (not induced) metabolic processes
  (choice of suitable nuclides as tracer)

- labeling should not modify tracer dynamics in body

- conservation of physiological concentrations of metabolic
  substances

- low radiation exposure (comparably short half-life)

- cost-benefit ratio

definitions:

Z: atomic number; number of protons in nucleus

A: mass number; number of nucleons in nucleus
(protons + neutrons)

N: number of neutrons in nucleus: $N = A - Z$
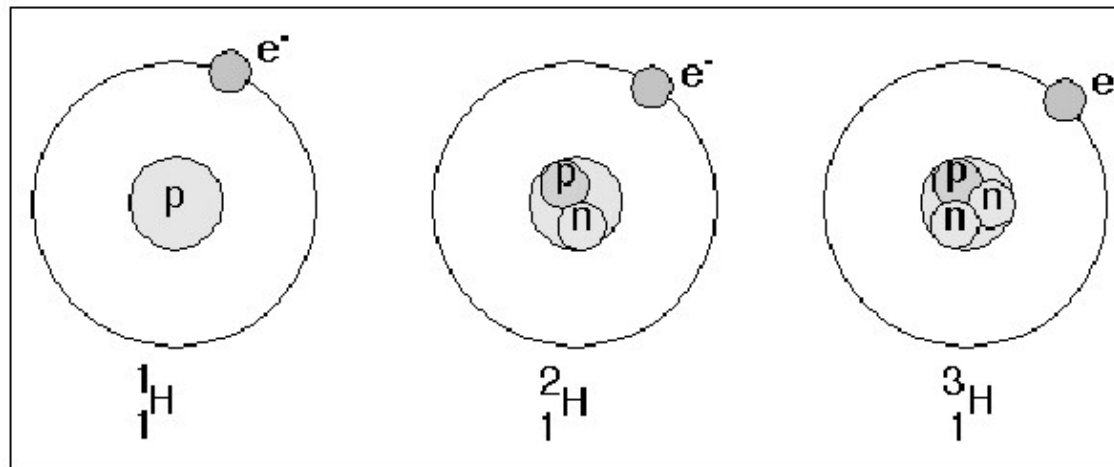
X: symbol of chemical element

$$^A_Z X$$

$$^1_1 H$$
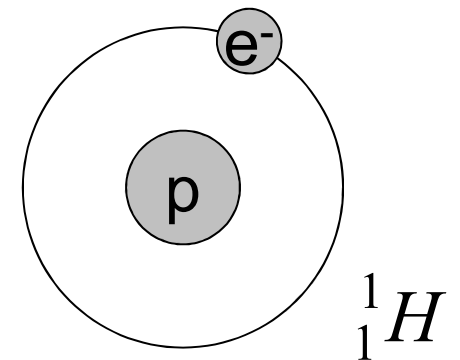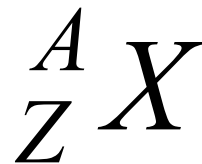
definitions:

nuclide: type of atom with type of nucleus defined by N and Z

radionuclide: nuclide with measurable decay rate (radioactive, unstable)

isotopes: nuclides with same atomic number Z but different
N and A → same element

isobars: nuclides with same mass number A (but Z and N differ)
→ different element
isotones: nuclides with different number of neutrons N (but Z and A differ)
→ different element

radionuclide for nuclear medical imaging:

requirements:

- must bind to targeted molecules related to metabolism
- stabile isotopes must be abundant in biochemical molecules
  (or their analogs):

  carbon (C), nitrogen (N), oxygen (O),
  hydrogen (H), fluorine (F)

- half-life

- path length in tissue

ionizing radiation:

γ	gamma rays	photons
β^-, e^-	beta rays	electrons
β^+, e^+		positrons
p		protons
n		neutrons
α	alpha rays	helium nucleus 2 protons + 2 neutrons

path length (penetration power) of ionizing radiation:

type of radiation	energy [MeV]	path length air	water
α	1	0.6 cm	0.008 mm
	6	5.0 cm	0.06 mm
β	0.1	10 cm	0.13 mm
	1	300 cm	4.2 mm
	3	1200 cm	15.0 mm
γ	0.01	1 m	0.15 cm
	0.1	230 m	2.7 cm
	1	190 m	22.0 cm
	10	380 m	45.0 cm

radioactive decay:

α - decay	${}^{226}_{88}\text{Ra} \longrightarrow {}^{222}_{82}\text{Rn} + {}^{4}_{2}\alpha + \gamma$
β^- -decay	${}^{131}_{53}\text{J} \longrightarrow {}^{131}_{54}\text{Xe} + e^- + \overline{\nu} + (\gamma)$
	$n \longrightarrow p + e^- + \overline{\nu}$
β^+ -decay	${}^{11}_{6}\text{C} \longrightarrow {}^{11}_{5}\text{B} + e^+ + \nu + (\gamma)$
	$p \longrightarrow n + e^+ + \overline{\nu}$
electron capture	${}^{201}_{81}\text{Tl} \longrightarrow {}^{201}_{80}\text{Hg}^m$
	$p + e \longrightarrow n$
isomeric transition (metastable nuclides)	${}^{99}\text{Tc}^m \longrightarrow {}^{99}\text{Tc} + \gamma$
spontaneous fission	${}^{236}_{92}\text{U} \longrightarrow {}^{99}_{42}\text{Mo} + {}^{133}_{50}\text{Sn} + 4{}^{0}_{0}n$

15

radioactive decay:

stability of an element depends on ratio between
atomic number (Z) and number of neutrons (N)
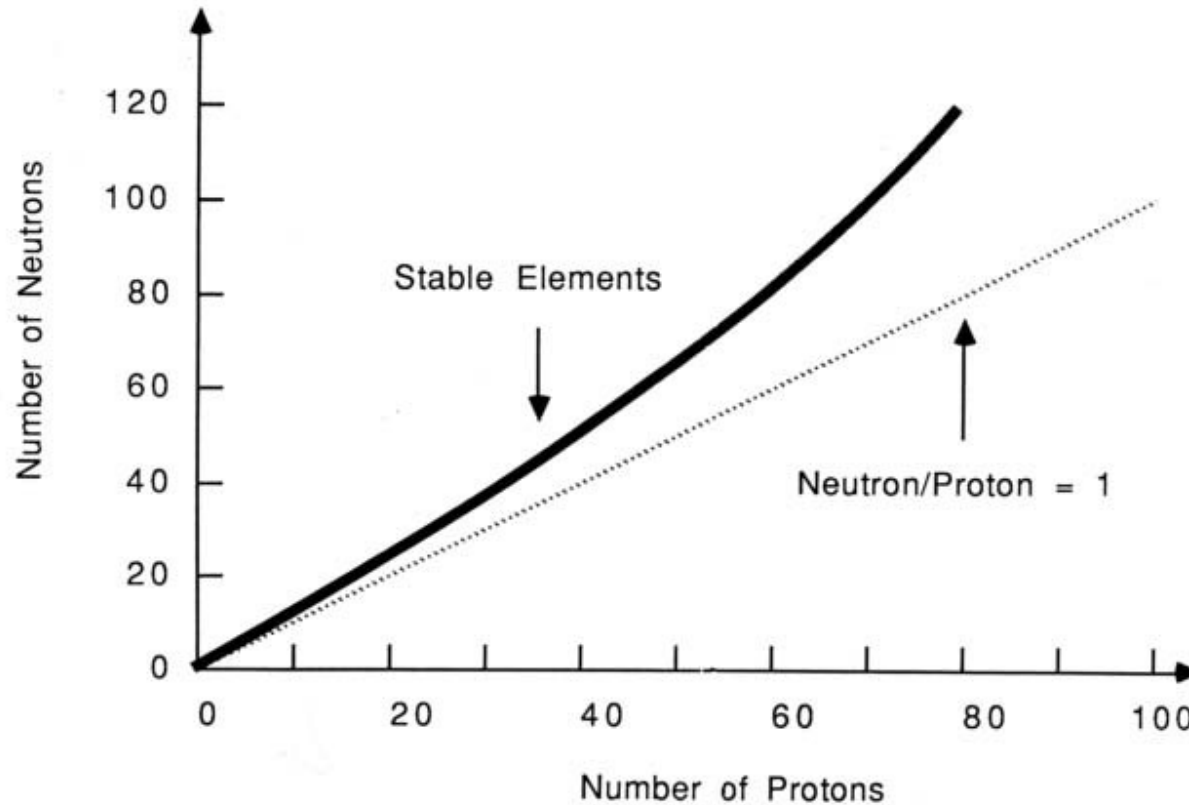
radioactive decay:

decay law:

$$N(t) = N_0 e^{-\lambda t}$$

where:

$N(t)$ = number of nuclides at time t

N_0 = number of nuclides at $t = 0$

λ = decay constant [τ^{-1}]

half-life:

$$T_{1/2} = \frac{\ln 2}{\lambda}$$

radioactive decay:

activity of a radioactive substance:
(number of decays per time unit)

$$A(t) = -\frac{dN}{dt} = \lambda N_0 e^{-\lambda t} = A_0 e^{-\lambda t}$$

unit: number of decays/second = Becquerel = Bq
(former: Curie (Ci); 1 Ci = $3.7 \cdot 10^{10}$ Bq)

typical activities for nuclear medical diagnosis:

100 MBq - 1000 MBq

generation of radionuclides:

- naturally occurring radioactive isotopes have too long half-life
- not of relevance for nuclear medical imaging
$\rightarrow$ synthetic radionuclides

nuclear fission	$^{235}_{92}U + \,^{1}_{0}n \longrightarrow \,^{236}_{92}U \longrightarrow \,^{99}_{42}Mo + \,^{133}_{50}Sn + 4\,^{0}_{0}n$
neutron bombardment	$^{98}_{42}Mo + \,^{1}_{0}n \longrightarrow \,^{99}_{42}Mo + \gamma$ $^{98}_{42}Mo(n,\gamma)\,^{99}_{42}Mo$
bombardment with charged particles (e.g. cyclotron) requires E(p) $\geq$ 10 MeV Coulomb wall of nucleus	$^{18}_{8}O + p \longrightarrow \,^{18}_{9}F + n$ $^{18}_{8}O(p,n) \longleftarrow \,^{18}_{9}F$

radionuclide generator

production of $^{99}Tc^m$ from ^{99}Mo

- ^{99}Mo from nuclear reactor (e.g. n-capturing)
- transport to clinic in lead container as
  $Na^+MoO_4^-$ ($T_{1/2}$ = 66.7 h)
- $^{99}Mo \rightarrow ^{99}Tc^m$ ($T_{1/2}$ = 6.03 h)
- pertechnetate ($Na^+TcO_4^-$) water soluble
- elution
- filling a syringe (NaCl) and injection

- enough new $^{99}Tc^m$ after 24h
- repeat elution ("milking")
- generator exhausted after 1 week

radionuclide generator (Moly generator)

saline solution

parent and daughter

(^{99}Mo and ^{99}Tc^m)

lead shielding

glass column

alumina (AL$_2$O$_3$)

filter (glass frit)

daughter (^{99}Tc^m)

eluted vial
(^{99}Tc^m)
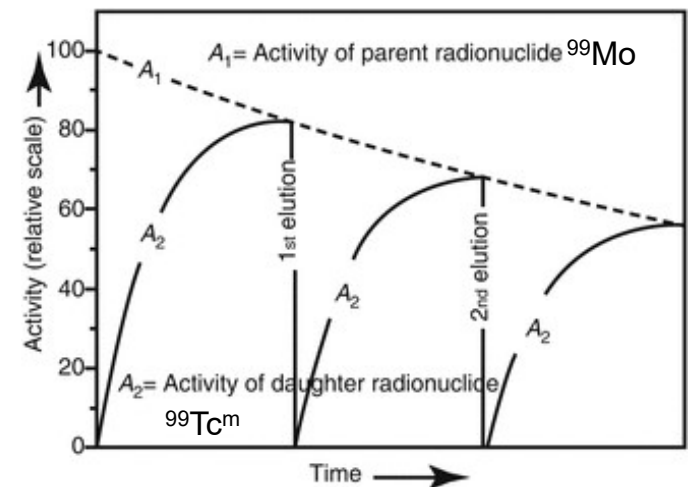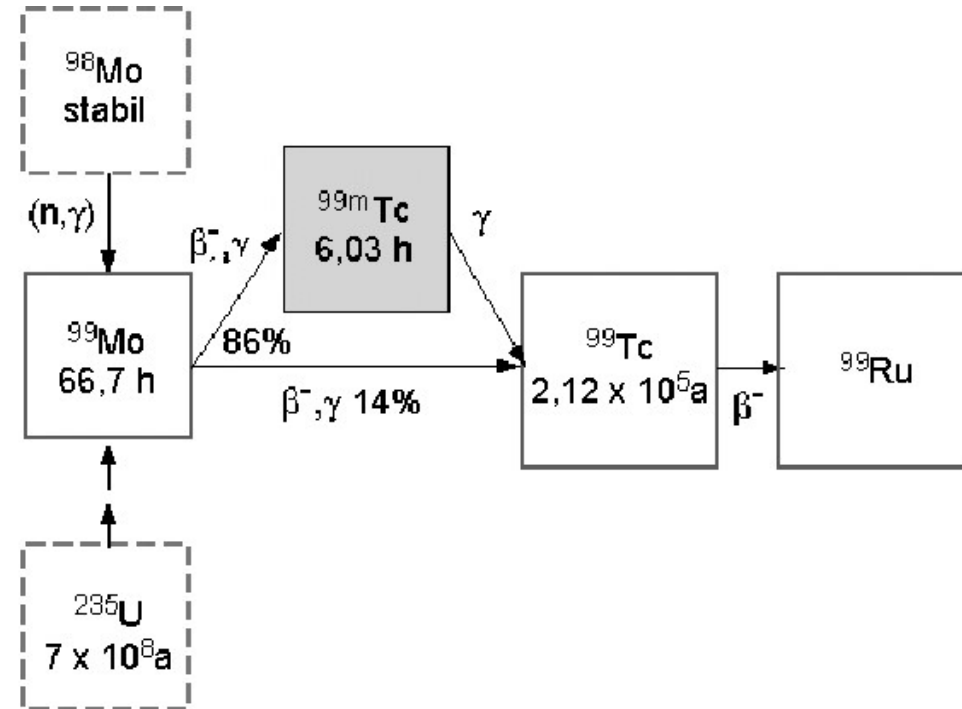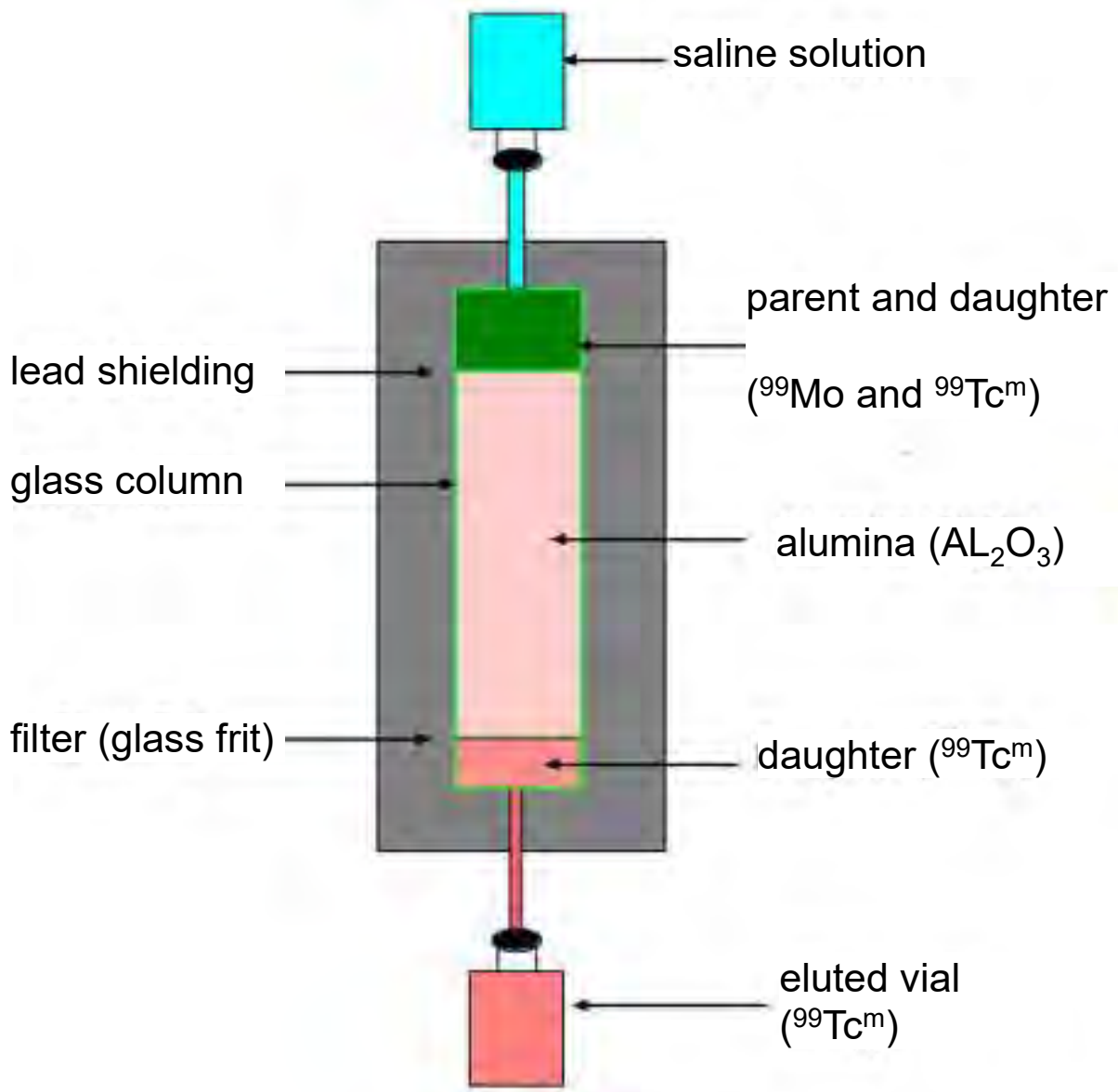
nuclear medical imaging techniques

radionuclides for diagnostic purposes:

nuclide	γ-energy keV	half-life	decay process (MeV)	production
^{11}C	511	20,3 min	β^+ (0,97 MeV)	cyclotron
^{13}N	511	9,93 min	β^+ (1,2 MeV)	cyclotron
^{15}O	511	124 s	β^+ (1,74 MeV)	cyclotron
^{18}F	511	110 min	β^+ (0.635 MeV) EC	cyclotron
^{67}Ga	92 185 296 388	78 h	EC	cyclotron

radionuclides for diagnostic purposes:

nuclide	γ-energy keV	half-life	decay process (MeV)	production
^{81m}Kr	190	13 s	IT	Generator ^{81}Rb
^{99m}Tc	140	6,0 h	IT	Generator ^{99}Mo
^{111}In	173 247 23 (Cd-Kα)	3,8 d	EC	cyclotron
^{123}I	159	13,3 h	EC	cyclotron
^{133}Xe	81 31 (Cd-Kα)	5,3 d	β^-	nuclear reactor
^{195m}Au	262 68 (Cd-Kα)	30,5 s	IT	Generator ^{195}Hg
^{201}Tl	135 167 71 (Hg-Kα)	73 h	EC	cyclotron

radionuclides for diagnostic purposes:

- linking to atom resp. molecule (radiopharmaceutical)

tracer:

- only transport of radionuclides (blood, breathing air)

- diffusion into specific organs (perfusion)

- direct involvement in chemical processes (e.g. metabolism)

radiopharmaceuticals for diagnostic purposes:

bind radionuclides to pharmaceuticals that are specific for metabolic activities

gamma emitter

^{99m}Tc-sestamibi ($C_{36}H_{66}N_6O_6Tc$)   (perfusion of heart, cancer)

^{99m}Tc-labelled HMPAO (hexamethyl propylenamine oxime)   (perfusion of brain)

positron emitter

^{11}C $T_{1/2}$ = 20 min

(receptors of neurons, metabolic activity)

^{13}N $T_{1/2}$ = 10 min

NH_3 (blood flow, regional perfusion of heart)

^{15}O $T_{1/2}$ = 2.1 min

CO_2 (cerebral blood flow), O_2 (oxygen consumption of heart), H_2O (oxygen consumption of heart and blood perfusion)

^{18}F $T_{1/2}$ = 110 min

2-Deoxy-2-[^{18}F]-glucose (fluorodeoxyglucose)

(FDG, neurology, cardiology, oncology, metabolic activity)

usage in nuclear medical diagnosis:

- known activity of radiopharmaceutical when applied to the body

- activity can be estimated for subsequent times (decay law)

- distribution of activity A in the body: where, when, how much?

$$\mathrm{d}A/\mathrm{d}V = \mathrm{f}(x,y,z,t) = ?$$

- suitable recording of time-dependent activity distribution

- image reconstruction (like with x-ray-CT), films

- functional processes in body

detectors for γ-quanta   **(Geiger-Müller-type) counter**

schematic circuit diagram
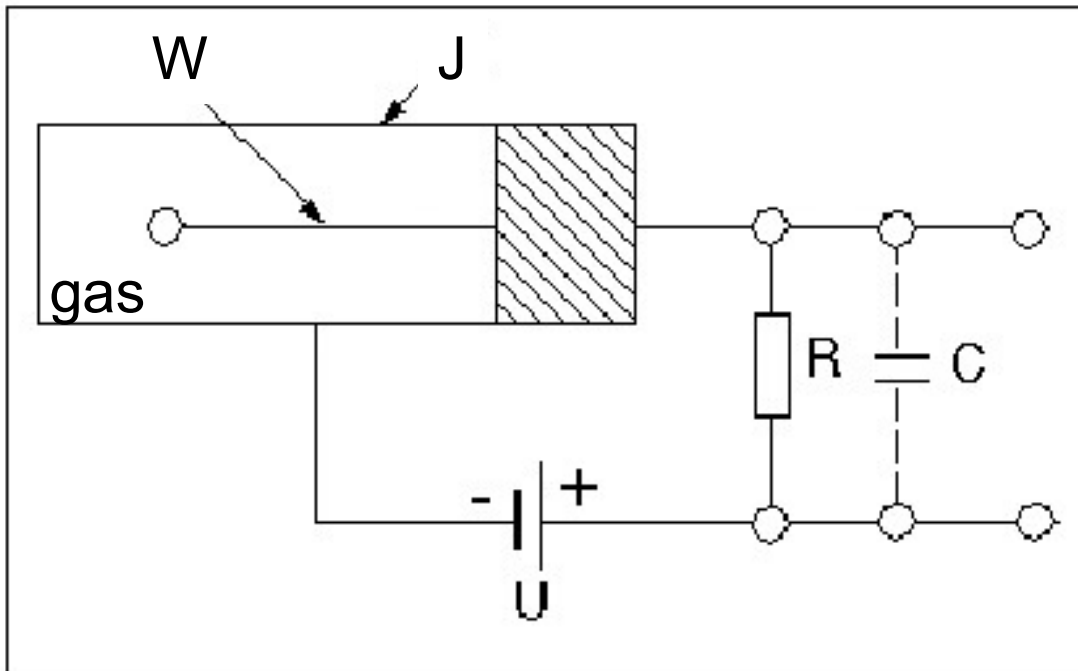
W = wire (anode)
J = jacket (cathode)
R = tube resistance
C = tube capacitance
U = tube voltage

detectors for γ-quanta   (Geiger-Müller-type) counter

mode of operation of counter depends on potential difference
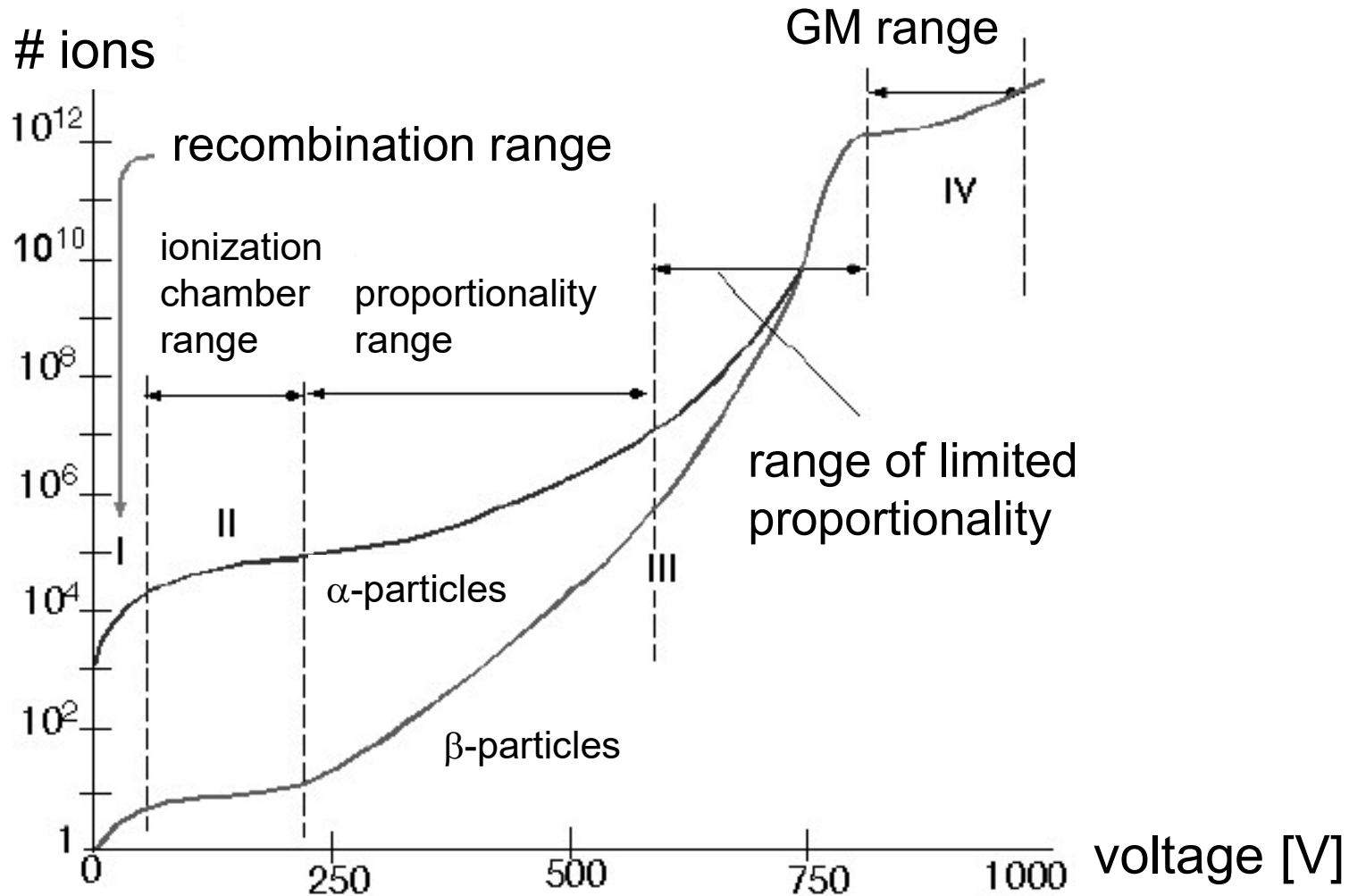
detectors for γ-quanta   **(Geiger-Müller-type) counter**

- **range I** (recombination area):
  potential difference not sufficient for charge separation (γ-quant induces
  ionization of gas); charge carriers (gas) recombine

- **range II** (ionization range):
  charge quantity transported via wire roughly proportional to induced
  charge quantity

- **range III** (proportionality range):
  charge amplification; strong acceleration of e$^-$ leads to ionization cascade;
  charge quantity transported via wire proportional to induced charge quantity

- **range IV** (Geiger-Müller range):
  charge quantity transported via wire independent of induced charge quantity;
  event counting (no analysis of pulse height)

detectors for γ-quanta   **scintillation counter**

photomultiplier

scintillation crystal

fiber optics   photo cathode   dynodes

γ-particle

counter

light quanta

1 2 3 4 5 6 7 8 9

Q

C

R

dynode voltage divider

- +

high voltage

30
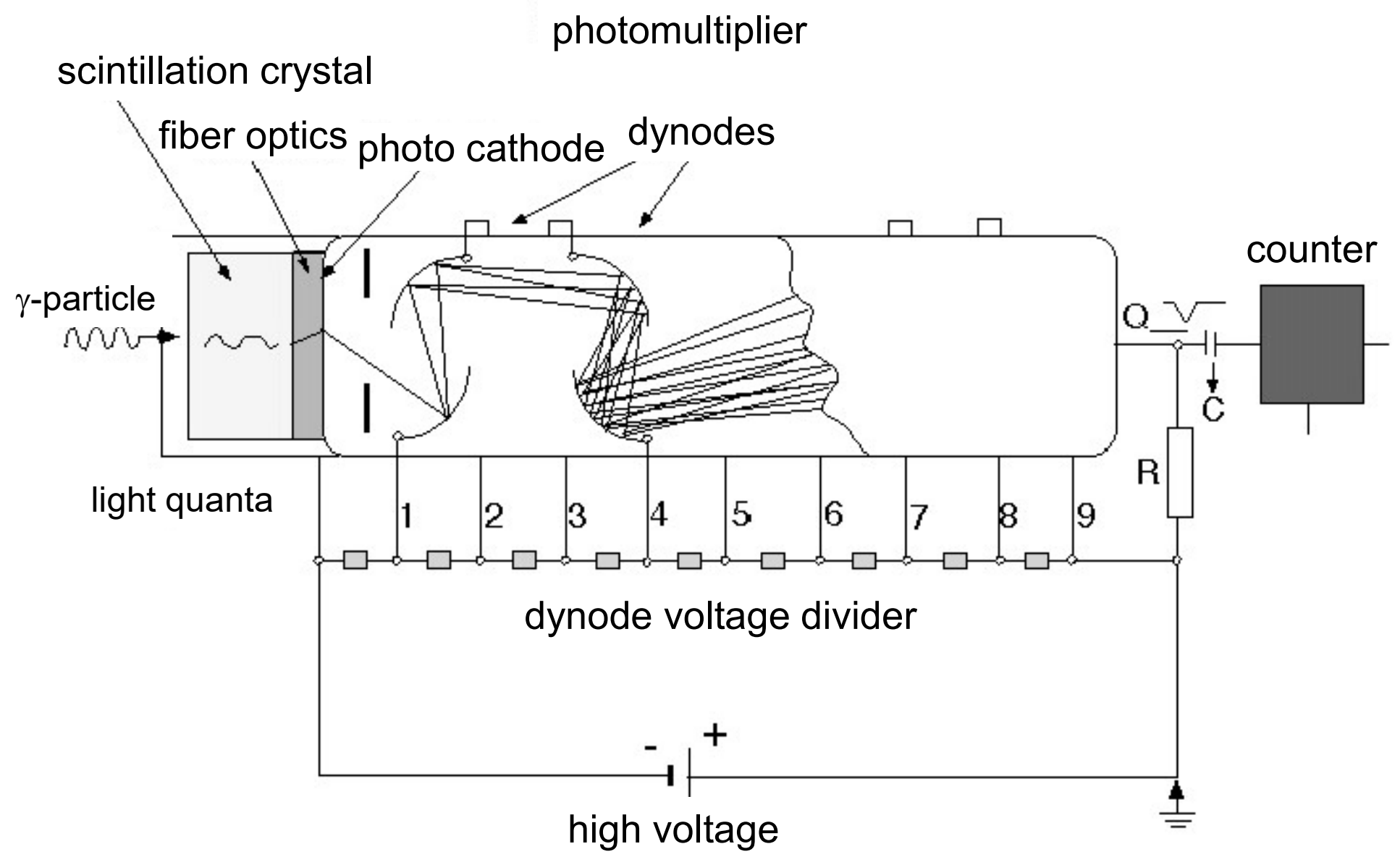
detectors for γ-quanta   **scintillation counter**

- scintillation crystal absorbs γ-quant; generation of photons
  (photoelectric effect and Compton-scattering)

- @full absorption: number of photons proportional to γ-energy:
  one light flash per γ-quant and $N_{photons} \sim E_\gamma$

- photomultiplier:
  release e⁻ in first dynode (photoelectric effect);
  accelerate to next dynode;
  each e⁻ generates secondary electrons;
  quantifiable impulses at output after about 10 dynodes

detectors for γ-quanta   scintillation counter

	NaI(Tl)	BGO $= Bi_4Ge_3O_{12}$
density (gcm^{-3})	3.67	7.13
→ atomic number	11 - 53	82 - 32 - 8
rel. luminous efficiency (norm. to NaI)	1.0	0.08
wavelength scintillation light (nm)	410	480
refraction index	1.78	2.15
decay time scintillation light (ns)	230	300
detector efficiency (%) thickness of crystal	(100 keV)	400 (keV)
20 mm	61	90
8 mm	52	84
4 mm	46	78

collimators

- define detection range for SPECT
  and planar scintigraphy
  (slice selection)

detector

collimator

- ideal: cylindrical tube

- material (γ-absorber): lead, tungsten

- the smaller the collimator's diameter the better the spatial resolution
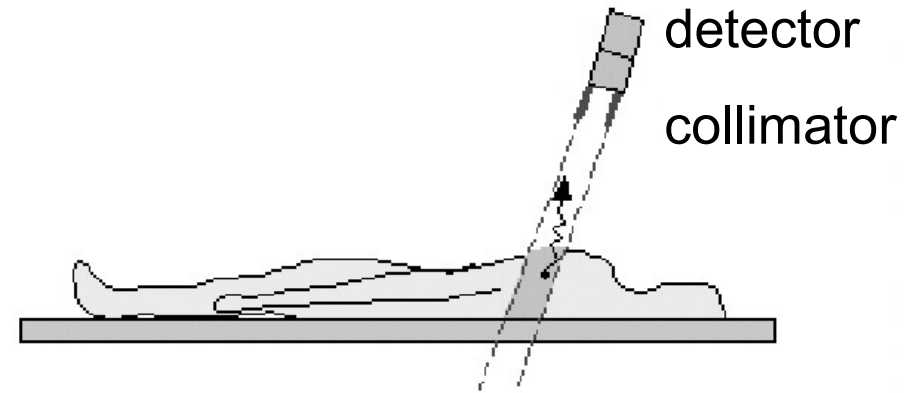
BUT:
- the smaller the collimator's diameter the smaller the number of
  detected quanta and the stronger the noise

point spread function of collimators

- move point-like γ-source along detector and
  register count rate in dependence on position
- observe penumbral region and plateau
- radius R of PSF from intercept theorem:

$$R = \frac{D}{L}\left(Z + \frac{L}{2}\right)$$

where:

    D = diameter of collimator
    L = length of collimator
    Z = distance collimator - γ-source

collimator element

point spread function

FWHM
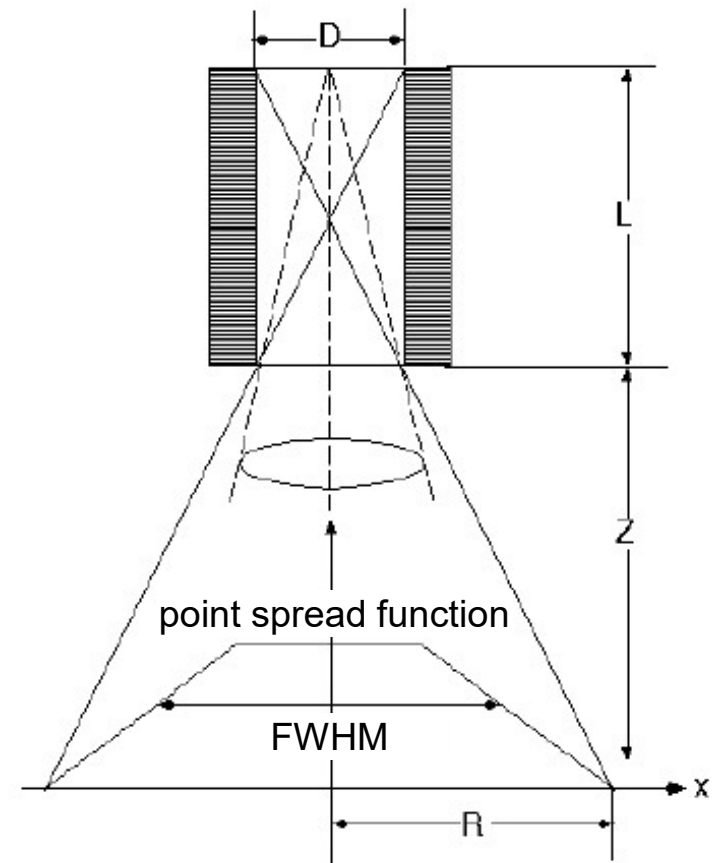
point spread function (PSF) the more narrow the smaller D/L and Z

typical parameters of collimators

		LEAP	HRES	UHRES	HSENS
L	[mm]	24	24	36	24
D_{eff}	[mm]	1,43	1,11	1,08	2,02
ε (relativ)		1,0	0,64	0,28	2,05
HWB					
at z = 0 mm	[mm]	4,2	4,0	3,9	4,6
at z = 100 mm	[mm]	8,9	7,4	5,8	12,2

LEAP = Low-Energy All Purpose   HSENS = High Sensitivity
HRES = High-Resolution ε = relative sensitivity
UHRES = Ultra-High Resolution   HWB = FWHM of point spread function

focusing collimators

distribution of iso-impulse lines ("sensitivity club")
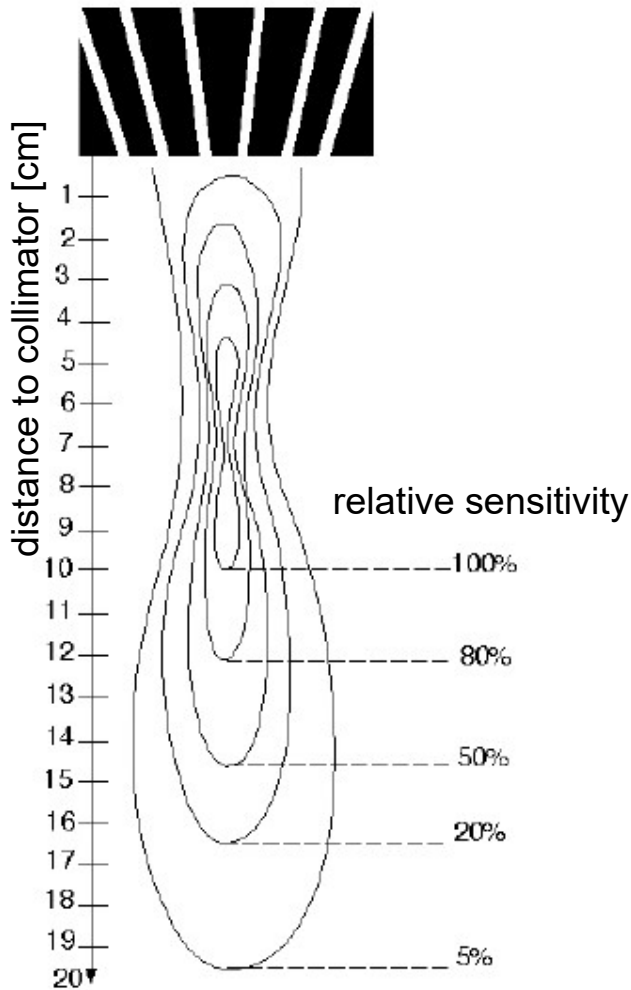
point spread function
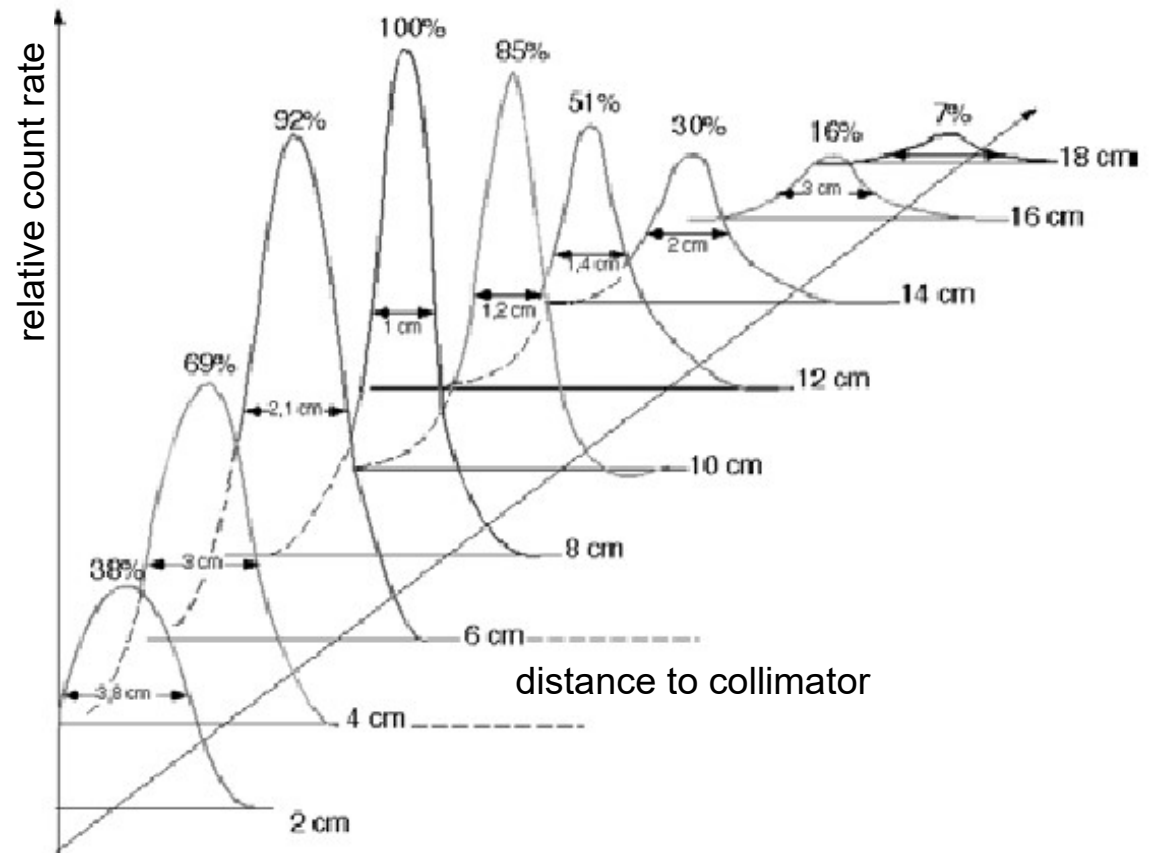
relative sensitivity

distance to collimator

relative count rate

distance to collimator [cm]

pulse height analyzer

photo effect

elastic
scattering

scattered
photon

scattered
photon

Compton
scattering

- e

pair production

+ e

Proton

nuclear reaction
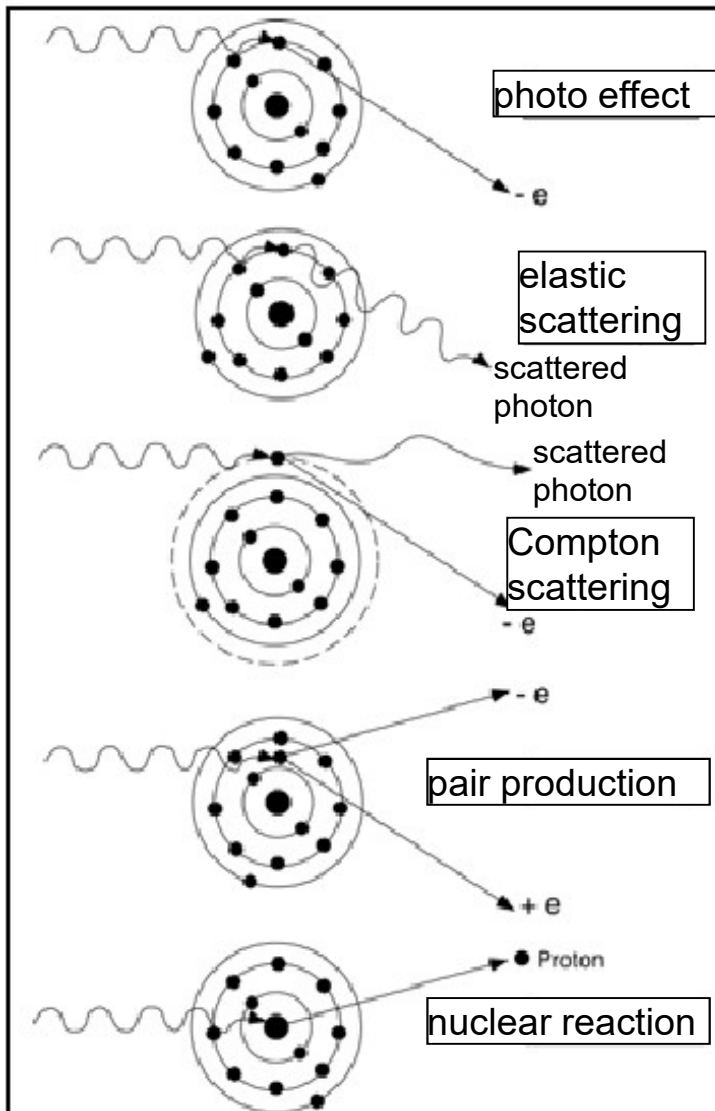
- scattering of γ-quanta in tissue mostly due to Compton-scattering

- imaging of site of Compton-scattering instead that of γ-emitter

- artifacts when imaging activity

reduction of amount of scattered γ-quanta with help of
pulse height analyzer

pulse height analyzer
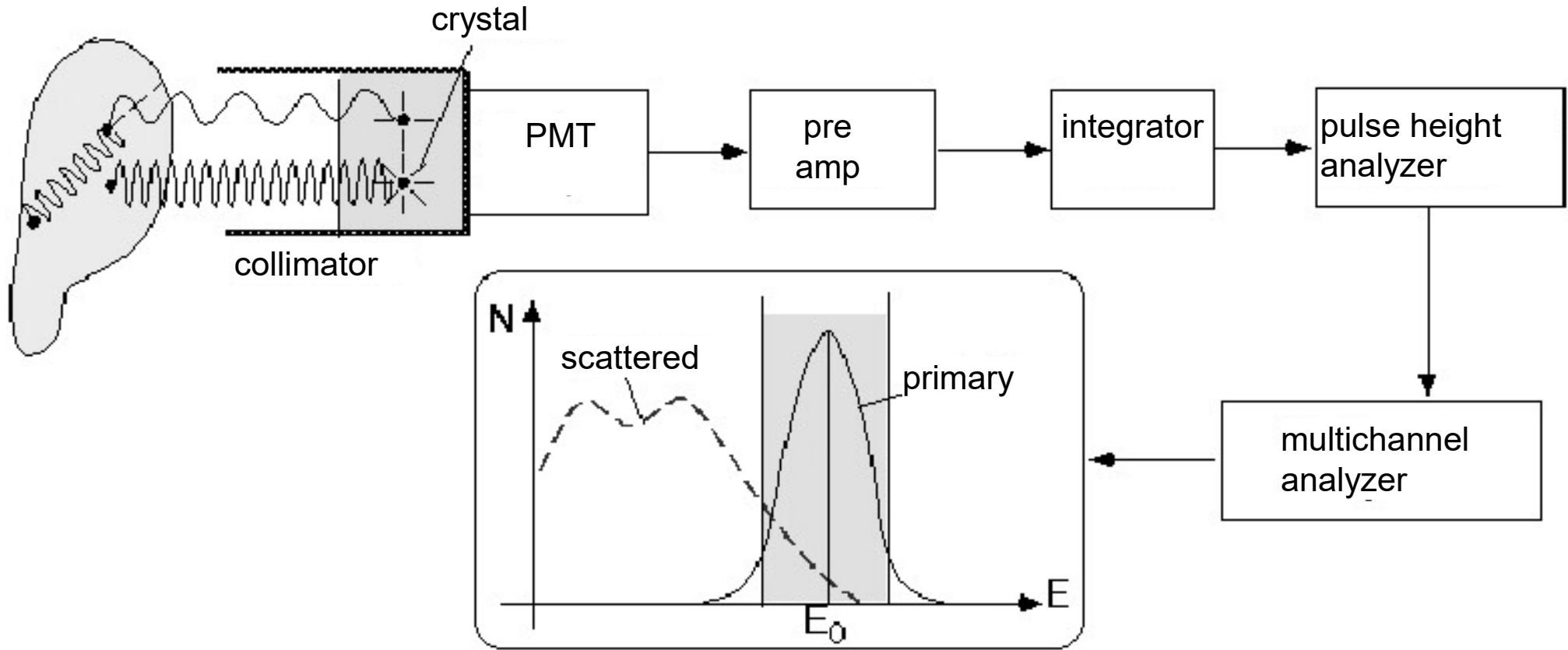
pulse height analyzer

assumptions (ideal detection and ideal detector):

- complete absorption of all γ-quanta in scintillator crystal
- uniform conversion of energy into light
- uniform number of photons onto dynode of PMT

$\Rightarrow$ area under curve of pulse (@output) ~ E_{γ}

- energy resolution of detector depends on statistics of generating differently many photons and photo-e$^-$ by γ-quant

pulse height analyzer

$E_{\gamma, \text{ scattered}} < E_{\gamma, \text{ primary}}$

define analysis window such that scattered γ-quanta
are optimally suppressed

- lower bound of window (threshold) too high:
  reduction of primary γ-quanta

- lower bound of window (threshold) too low:
  number of scattered γ-quant too high

$\Rightarrow$ choose threshold appropriately !

gamma-camera (Anger camera)

Hal Anger

idea: simultaneous recording of activity distribution over a large area of the body with high spatial resolution

naïve ansatz:
- one collimator for each detector, but: PMT too expensive !

Anger's ansatz:
- only few PMTs (37 - 100)
- high spatial resolution with help of resistance matrix

gamma-camera (Anger camera)

- scintillation flash light "seen" by various multiplier
- "center-of-mass" of multiplier signals corresponds to position (*x,y*) of absorption of γ-quant

$$x = \frac{k(x^+ - x^-)}{z}$$

$$y = \frac{k(y^+ - y^-)}{z}$$

$$z = x^+ + x^- + y^+ + y^-$$

- z = estimate of pulse height

gamma-camera (Anger camera)

output signals

resistance matrix

lead shielding

PMTs

fiber optics

NaI crystal

collimator

amplifier

differential amplifier

$(x^+ - x^-)$

$(y^+ - y^-)$

$x = \dfrac{x^+ - x^-}{z}$

$y = \dfrac{y^+ - y^-}{z}$

summation amplifier

$z = x^+ + x^- + y^+ + y^-$

pulse height analyzer

monitor

43
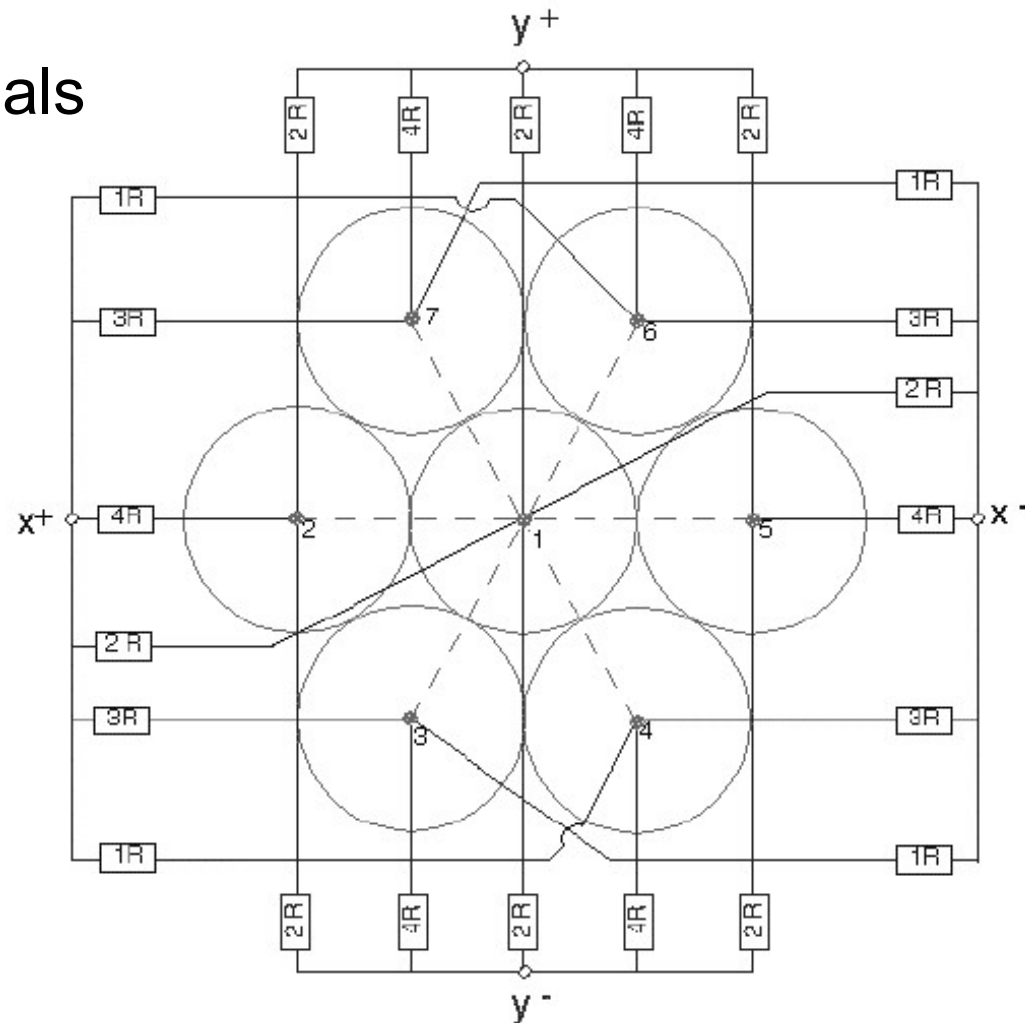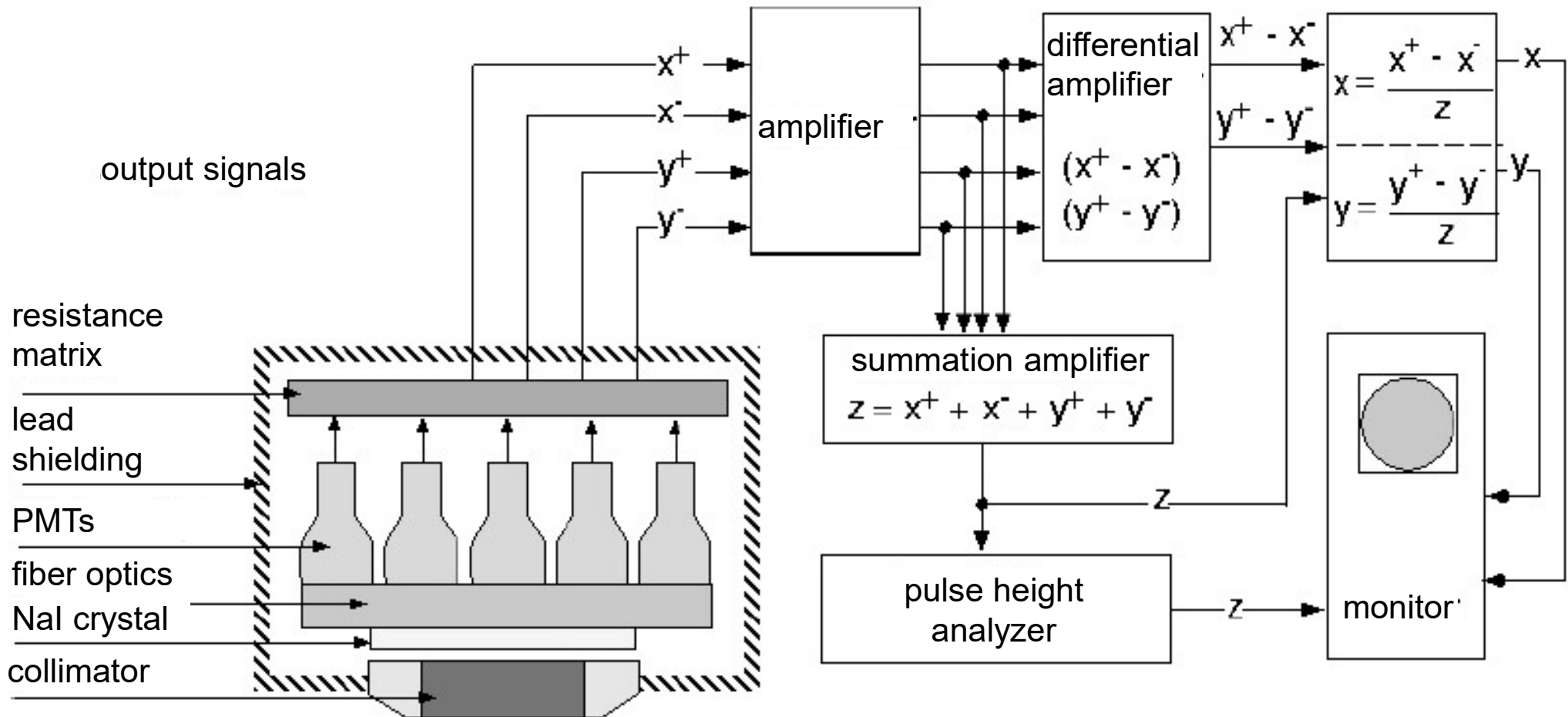
gamma-camera (Anger camera)

- typical specs:

      37 - 100 PMTs, diameter: 20 - 50 cm

      thickness scintillation crystal:

          6 mm (200 keV-quanta) - 12 mm (511 keV-quanta)

      spatial resolution: 3 - 5 mm

- high-quality gamma-camera requires uniform and stable
  sensitivity of PMTs

- regular calibration of system with known activity distribution;
  correction schemes

planar scintigraphy

planar scintigraphy

- fixed positioning of gamma-camera
  over region of interest

photomultiplier

crystal

collimator

- image pixel = integral over activity
  within a column beneath the collimator
  (width of column defined by collimator septa)

- compares to projection radiography (x-ray)

- increased sensitivity by using focusing collimators
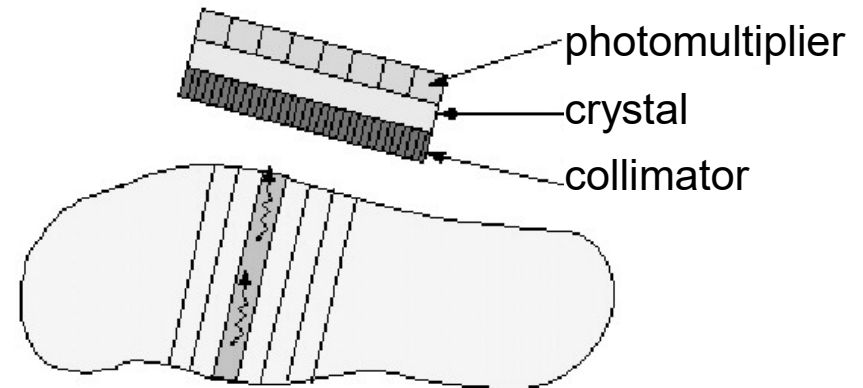
planar scintigraphy

fields of application

organ	diagnostic question	radiopharmaceuticals
heart	defects of cardiac septum ejection fraction	^{201}Th-Chlorid, ^{99}Tc-Phosphat
thyroid gland	tumor hyperfunction	^{131}J, ^{123}J ^{99}Tc-Pertechnetat
lung	ventilation	^{133}Xe, ^{99}Tc-Makroalbumin
kidney	perfusion secretion excretion	^{99}Tc-Chelate (z. B. Tc-DMSA, Tc-DTPA)
bones	tumor	^{99}Tc-Phosphate

^{99}Tc-compounds "travel" with blood; do not participate in metabolism
^{99}Tc short half-live, comparably low radiation exposure

nuclear medical imaging techniques

planar scintigraphy   **dynamical imaging**

- fixed positioning of gamma-camera over region of interest

- acquisition of data for a longer period of time

- averaged activity distributions from shorter time segments
  (typically 1 - 10 s); noise reduction

- spreading of tracer in body (movies)

- fields of application: heart, kidneys

planar scintigraphy   dynamical imaging

MUGA: Multi-gated Acquisition (heart)
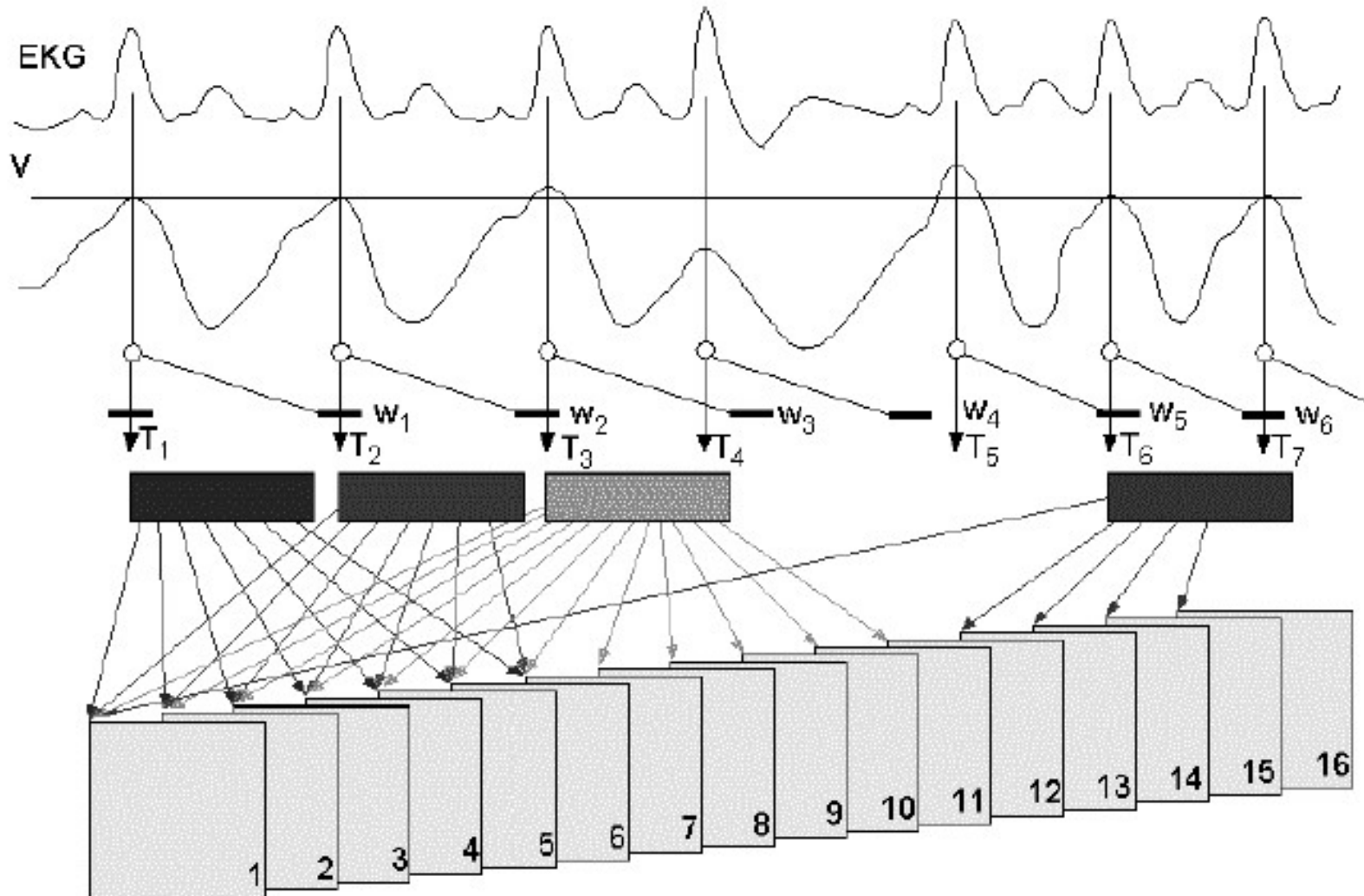
nuclear medical imaging techniques

planar scintigraphy　　　　　　　　**dynamical imaging**

kidneys

0-10 min　　　　　　10-20 min　　　　　　20-30 min

L　　　　R　　　　　L　　　　R　　　　　L　　　　R
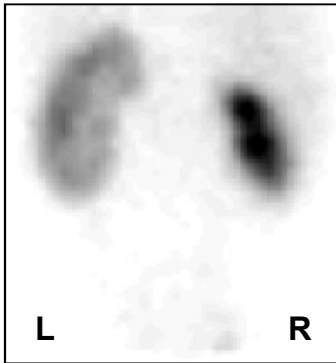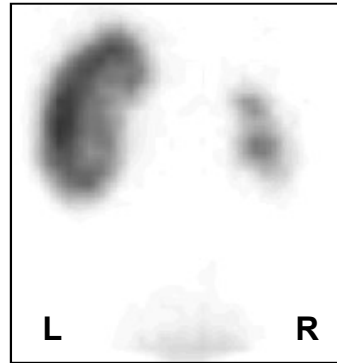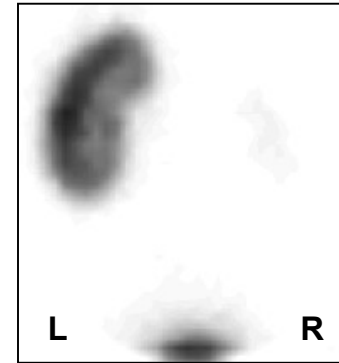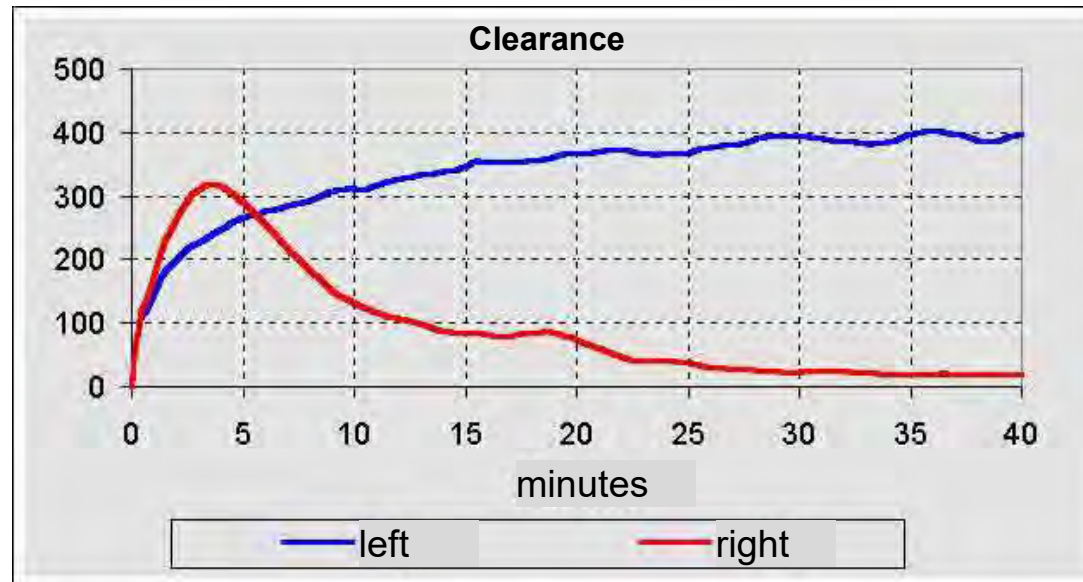
Tracer:

123J-Orthojod-Hippursäure
99mTc-MAG3
99mTc-DTPA

Clearance

left　　　　　right

minutes

planar scintigraphy

average radiation exposure

investigated organ	radiopharma-ceutical	applied activity [MBq]	energy dose/ examination		ion dose rate @distance 1 m from patient [pA/kg]
			critical organ [mGy]	gonads [mGy]	
thyroid gland	^{99m}Tc-Pertechnetat ^{131}Jodid	37 1,85	6 500	0,2 0,3	5 1,1
brain	^{99m}Tc-Pertechnetat (TcO$_4^-$)	370	60	2	43
lung	^{99m}Tc-MAA	74	5	0,05	11,5
liver spleen	^{99m}Tc-S-Kolloid ^{99m}Tc-S-Kolloid	111 111	12 3	0,15 0,15	14,3 14,3
kidneys	^{99m}Tc-DMSA	74	1	0,4	10
bones	^{99m}Tc-DPD	444	5	3	51,6

comparable to or even lower than x-ray diagnosis !

planar scintigraphy   whole-body scintigram

planar scintigraphy   **whole-body scintigram**

ventral   dorsal

nuclear medical imaging techniques

planar scintigraphy   whole-body scintigram

Radiopharmakon: 10 MBq/kg Körpergewicht Tc-99m Methylendiphosphonat

Hydrierung: ausreichende Flüssigkeitszufuhr (oral) zwischen Injektion und statischer Aufnahme der Knochenphase. Unmittelbar vor der Aufnahme Blase entleeren lassen.
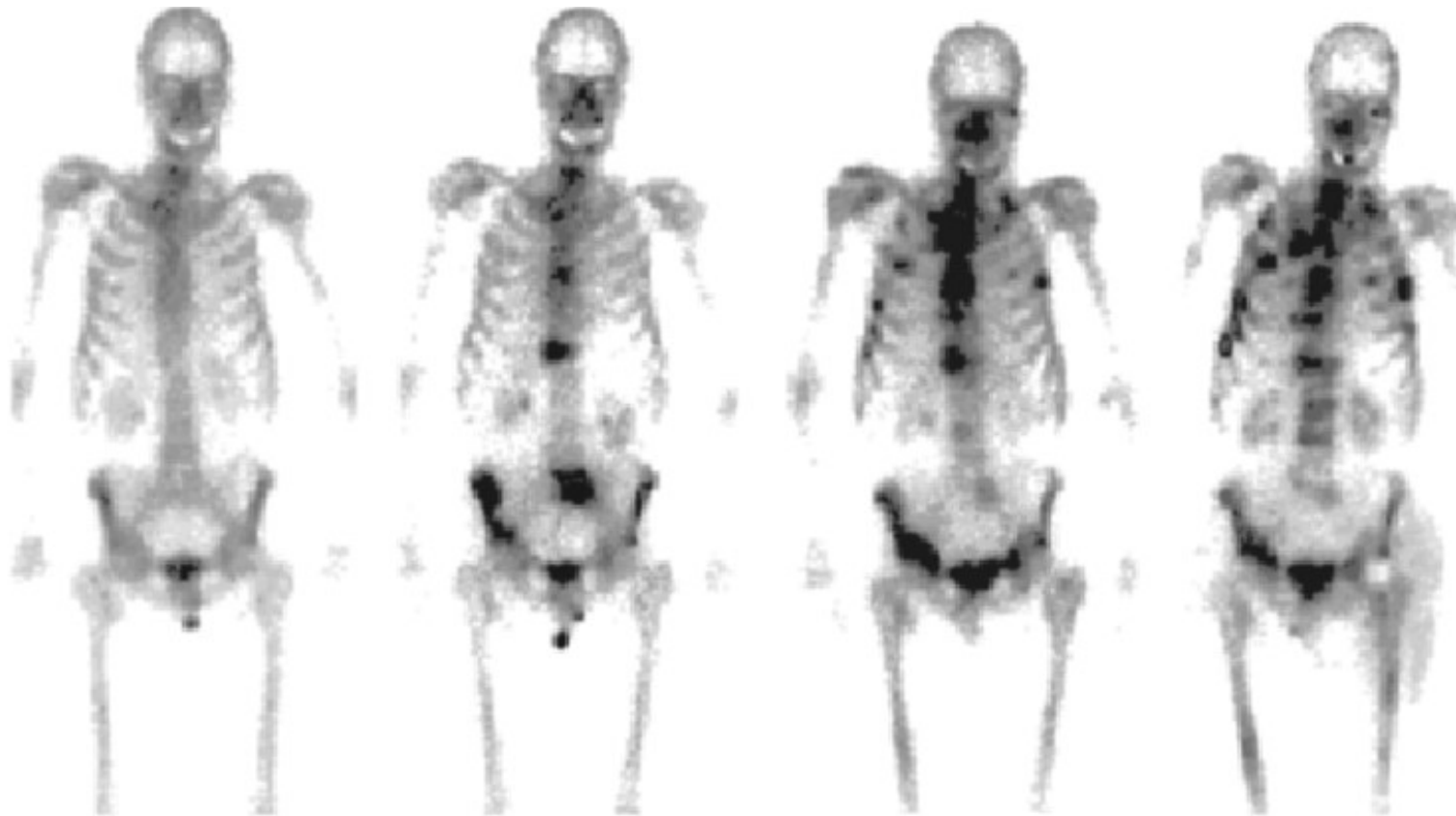
Januar 89   Juli 91   Januar 93   Juni 93

scintigraphic verification of progressive metastasis in a patient with prostate carcinoma

54

planar scintigraphy   thyroid gland

Untersuchungsgerät: Gammakamera mit hochauflösendem Kollimator
Radiopharmakon: 20-80 MBq Tc-99m Pertechnetat
Kameramessung: Messung der Spritze vor Injektion, Injektion, Messung der leeren Spritze p.i.
                     Kontrolle der Injektionsstelle auf paravenöse Injektion
                     Schilddrüsenmessung 15-25 min p.i. (Dauer 2-8 min)
Auswertung: Konturnahe ROI über der Schilddrüse, Untergrund-ROI caudal

$$TcTU\,(\%) = 100 * \frac{\text{Schilddrüsenimpulse - Untergrundimpulse}}{\text{Nettoimpulse der injizierten Aktivität}}$$
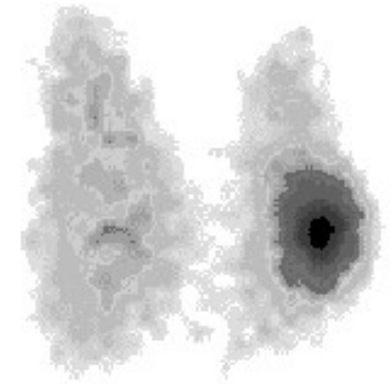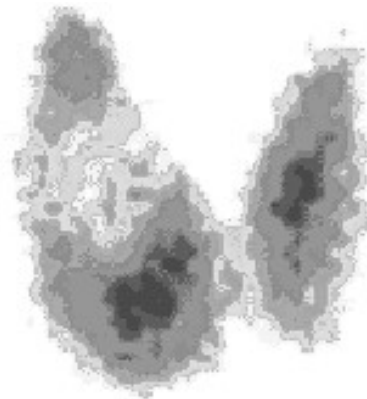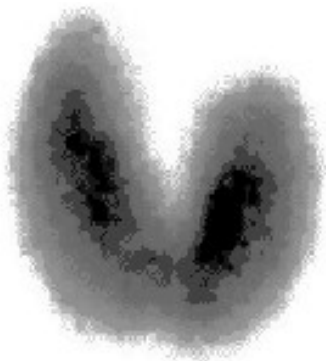
M. Basedow (homogenous,   cold thyroid nodule   hot thyroid nodule
generally increased uptake)   (carcinoma, cyst, inflammation, bleeding) (autonomous adenoma)

planar scintigraphy   **kidneys**

posterior   anterior
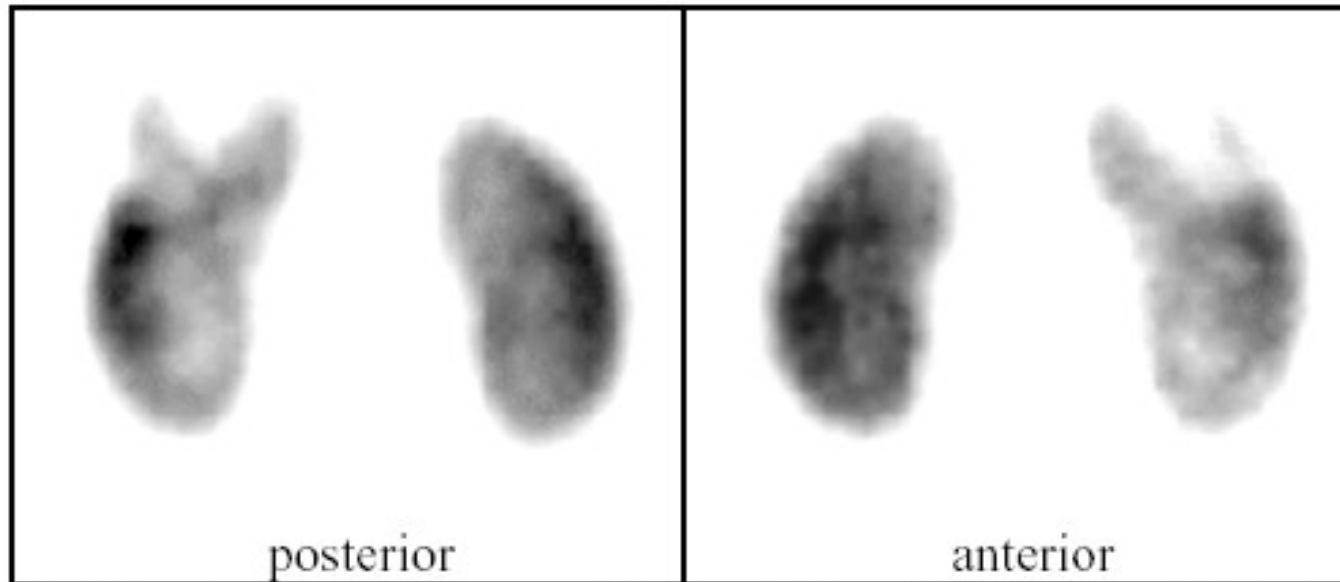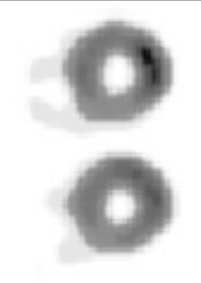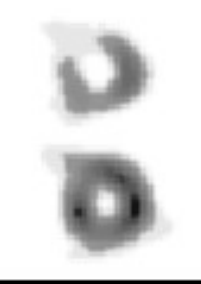
Speicherdefekt im oberen Pol der linken Niere einer 7-Jährigen nach rezidivierenden hochfieberhaften Harnwegsinfekten (30 MBq Tc-99m DMSA).

DMSA (**di**mercaptosuccinic **a**cid = Dimercaptobernsteinsäure)

planar scintigraphy   heart

upper scintigrams: during load lower scintigrams: at rest	SEPT ANT LAT INF	BASE ANT APEX INF	SEPT APEX LAT BASE
Beim gesunden Herz reichert sich die Aktivität sowohl in Ruhe als auch unter Belastung im gesamten Herzmuskel gut an. *(normal)*			
Irreversible Defekte wie Infarktnarben stellen sich in beiden Untersuchungen gleich minderspeichernd dar. Das vital chronisch ischämische Myokard (hibernating myocardium) hat ein Speichermuster ähnlich der Narbe, füllt sich jedoch nach Reinjektion von Thallium ganz oder teilweise auf. *(infarct)*			
Eine reversible Ischämie stellt sich durch die im Vergleich zu gesunden Myokard geringere Durchblutung besonders in der Belastungsuntersuchung minderspeichernd dar während in der Ruhe der Defekt weniger ausgeprägt erscheint oder ganz verschwindet. *(hypoperfusion)*			

planar scintigraphy   lung

lung perfusion scintigraphy

normal   pathologic
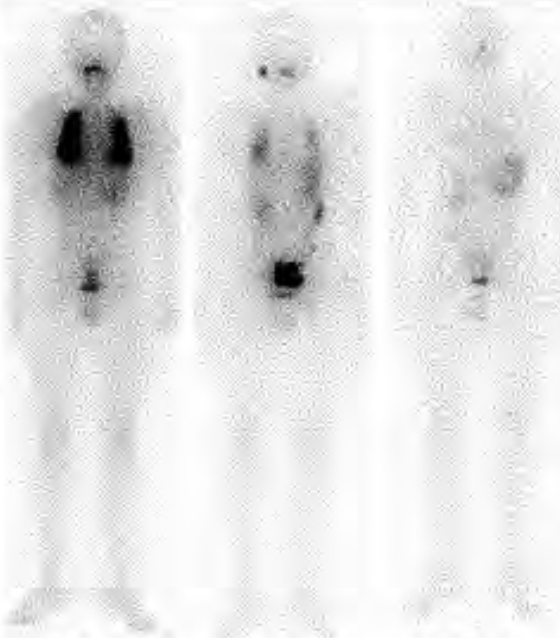
Tracer:
99mTc-markierte Partikel

planar scintigraphy   thyroid gland

Anreicherung von I-131 in den Metastasen eines hochdifferenzierten Schilddrüsen-karzinoms.

Szintigramme nach 1., 2. und 4. Therapie bei einem Kind aus Weißrußland, bei dem im Alter von 13 Jahren ein Schilddrüsenkarzinom infolge des Reaktorunglücks in Tschernobyl diagnostiziert wurde.

Nach 4 Therapien mit jeweils 6 GBq I-131 ist die bei der 1.Therapie erkennbare ausgedehnte diffuse Metastasierung der Lunge verschwunden, es sind keine krankheitsbedingten Anreicherungen mehr erkennbar.

02/95   12/95   07/96

Single Photon Emission Computed Tomography (SPECT)

Single Photon Emission Computed Tomography (SPECT)

employ tomographic methods to reconstruct - from projections - the **distribution of some activity A** in a sectional plane of the body

x-ray CT   **SPECT**

$$\ln\left(\frac{J_0}{J}\right) = \int \mu(x, y)\, d\ell \qquad Signal = \int A(x, y)\, d\ell$$

- identical algorithms
- different resolution
      (needle-like beam $\leftrightarrow$ sensitivity club)
- different signal statistics

Single Photon Emission Computed Tomography (SPECT)

	x-ray CT	SPECT
matrix size	512 x 512	128 x 128
# projections	> 1000	100 - 200
# detectors	~ 800	37 - 100 (photomultiplier)
resolution	0.5 mm	10 - 15 mm

reconstruction algorithms for SPECT:
- *standard*: filtered back projection; however, high noise level
  requires filtering at relatively low spatial frequencies

- *better*: iterative image reconstruction and taking into account
  absorption processes in the body

Single Photon Emission Computed Tomography (SPECT)

photomultiplier

crystal

collimator
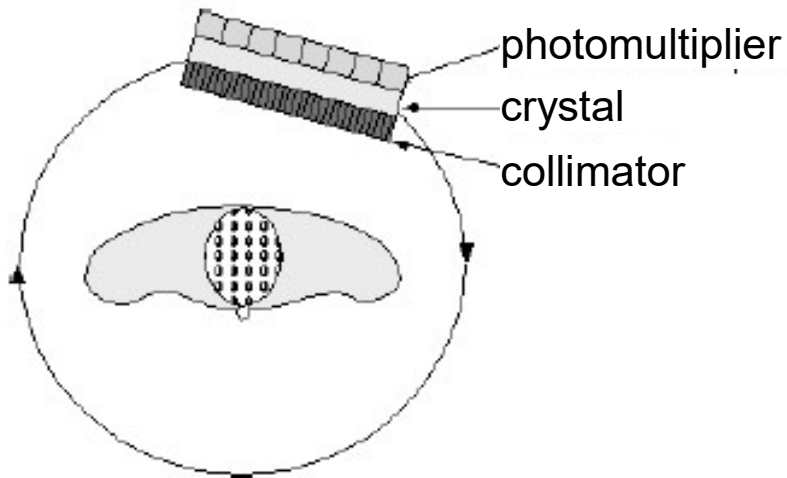
single probe head, circular orbit

higher spatial resolution, since FWHM of PSF depends on distance between detector and source
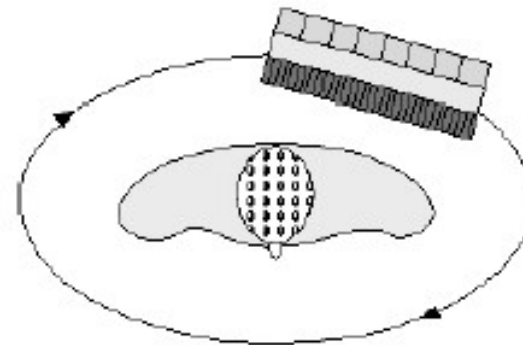
single probe head, elliptic orbit
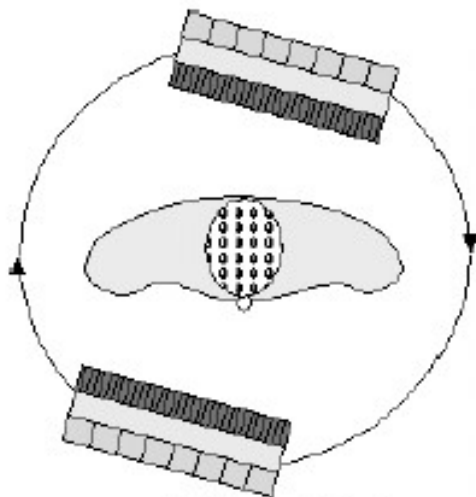
dual probe head

more projections ↔ better signal-to-noise ratio
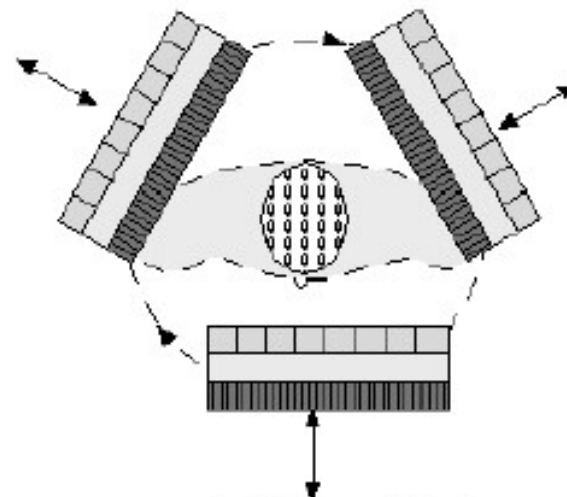
triple probe head

Single Photon Emission Computed Tomography (SPECT)

©Fototeam DRNN

dual probe head SPECT System
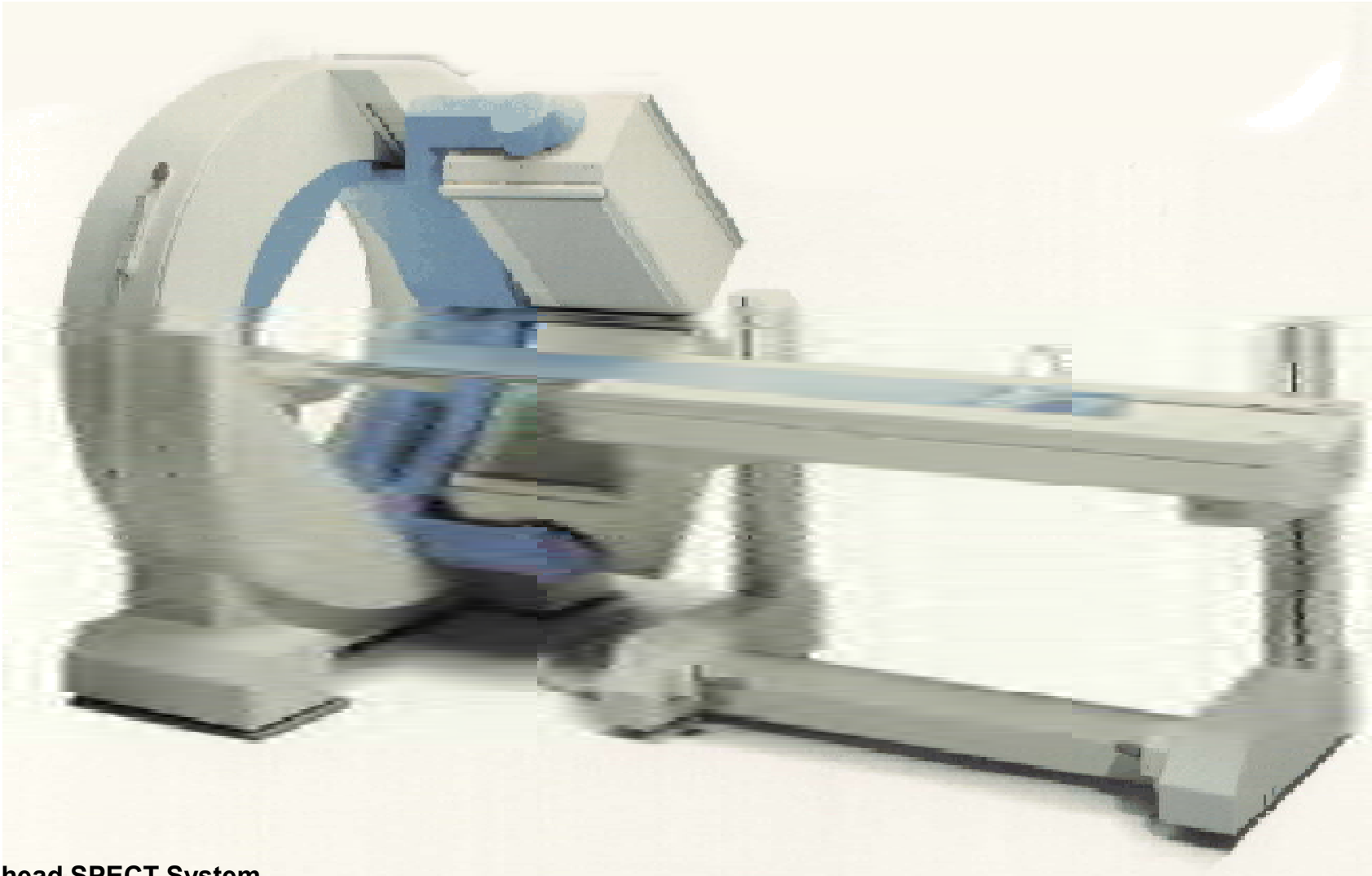
Single Photon Emission Computed Tomography (SPECT)

dual probe head SPECT System

Single Photon Emission Computed Tomography (SPECT)

imaging errors

physical reason:
  - absorption of γ-quanta between source and detector

technological reasons:
  - no true line integrals with collimators
  - amount of Compton-scattered quanta (despite use of pulse-height analyzer)
  - failure of photomultiplier

example:
- 140 keV radiation of ^{99}Tc; fixed field-of-view
-   5 cm tissue atop organ of interest: rel. amount of γ-quanta: 50 %
- 15 cm tissue atop organ of interest: rel. amount of γ-quanta: 10 %
$\Rightarrow$ large amount of artifacts when using back projection

Single Photon Emission Computed Tomography (SPECT)

imaging errors due to "wrong" detections
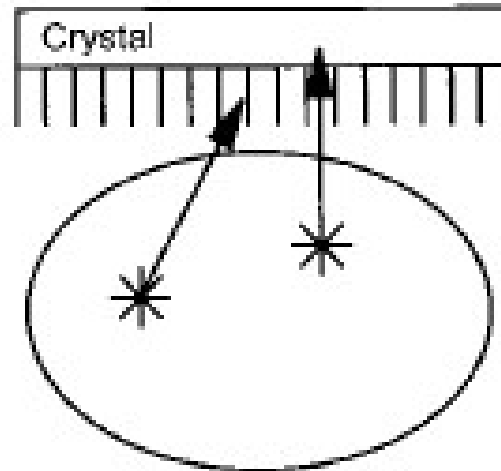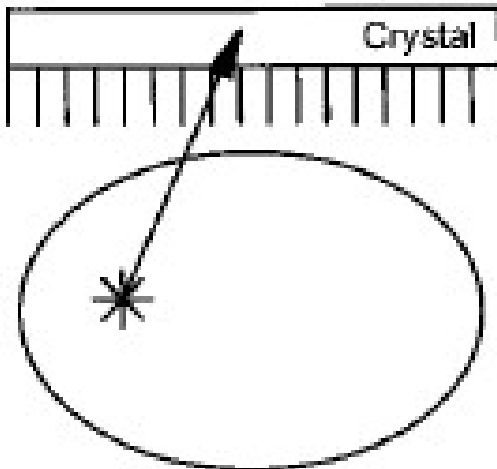
large field-of-view   Compton scattering   wrong coincidences
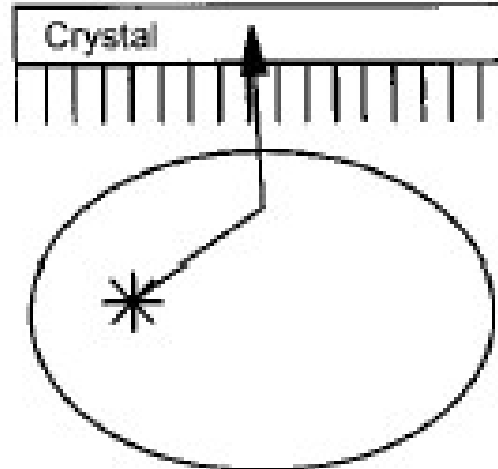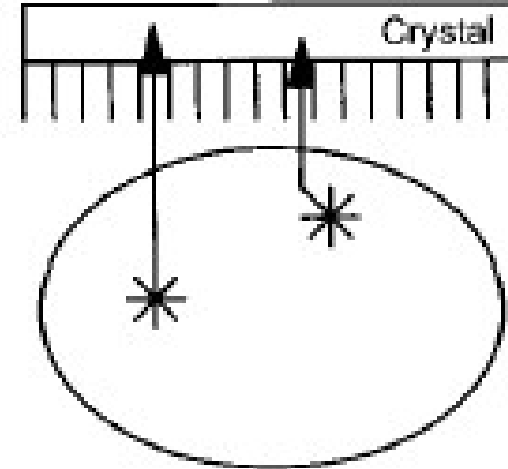
Single Photon Emission Computed Tomography (SPECT)
imaging errors due to failure of photomultiplier
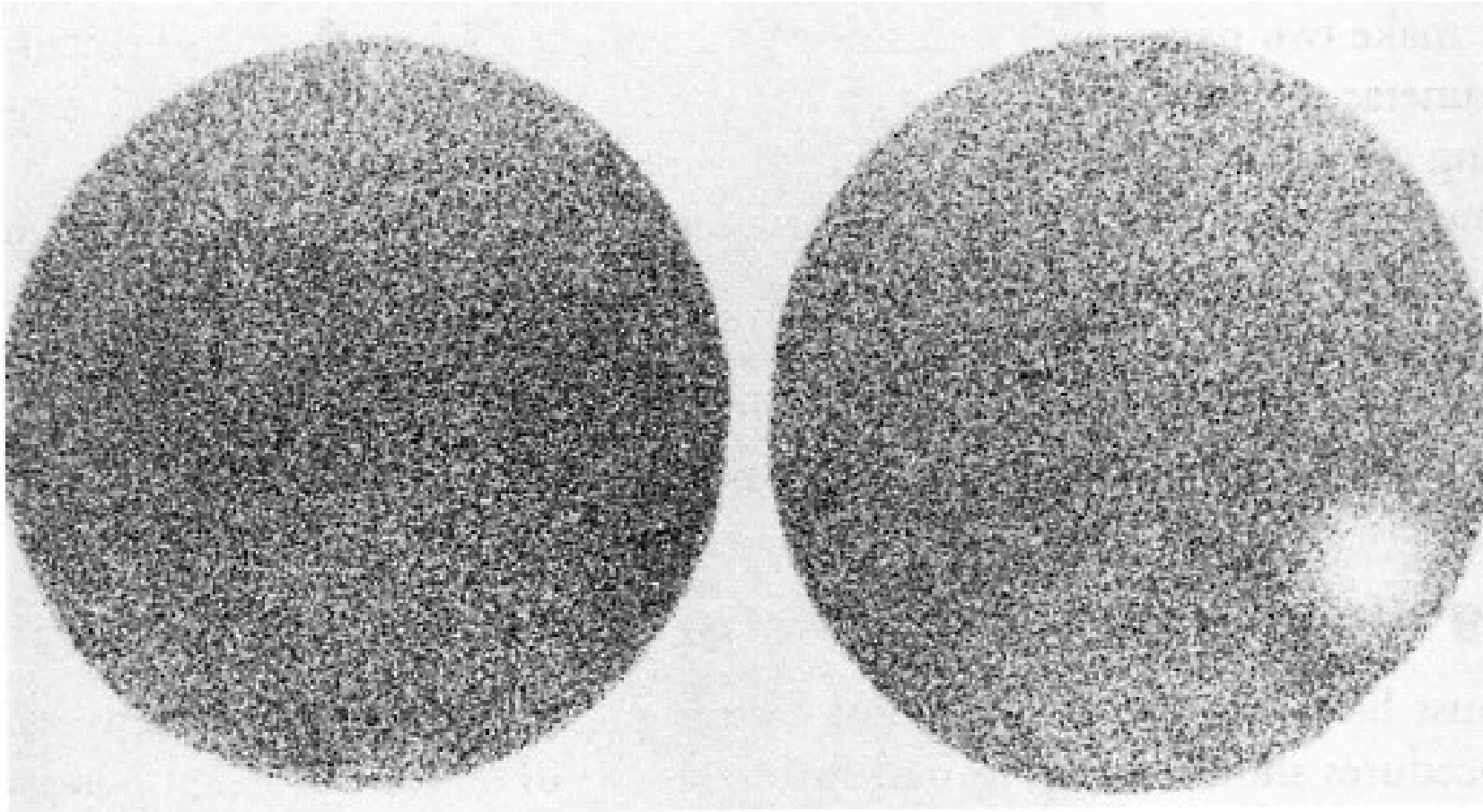
Single Photon Emission Computed Tomography (SPECT)

imaging errors due to spatial nonlinearities

impact of
detector
geometry
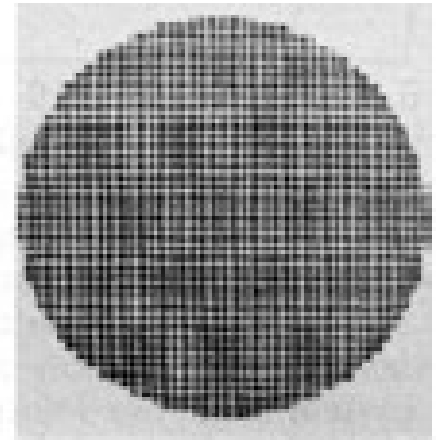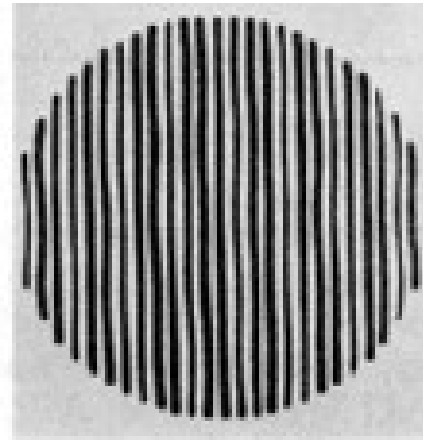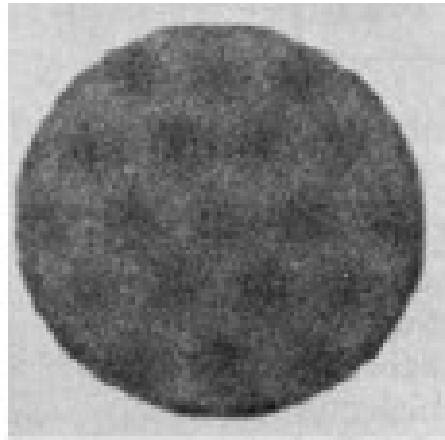
minimization
with appropriate
correction schemes
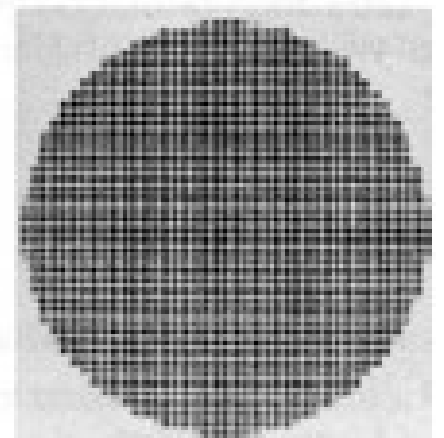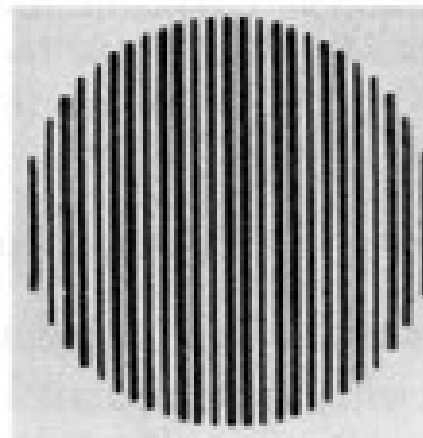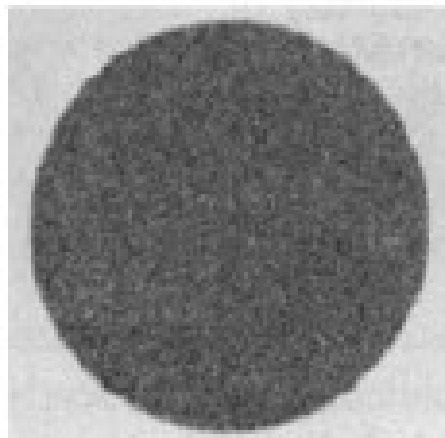
Single Photon Emission Computed Tomography (SPECT)

impact of filter characteristics on back projection

Butterworth 5. order $F_c=0.15 \cdot F_{Nyq}$	Butterworth 5. order $F_c=0.27 \cdot F_{Nyq}$	ramp filter
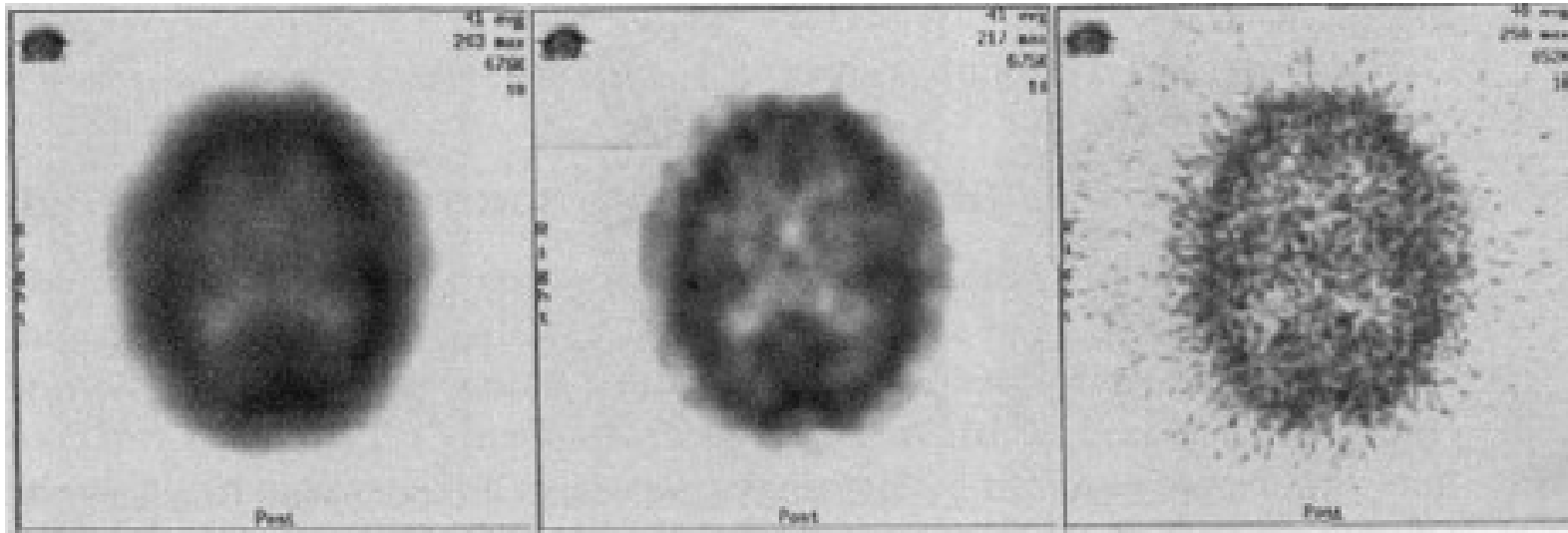
Single Photon Emission Computed Tomography (SPECT)

simplified attenuation correction

signal at anterior position
$$S_A = k \cdot A \cdot e^{-\mu x}$$

k = calibration factor
A = activity at position x
μ = mean attenuation
    coefficient of tissue

signal at posterior position
$$S_P = k \cdot A \cdot e^{-\mu(D-x)}$$

anterior

posterior
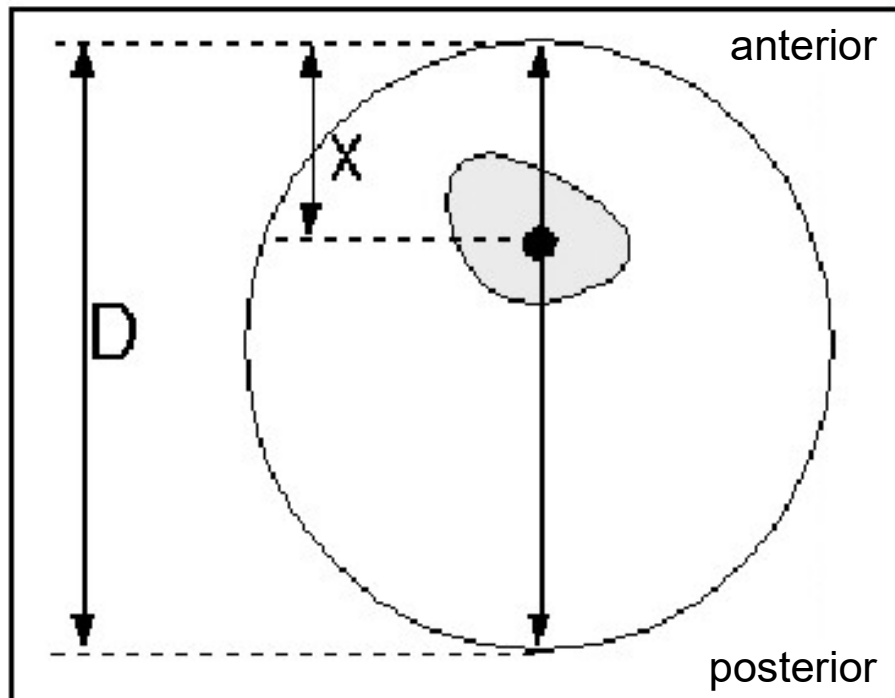
geometrical mean:

$$S_{GM} = \sqrt{S_A \cdot S_P} = k \cdot A \cdot e^{-\mu D/2}$$

recording of $\mu \cdot D$ via transmission measurement:

$$\ln\left(\frac{J_0}{J}\right) = \mu \cdot D$$

71

Single Photon Emission Computed Tomography (SPECT)

attenuation correction
cylindrical test system with known concentration of radionuclide
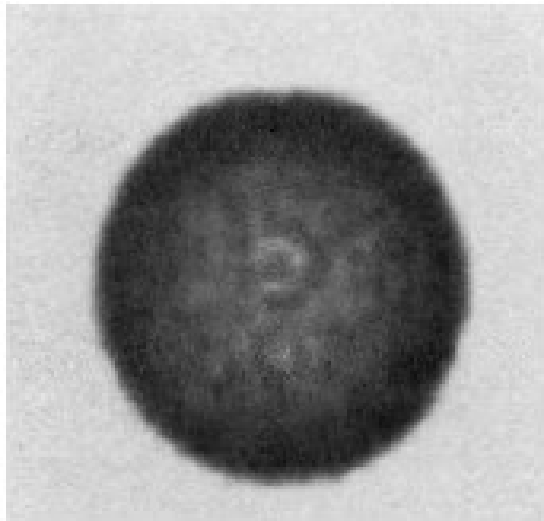
| without correction | μ optimum | μ too large |
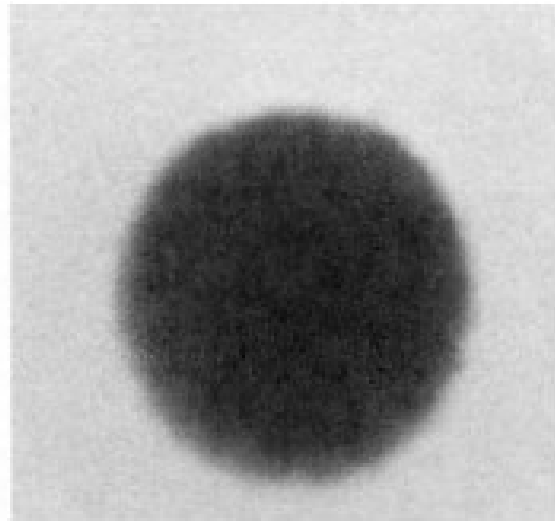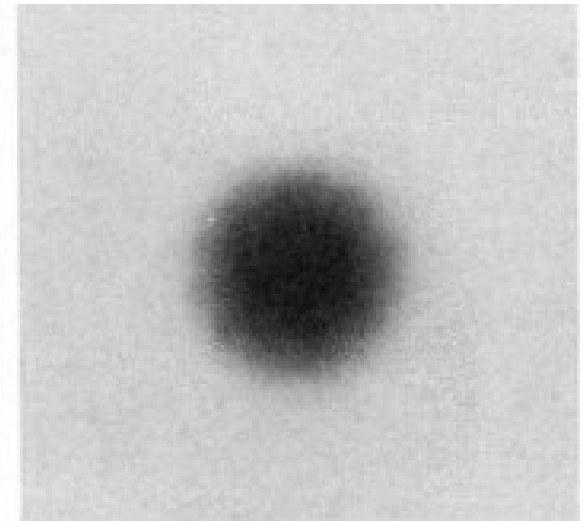
Single Photon Emission Computed Tomography (SPECT)

fields of application

- comparable to planar scintigraphy

- SPECT advantageous, if 3D activity distribution of interest

- cardiology
  vitality testing of cardiac muscle
  perfusion of myocardium (^{99}Tc or ^{201}Tl)
  balloon dilatation or bypass surgery

- neurology
  Alzheimer's disease, brain death

- epileptology
  localization of epileptic focus

Single Photon Emission Computed Tomography (SPECT)
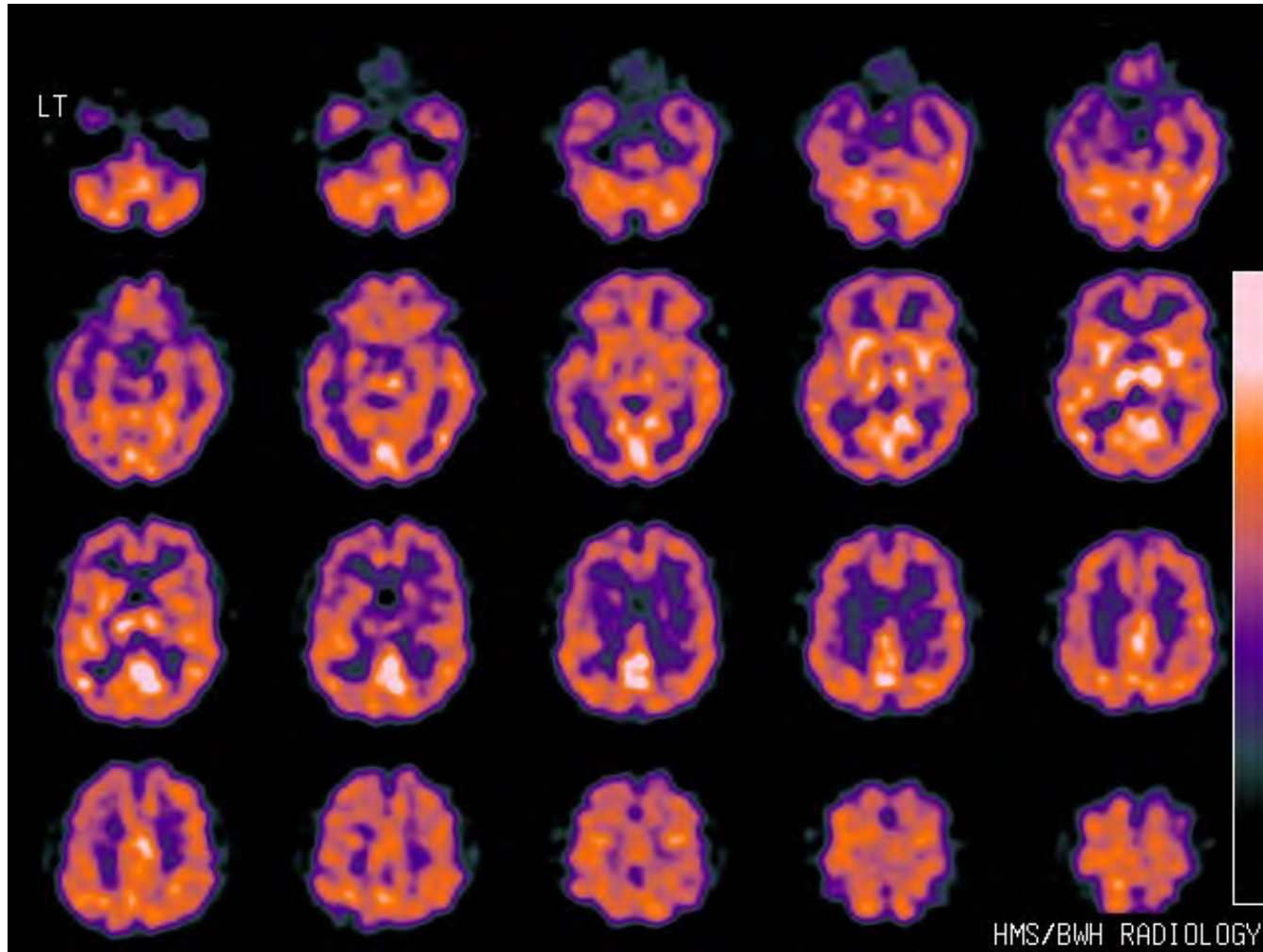
^{99m}Tc-HMPAO
(hexamethylpropylene-amine-oxime)

normal finding
adult male

Single Photon Emission Computed Tomography (SPECT)
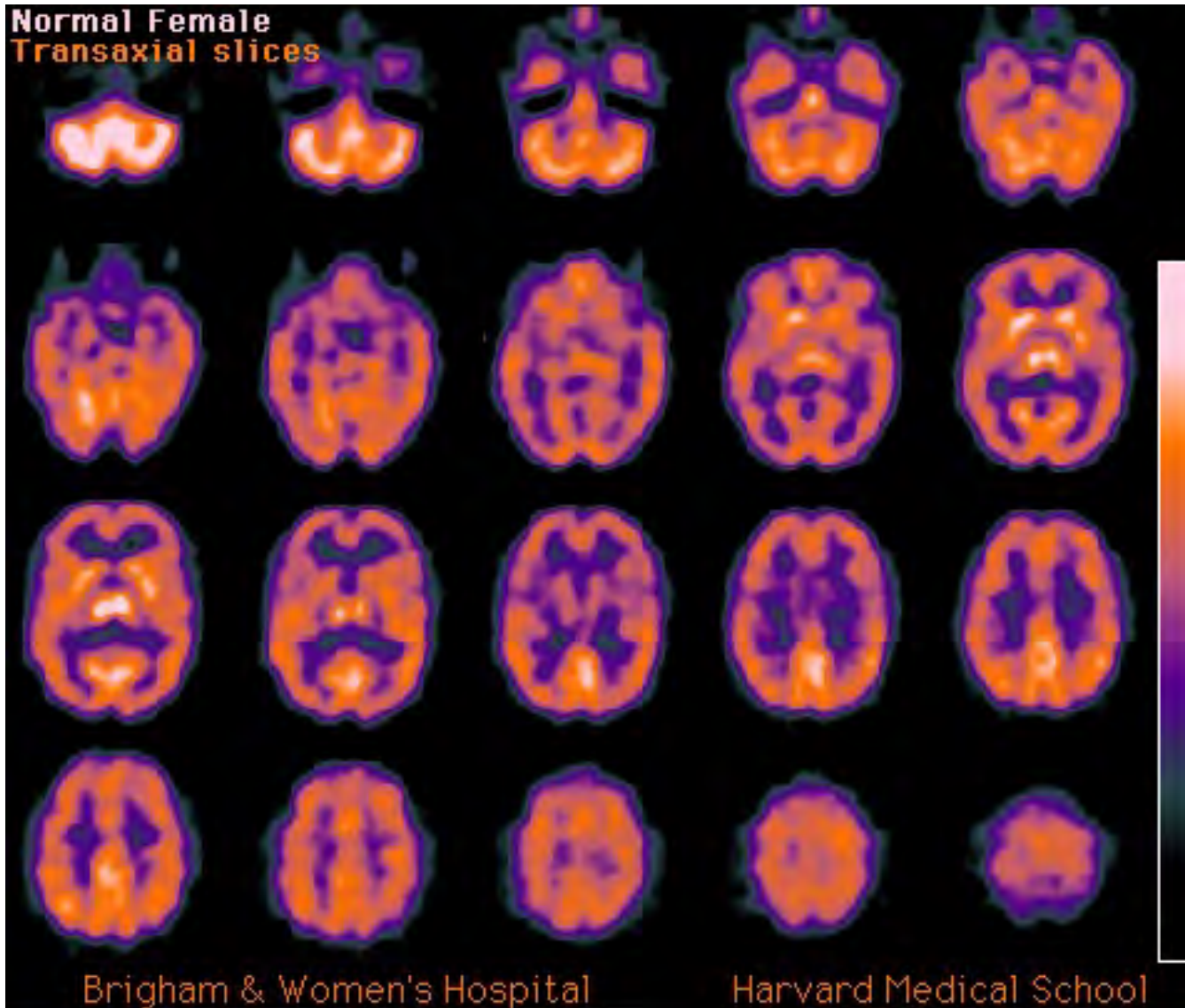
^{99m}Tc-HMPAO
(hexamethylpropylene-amine-oxime)

normal finding
adult female

Single Photon Emission Computed Tomography (SPECT)
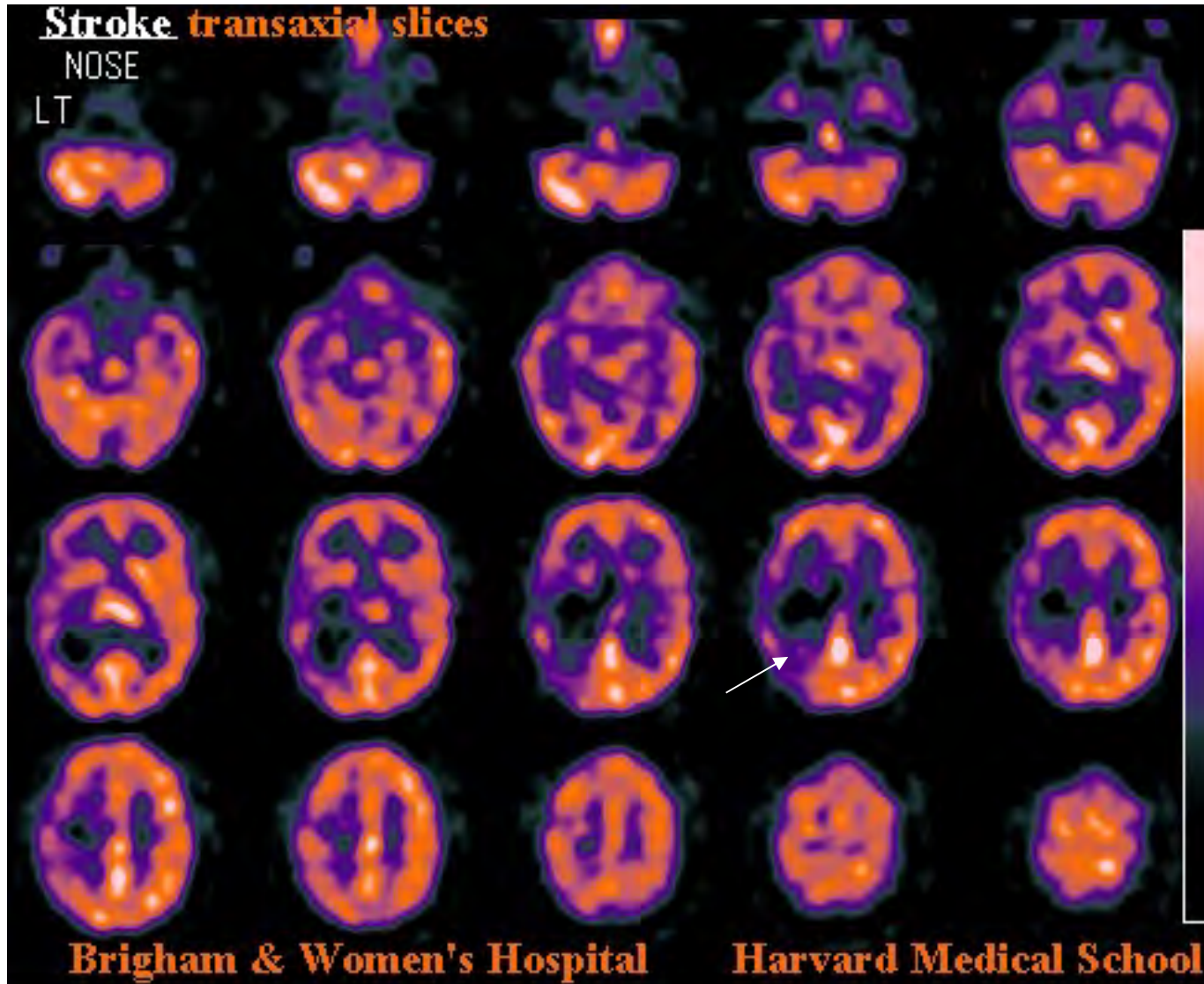
^{99m}Tc-HMPAO
(hexamethylpropylene-amine-oxime)

stroke

Single Photon Emission Computed Tomography (SPECT)
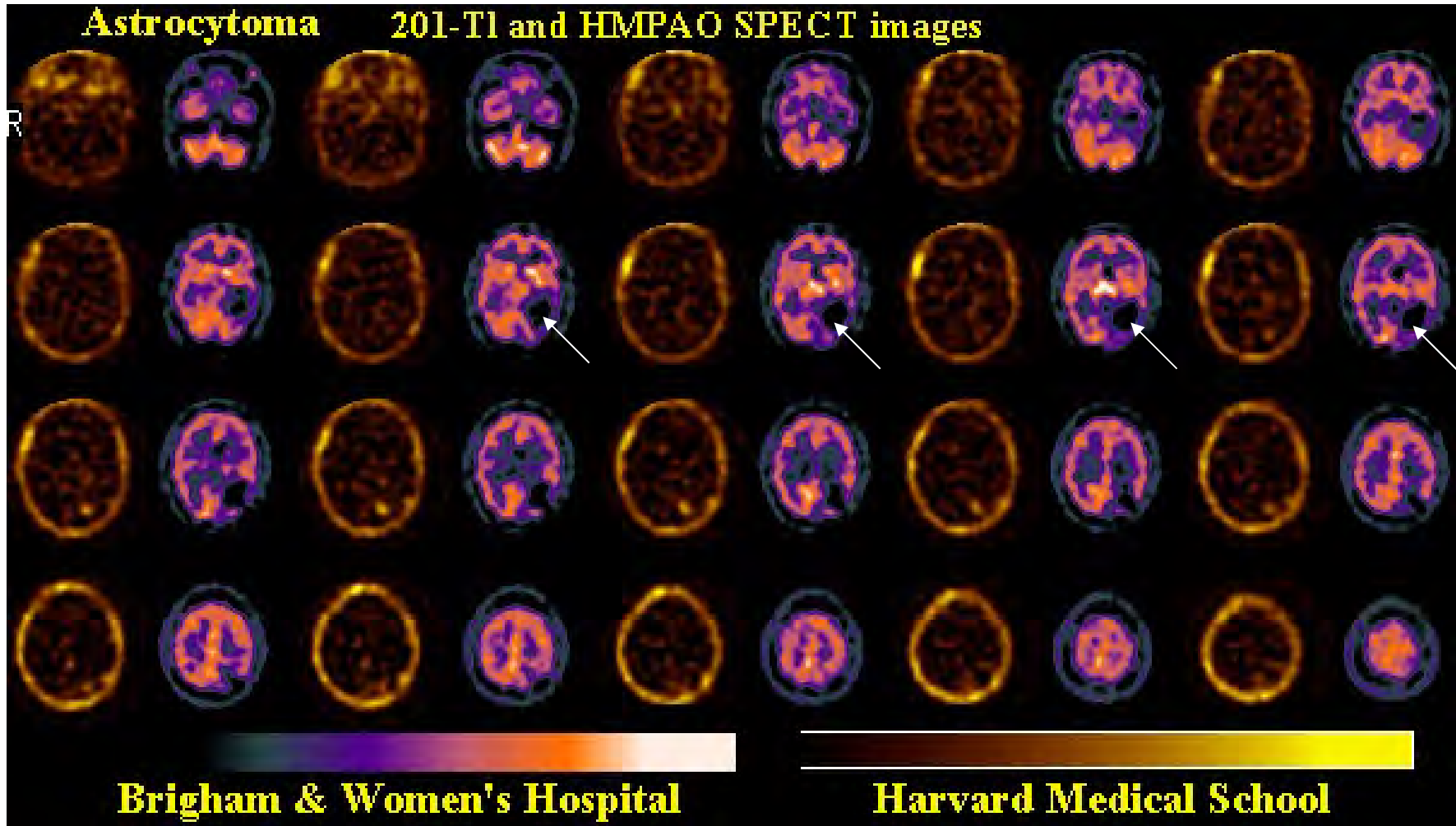
99mTc-HMPAO
(hexamethylpropylene-amine-oxime)

astrocytoma

Single Photon Emission Computed Tomography (SPECT)
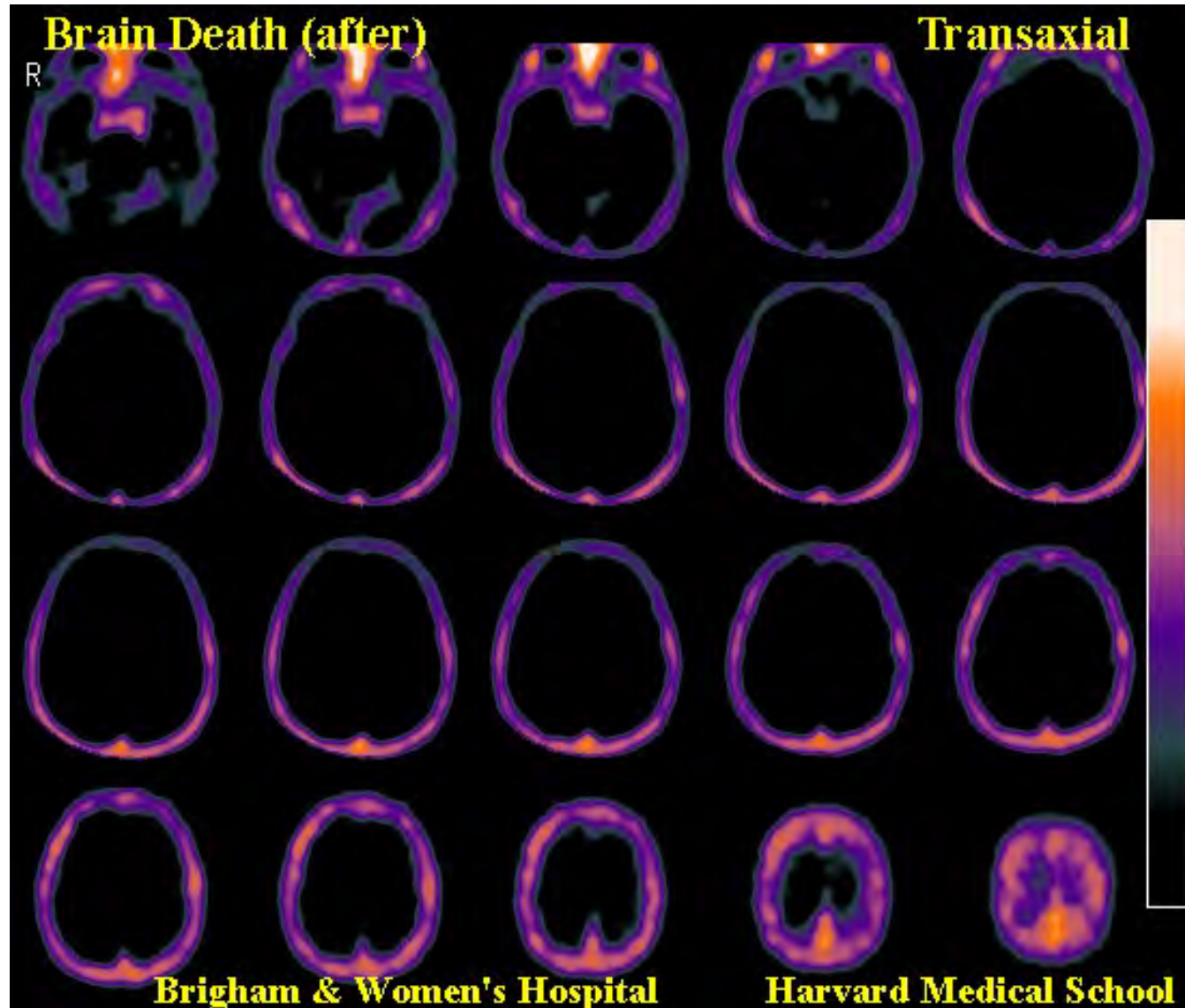
^{99m}Tc-HMPAO
(hexamethylpropylene-amine-oxime)

brain death

Single Photon Emission Computed Tomography (SPECT)
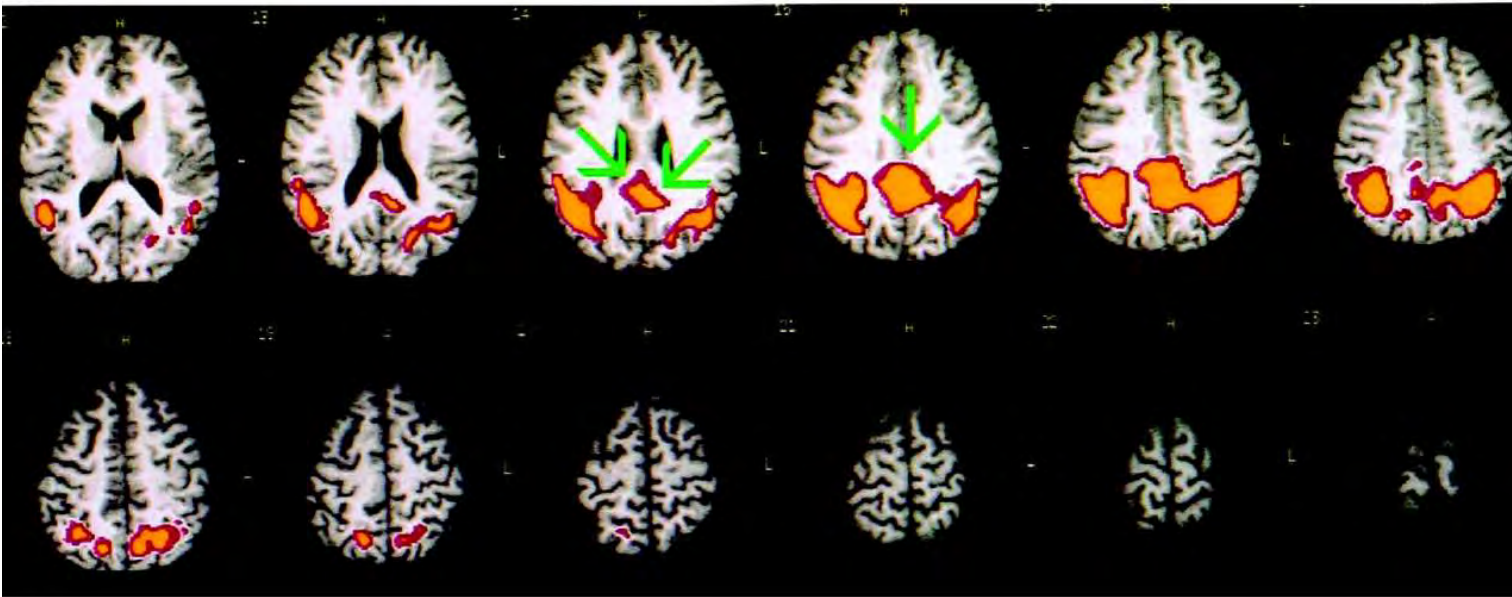
diminished regional blood flow in posterior cingulate gyrus in patient with M. Alzheimer

Tracer:
^{99m}Tc-hexamethyl-propyleneamine-oxime

(Bonte et al. J Nucl Med 2004)

early diagnosis of M. Alzheimer ?
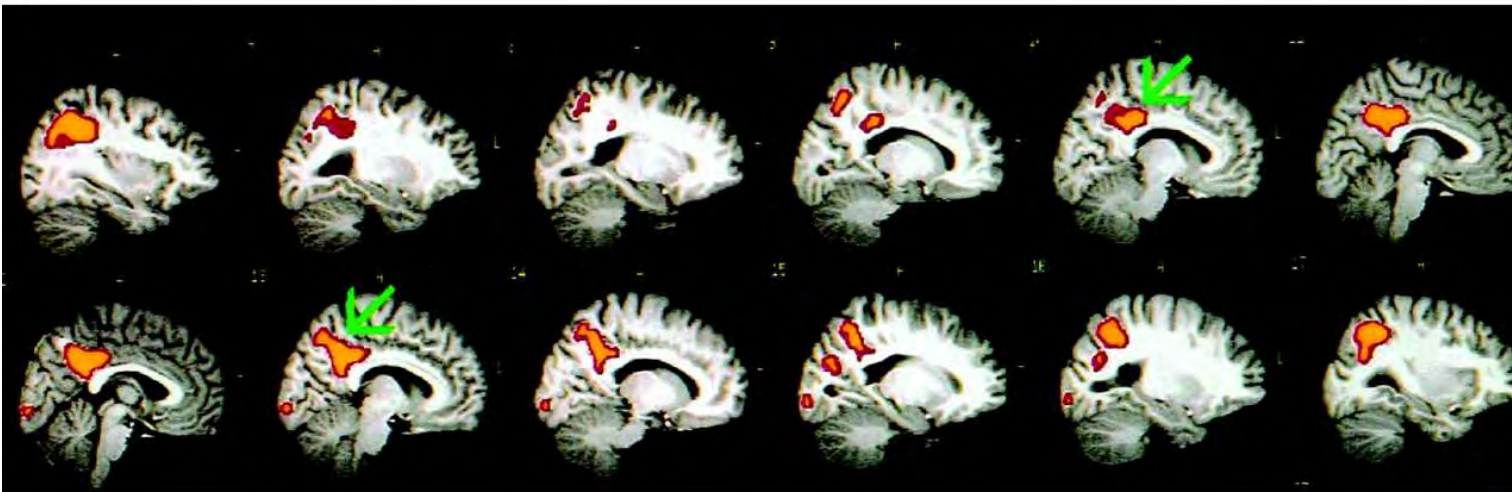
Single Photon Emission Computed Tomography (SPECT)
application example: heart
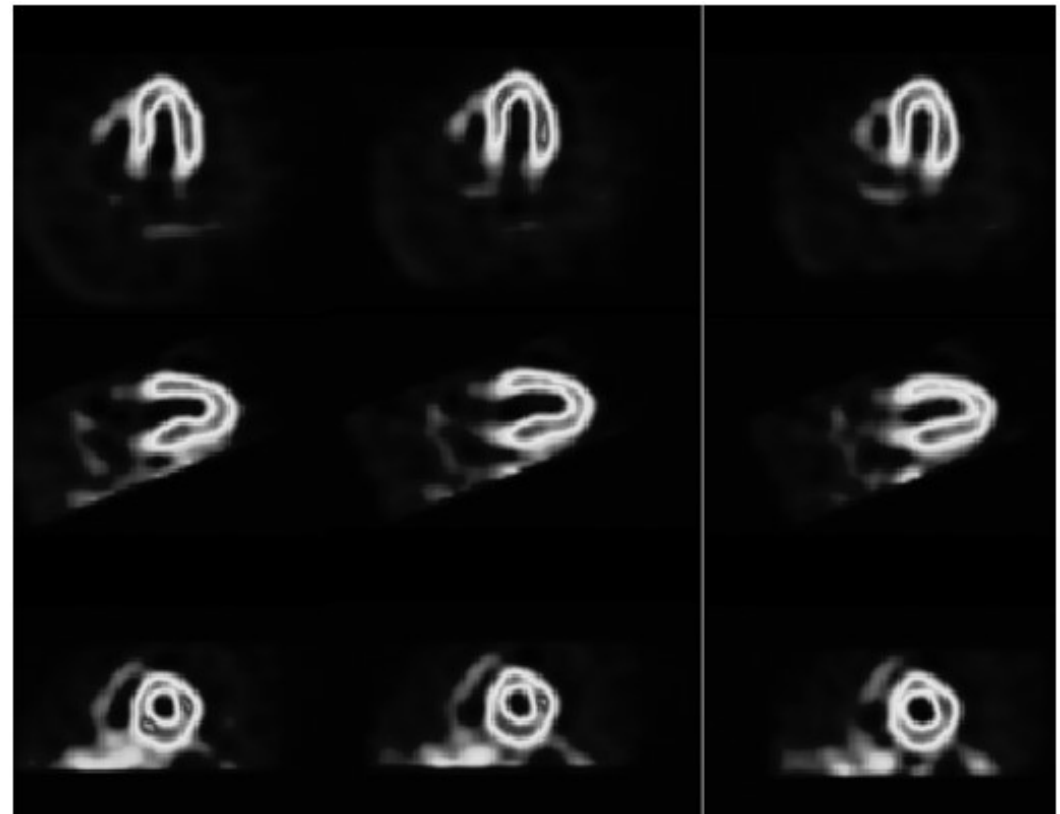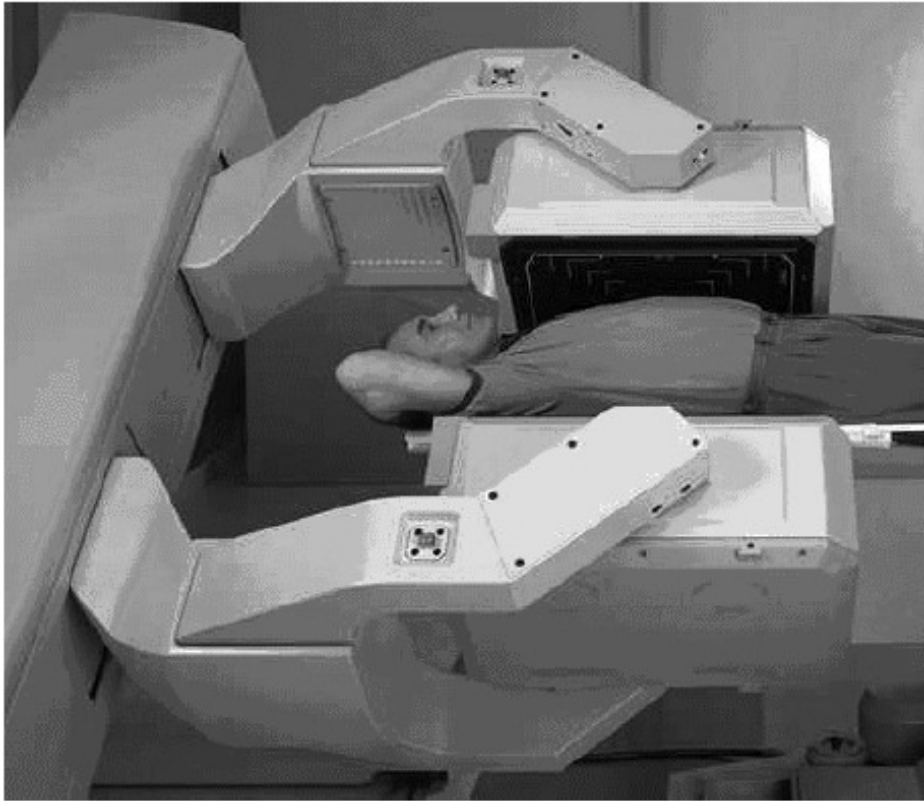
Single Photon Emission Computed Tomography (SPECT)
application example: whole-body scan

Single Photon Emission Computed Tomography (SPECT)
application example: neurology
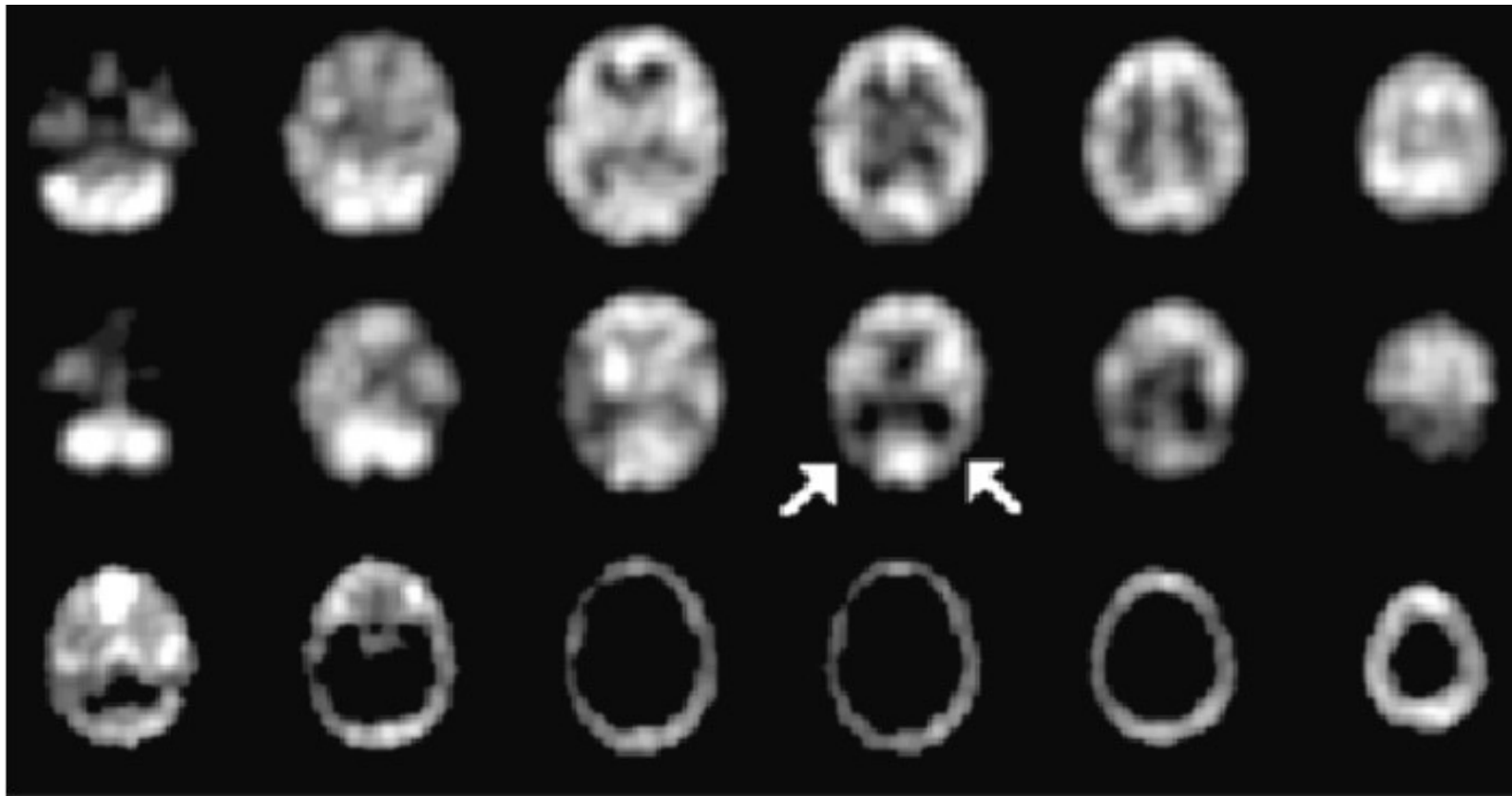
normal finding

M. Alzheimer:
parieto-occipital
perfusion decline

abolished
perfusion
brain death

Single Photon Emission Computed Tomography (SPECT)
SISCOM: Subtraction SPECT co-registered to MRI

^{99m}Tc-HMPAO
(hexamethylpropylene-amine-oxime)

^{99m}Tc-ECD
(ethyl cysteinate diethylester)
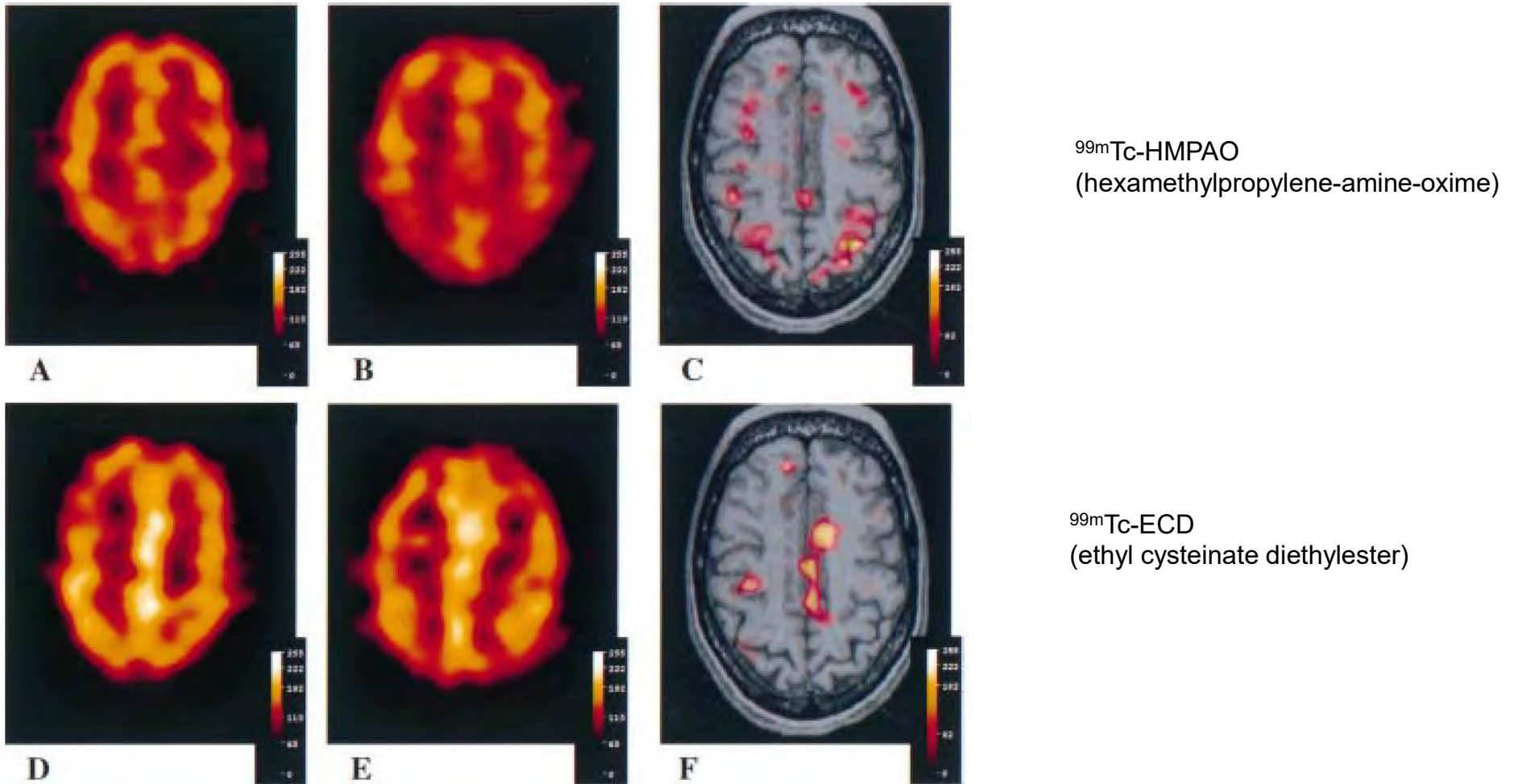
Figure 1   SPECT images of a patient with intractable non-lesional extratemporal seizures. The initial SPECT studies were done with ^{99m}Tc-HMPAO: ((A) postictal image, (B) interictal image, and (C) SISCOM). The injection was postictal, resulting in a non-localising SISCOM image. A repeat ictal study and an interictal study were performed using ^{99m}Tc-ECD ((D) ictal image, (E) interictal image, and (F) SISCOM). The ictal injection of ^{99m}Tc-ECD resulted in a localised SISCOM abnormality in the left mesial frontal lobe, which was concordant with seizure semiology and with ictal EEG localisation.

O'Brien et al.,
J Neurol Neurosurg Psychiatry 1999;66:331–339

Single Photon Emission Computed Tomography (SPECT)
application example: epilepsy
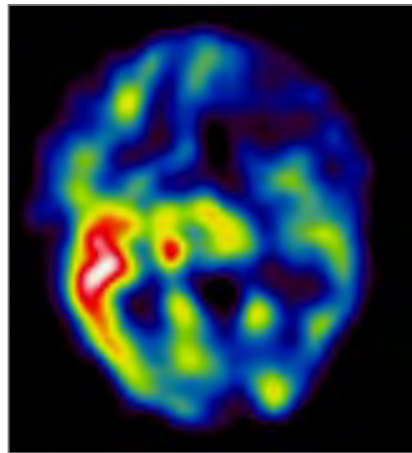
ictal SPECT
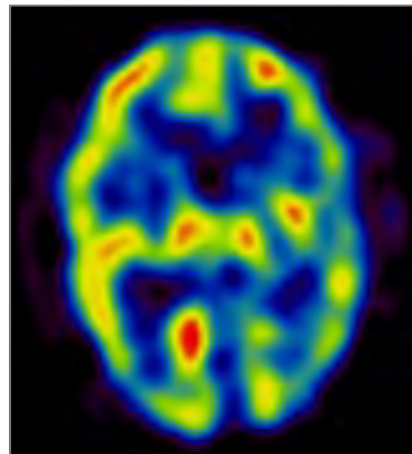
interictal SPECT

Positron Emission Tomography (PET)

Positron Emission Tomography (PET)

- radioactive labelling of biological substance
  with **positron emitter** (^{11}C, ^{13}N, ^{15}O, ^{18}F, ^{30}P)

  e.g. ^{15}O- water, ^{18}F- de-oxyglucose

- register γ-particles emitted from the body

- reconstruction of non-overlapping tomographic images

- quantitative assessment of activity concentration

- bio-kinetic models to assess transport- and metabolic rates

Positron Emission Tomography (PET)

1953: first clinical PET (Brownell (left) and Aronow)
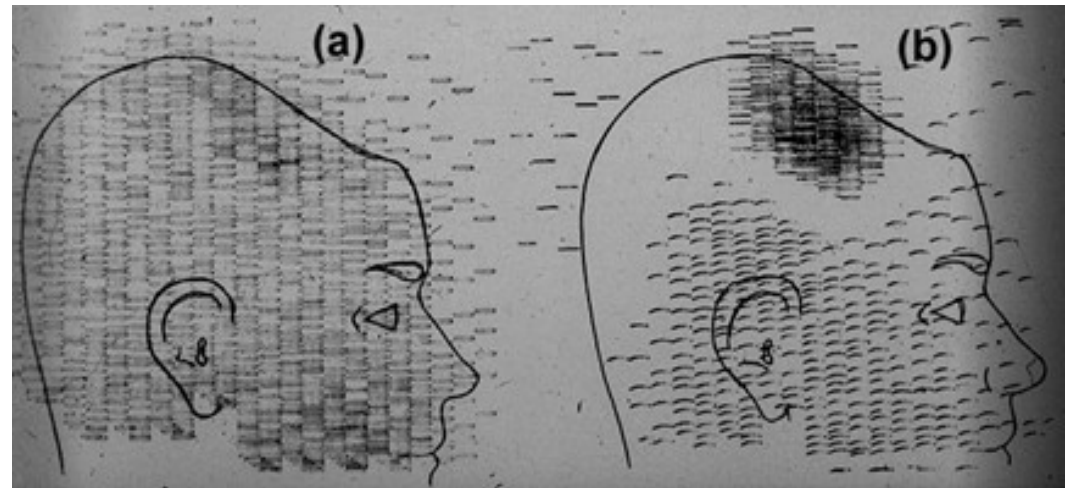
Aus: BROWNELL, G.L., W.H. SWEET, Localization of brain tumors with positron emitters, *Nucleonics 1953*, 11:40-45.

Positron Emission Tomography (PET)
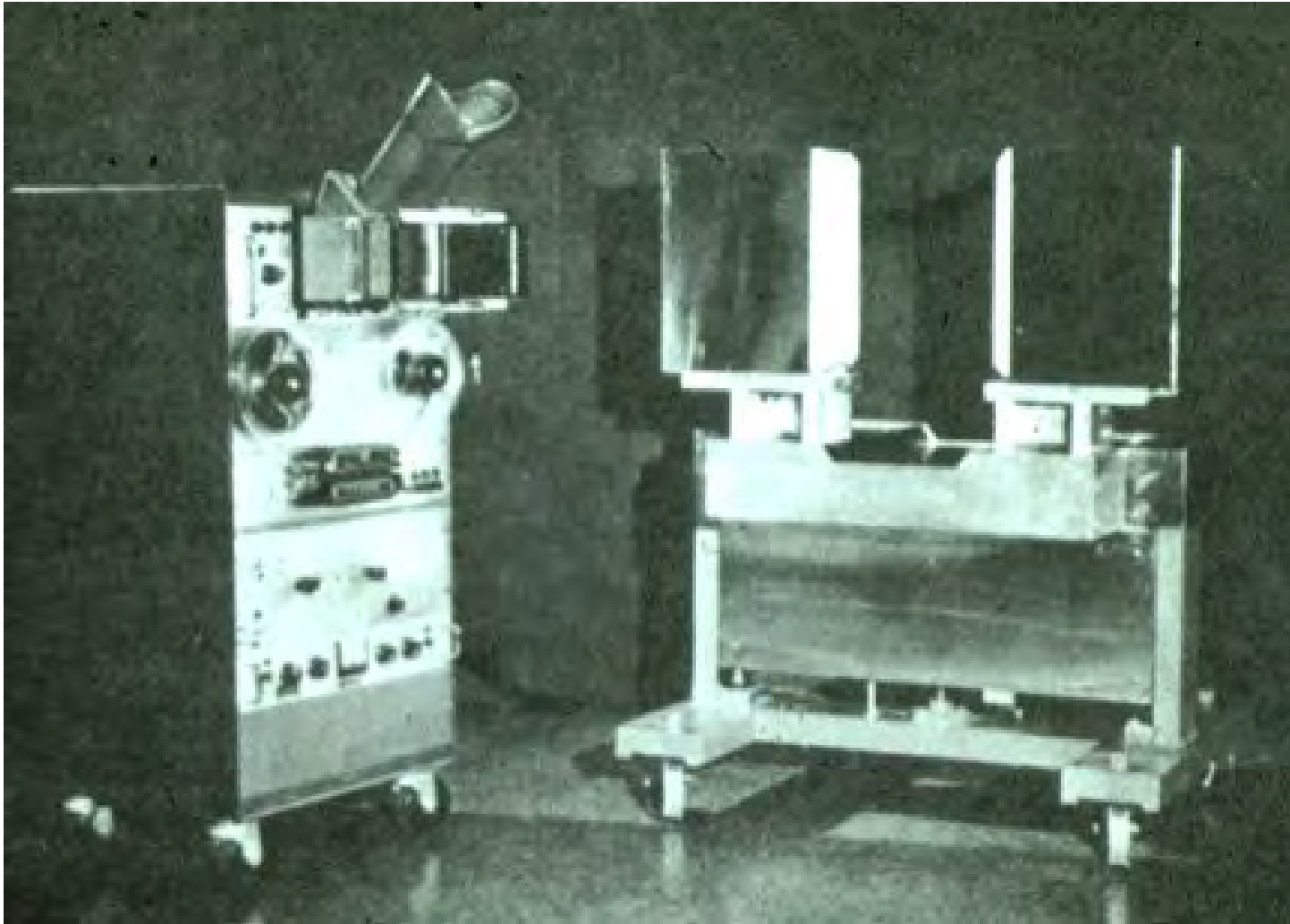
1962: Hybrid-PET (9 detectors in 2 rows, 3 detectors from one side in coincidence with one detector from opposite side)

Positron Emission Tomography (PET)

1968-1971: PC-I, first tomographic system
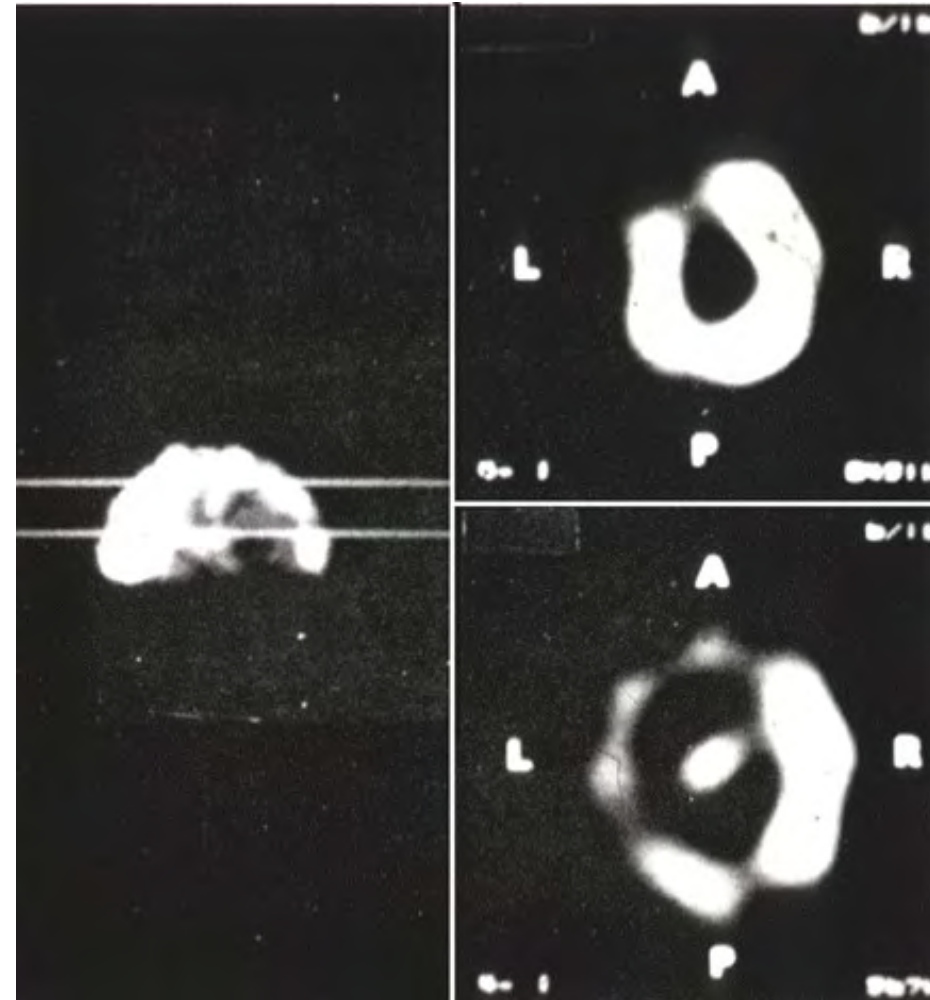
Brain study using PC-I and ^{68}Ga. Two lines on 2D-image show the levels of tomographic slices.
A tumor is clearly observable in the lower transverse slice.
Original images were presented by David Chesler at the
Meeting on Tomographic Imaging in Nuclear Medicine, September 15-16, 1972

89

Positron Emission Tomography (PET)

1971-1976: PC-II (Physics Research Lab, U Washington)

Positron Emission Tomography (PET)
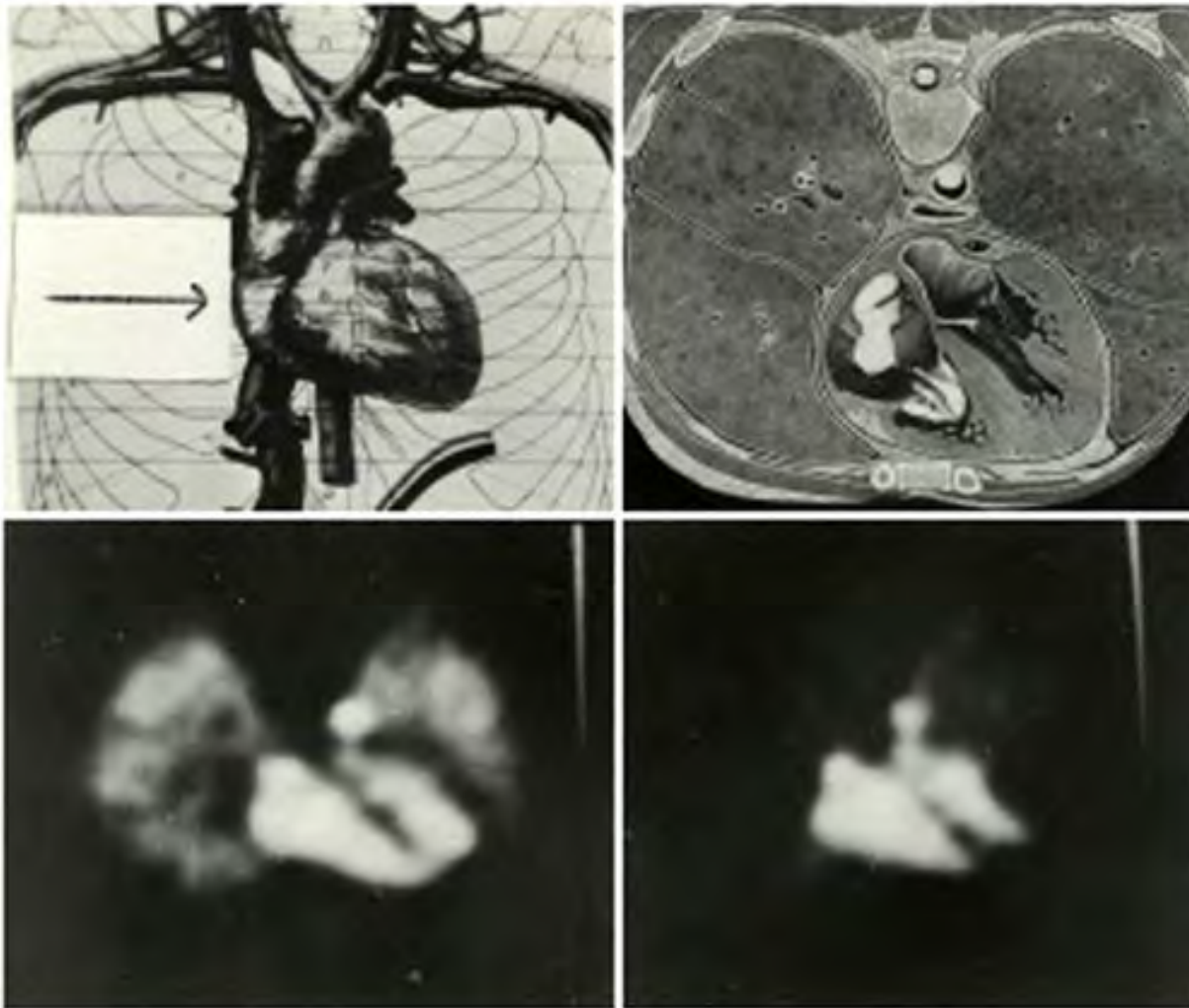
Top level: A-P anatomical illustration of heart and major vessels (left). Anatomical transverse section at the level shown in left.
Lower level: Transverse section image of blood pool using inhalation of ^{60}Co corresponding the image on top right, uncorrected for absorption (left).
Same as left with absorption correction (right).

Positron Emission Tomography (PET)

PC-II

Brain study using ^{68}Ga-ATP. Lower panel shows 4 tomographic coronal slices and the arrow points the tumor.
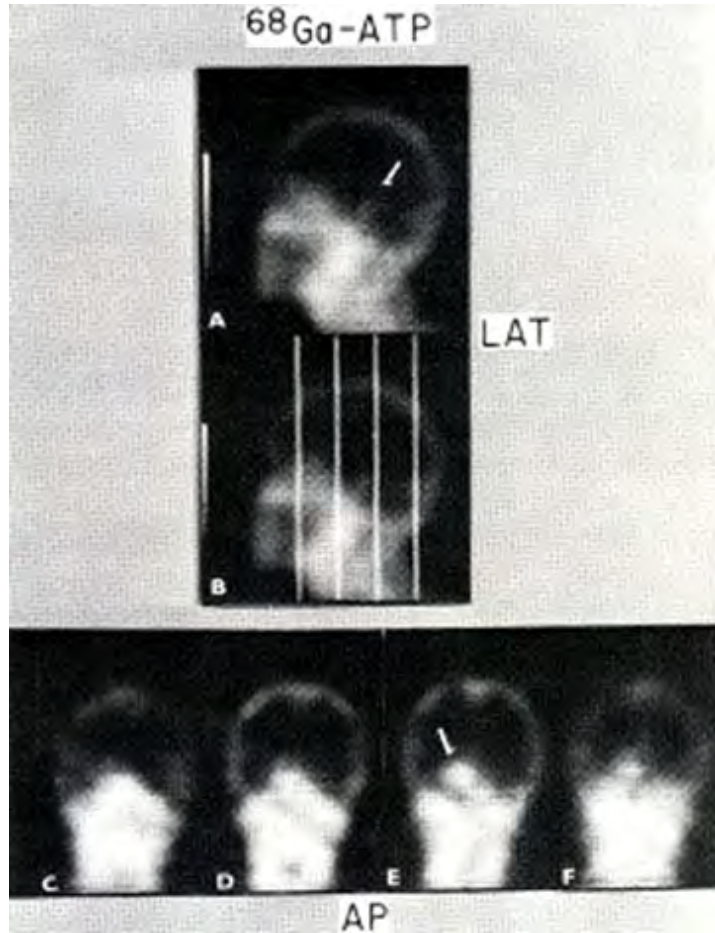
Brain study of the normal control patient using ^{18}F 2-fluoro-2-deoxy-D-glucose and PC-II.

Positron Emission Tomography (PET)

PCR-I und II: circular
and cylindrical PET
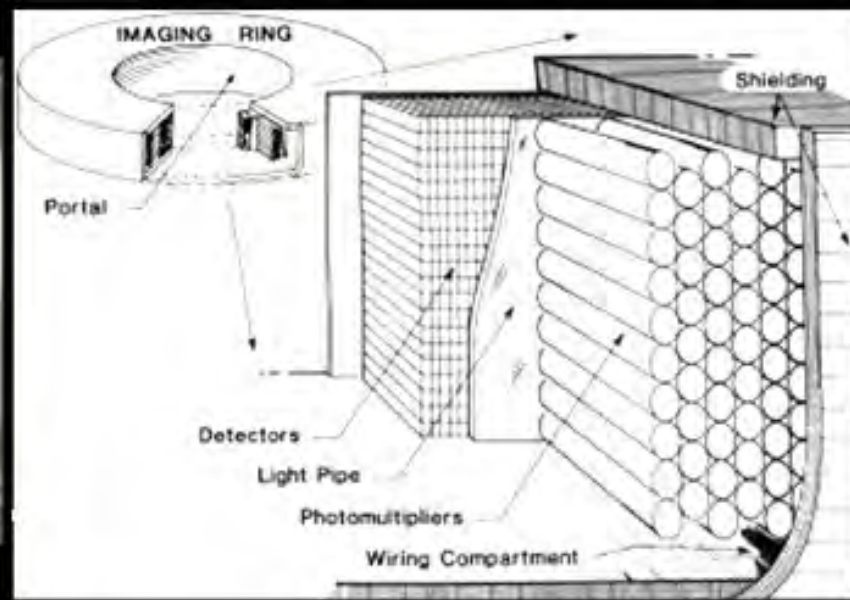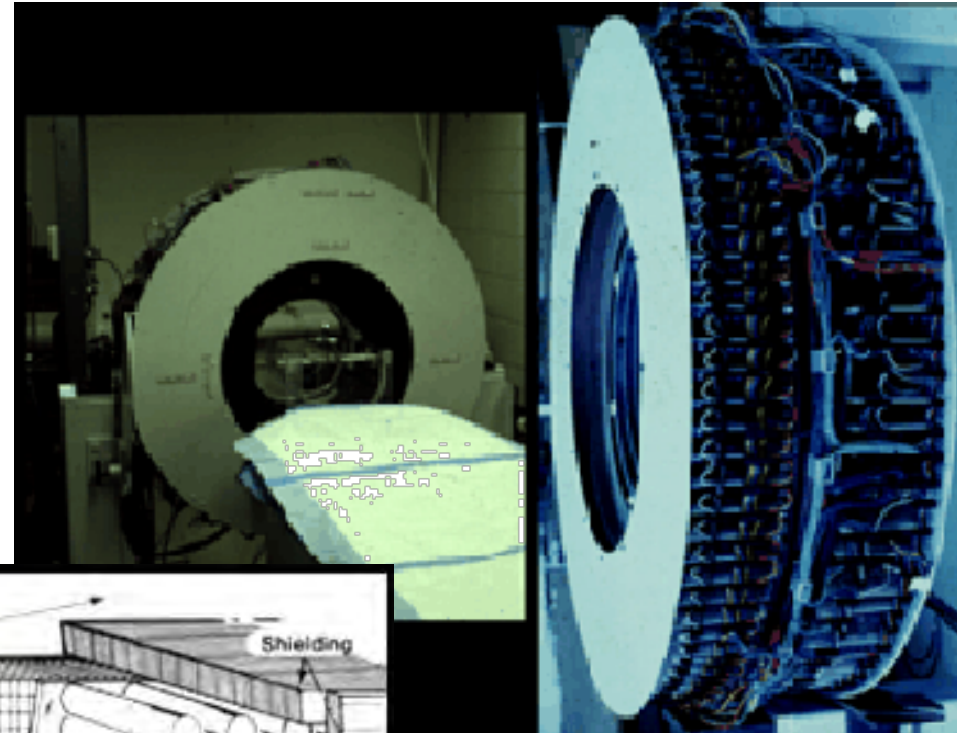
Positron Emission Tomography (PET)
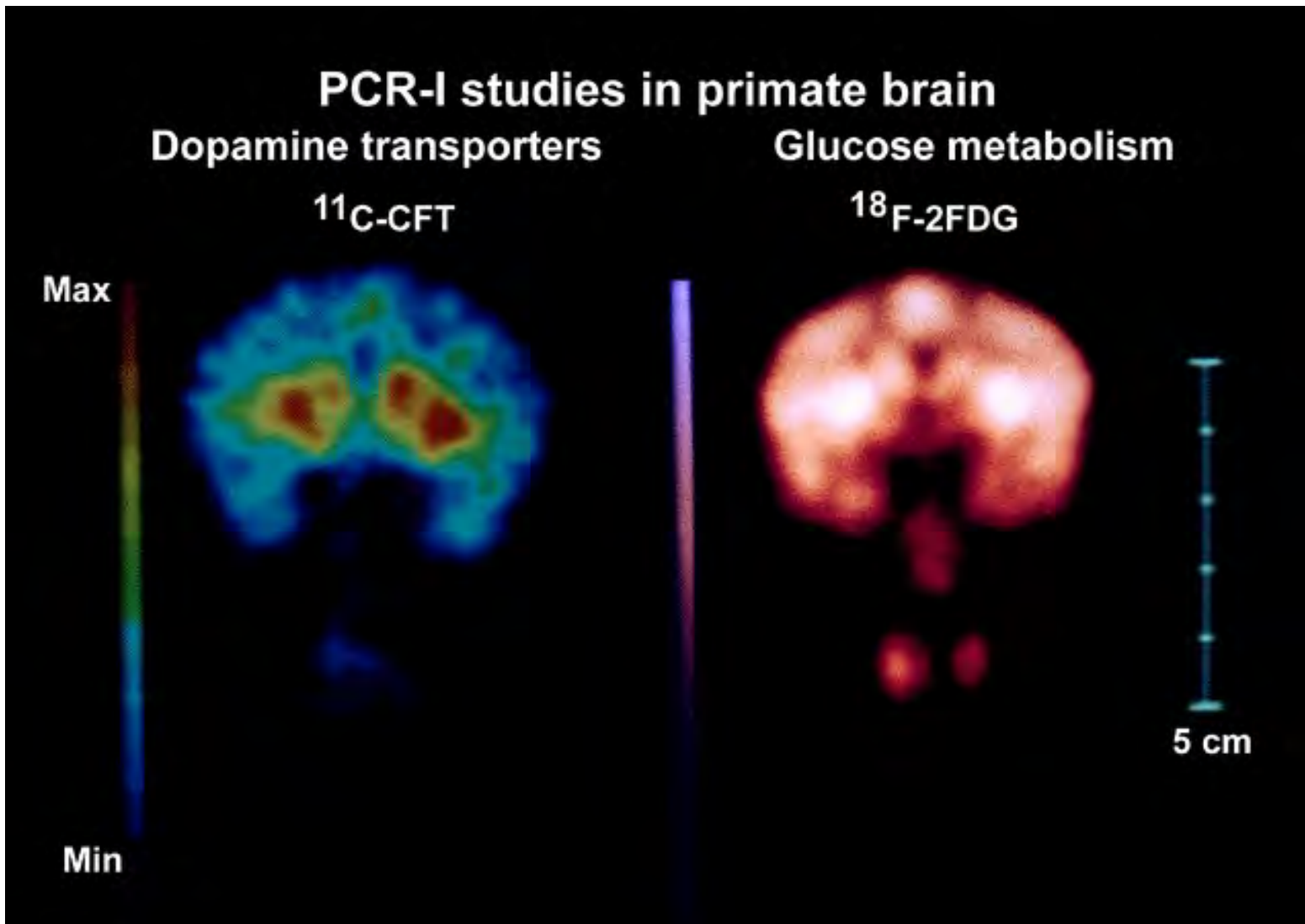
PCR-I studies in primate brain

Dopamine transporters — ^{11}C-CFT

Glucose metabolism — ^{18}F-2FDG

Positron Emission Tomography (PET)

Physics Research Laboratory, Massachusetts General Hospital
Division of Radiological Sciences, Massachusetts Institute of Technology
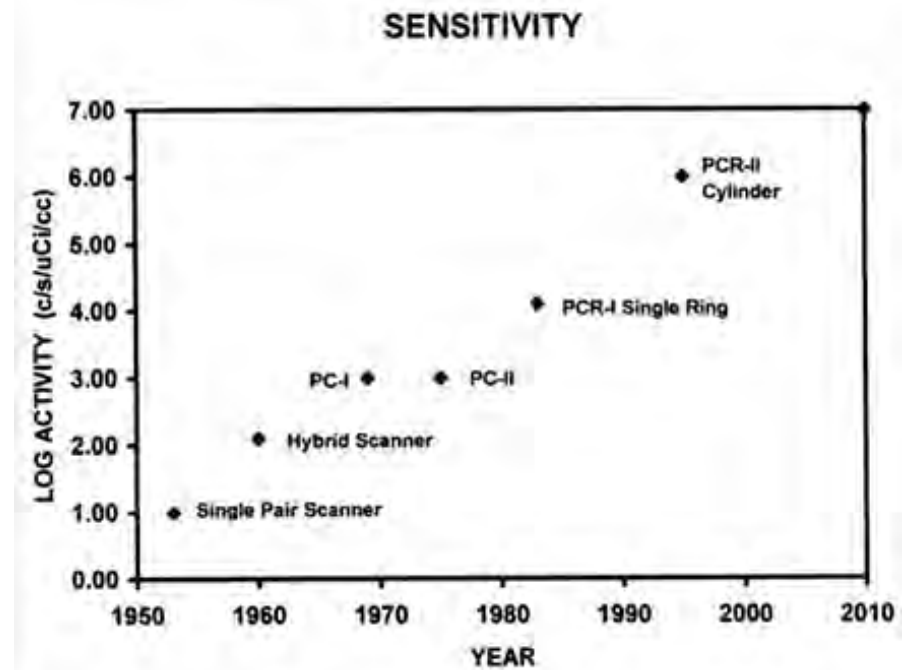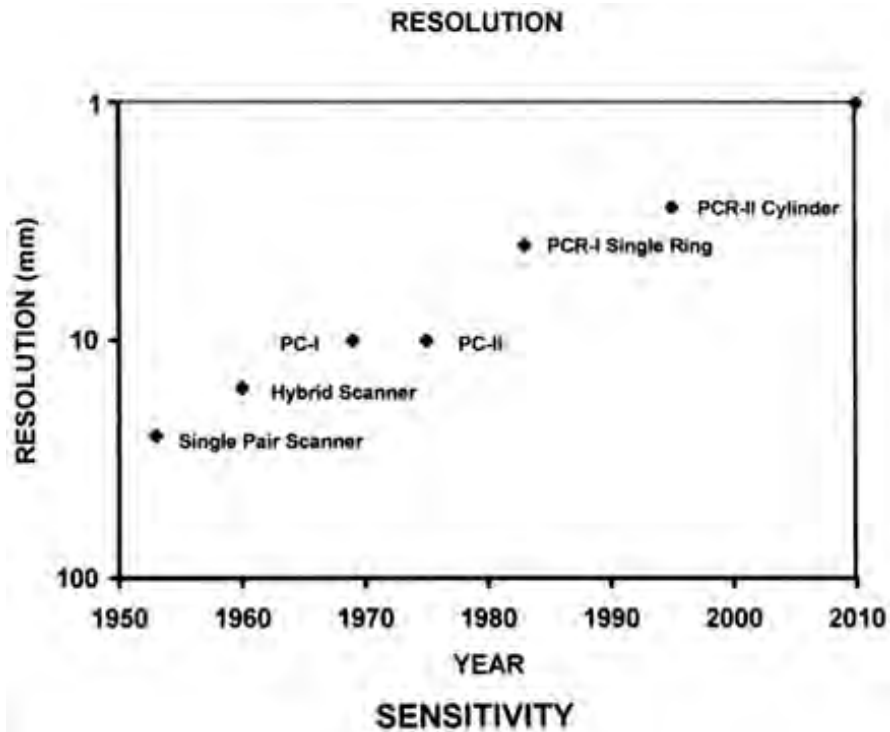
Positron Emission Tomography (PET)

physical fundamentals

positron emission (β^+ decay):
proton-to-neutron conversion with emission of positron and (electron) neutrino

$$p \rightarrow n + e^+ + \nu_{e^-} \qquad (e.g.: {}^{11}_{6}C \rightarrow {}^{11}_{5}B + e^+ + \nu_{e^-})$$
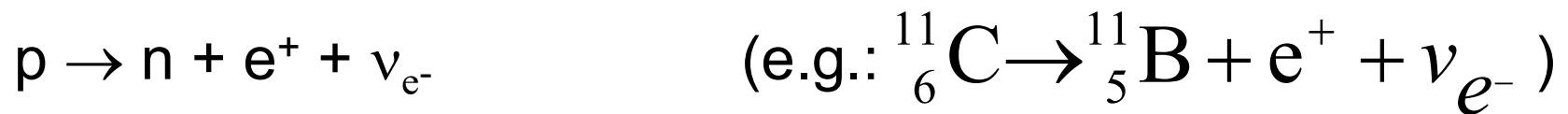
positron/electron annihilation:
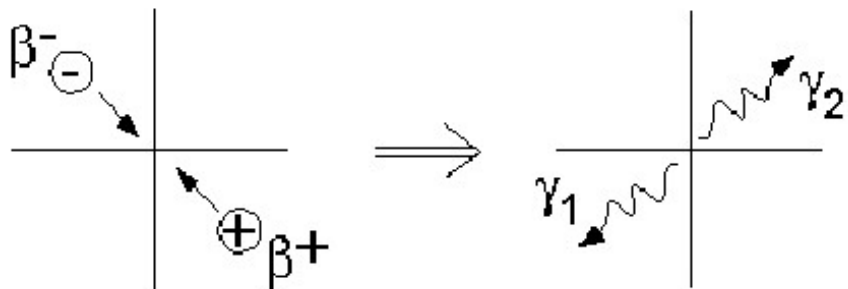
E_γ = 511 keV   (conservation of energy)
α = 180°   (conservation of impulse)
$\Delta\alpha$ = ±0.3°   (stat. distribution of rest impulse)

Positron Emission Tomography (PET)

	half-life [min]	E_{max} [MeV]	R_{max} [mm]	R_{avg} [mm] (in H_2O)
^{11}C	20.4	0.97	5.0	0.3
^{13}N	9.9	1.19	5.4	1.4
^{15}O	2.1	1.72	8.2	1.5
^{18}F	109.7	0.64	2.4	0.2

↑

**lower bound of spatial resolution of PET depends on
mean free path of e^+ to place of annihilation**

Positron Emission Tomography (PET)

electronic collimation   **coincidence detection**

511 keV

e⁺

γ

511 keV

e⁻

line of response (LOR)

γ

**coincidence
(10 - 20 ns)**
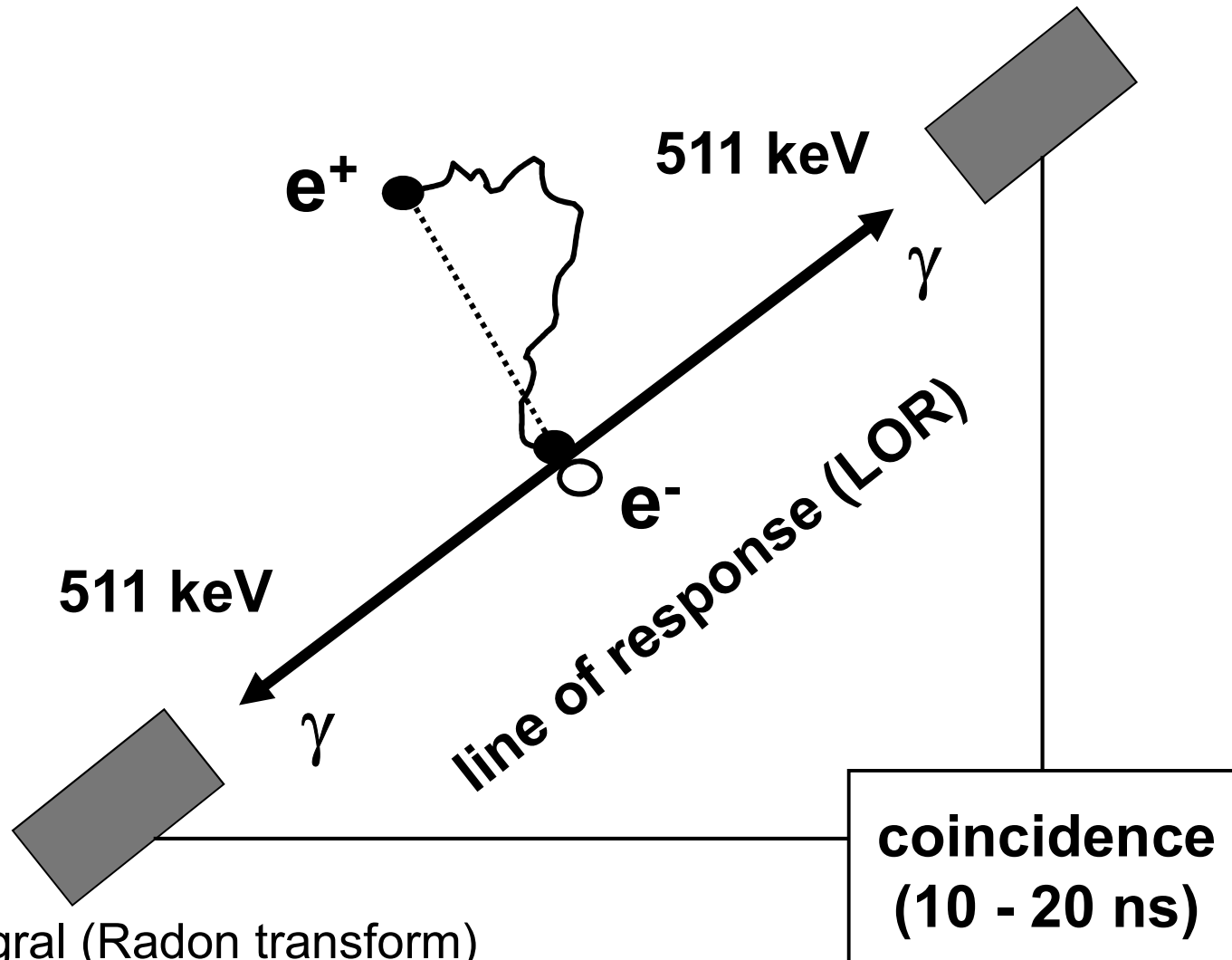
LOR = line integral (Radon transform)

Positron Emission Tomography (PET)

coincidence detection

$2\tau \approx 10$ ns
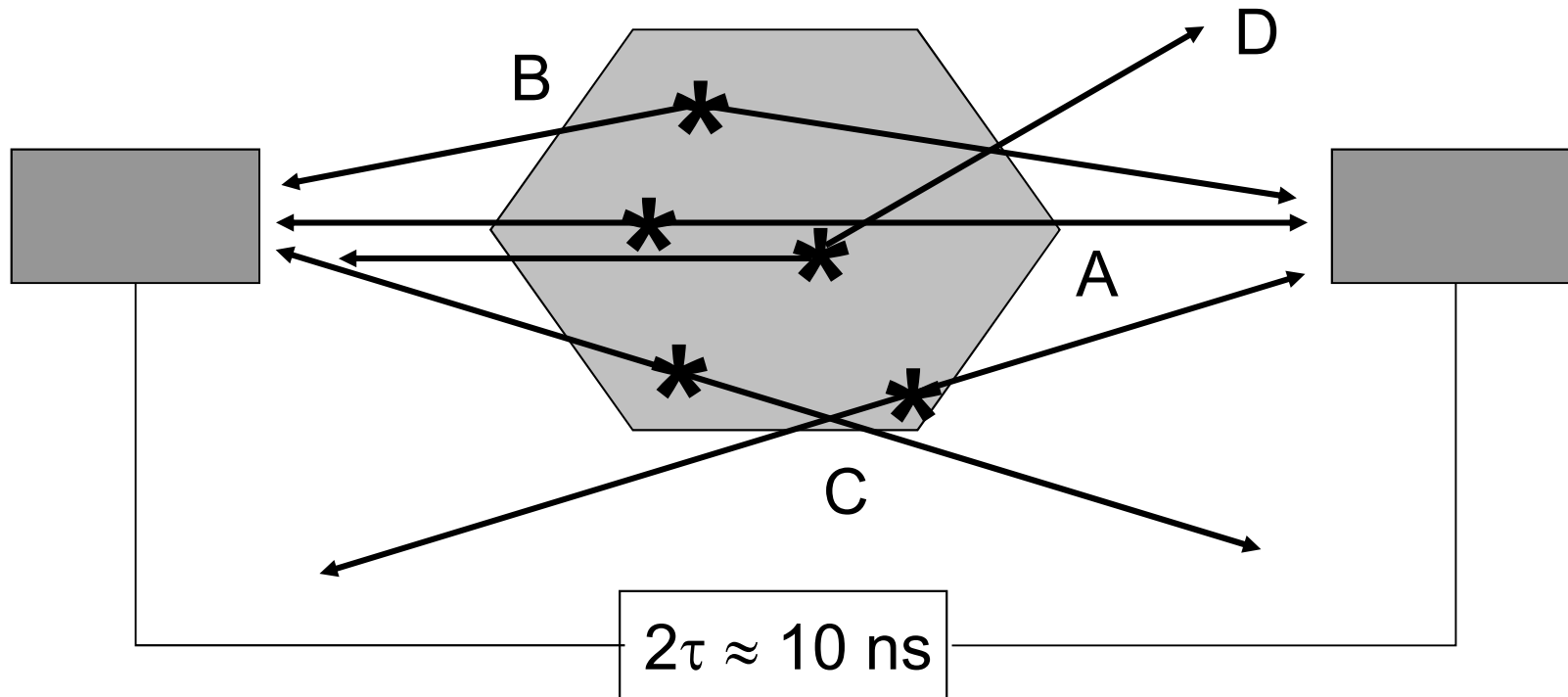
true (A), scattered (B), random coincidences (C); scattering (D)

Positron Emission Tomography (PET)

coincidence detection
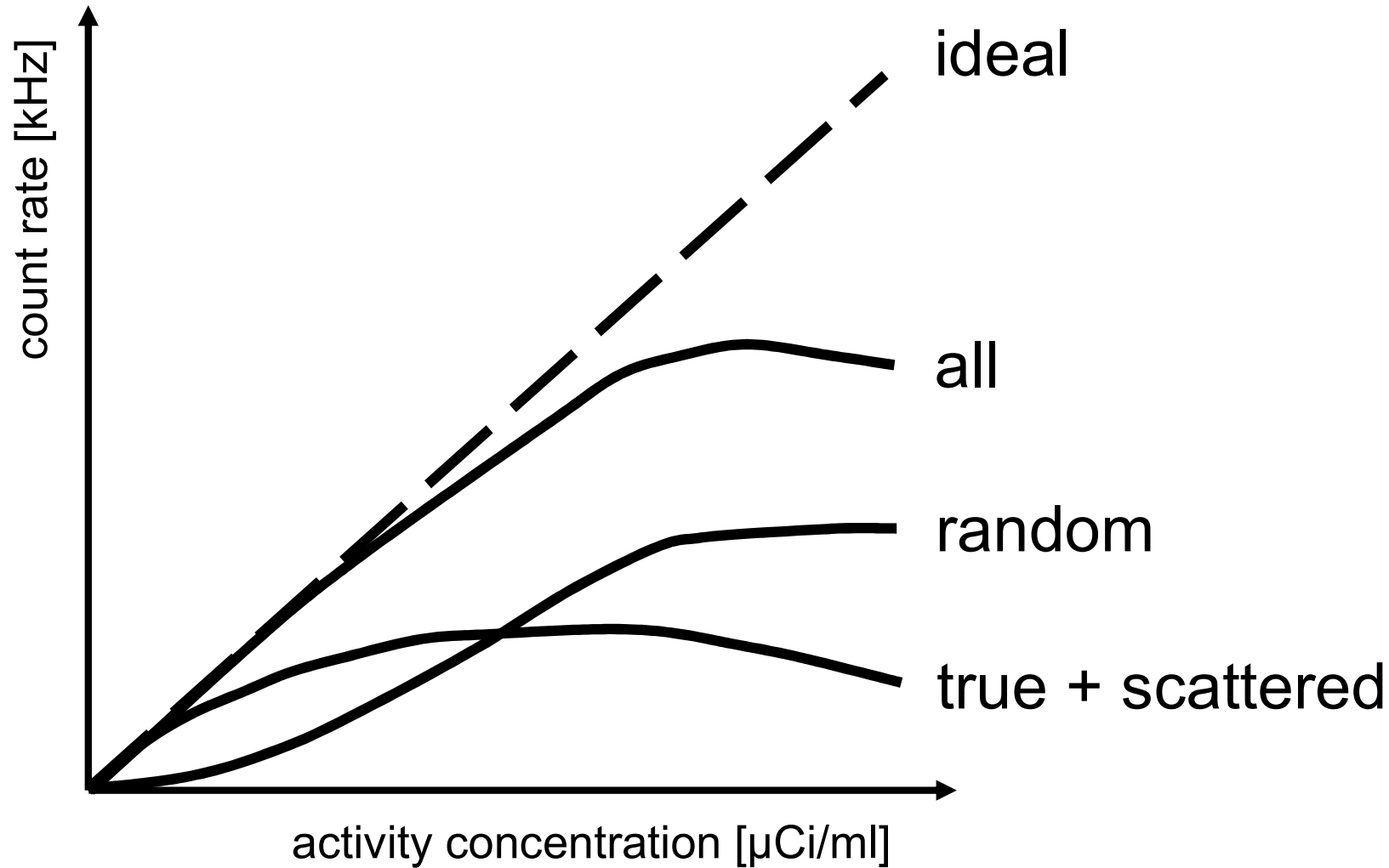
Positron Emission Tomography (PET)

coincidence detection

use of collinearity (electronic collimation) avoids necessity of using lead collimators

results in higher sensitivity:
> 1000 when compared to SPECT
(reduces necessary amount of isotopes)

intrinsic resolution of pair of coincidence detectors:
- depends on size of detectors
- corresponds to half the width of a detector

Positron Emission Tomography (PET)

scintillation crystals and detectors

given: high-energetic radiation (511 keV)

requirements:

- high density and atomic number
(large cross section for photo absorption)

- high luminous efficiency
(efficient segregation of background events)

- high spatial resolution

- short decay time of scintillation light
(temporal resolution, count rate (max. 10^6 events/sec)
narrow coincidence window)

Positron Emission Tomography (PET)

scintillation crystals

first PET systems:

thallium-doped sodium-iodide (NaJ:Tl)

high luminous efficiency, wave length: 410 nm; scint.-decay time: 230 ns; attenuation length (511 keV): 30 mm, leads to diminished sensitivity for γ-quanta (thicker crystals lead to diminished spatial resolution)

most often used:

bismuth-germanate ($Bi_4Ge_3O_{12}$=BGO)

high sensitivity due to high atomic number; but: luminous efficiency only 15 % of NaJ:Tl; wave length: 480 nm; scint.-decay time: 300 ns; attenuation length (511 keV): 11 mm

since 1992:

cerium-doped lutetium-oxy-orthosilicate (LSO:Ce)

high sensitivity due to high atomic number; luminous efficiency 75 % of NaJ:Tl; wave length: 420 nm; scint.-decay time: 40 ns; attenuation length (511 keV): 12 mm

Positron Emission Tomography (PET) detectors

photomultiplier

BGO crystal
e.g., 64 units on 4 PMT
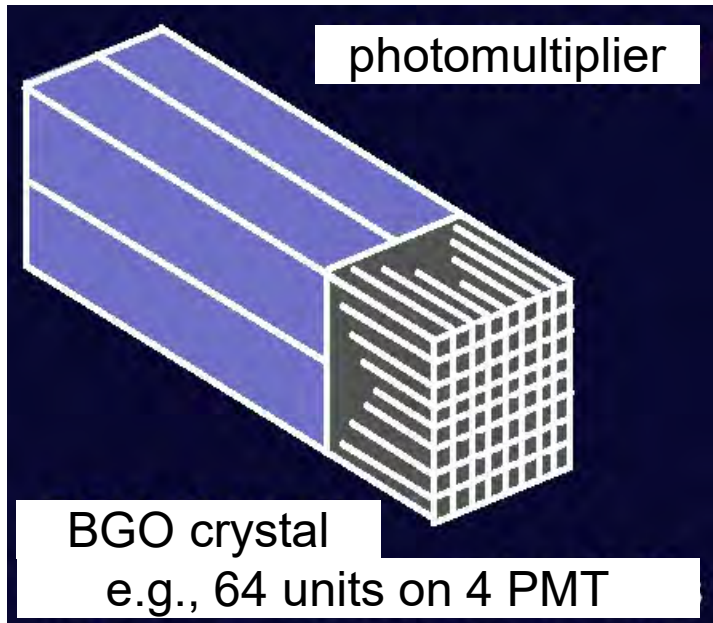
– γ-quant in crystal:
photoelec. effect, Compton scattering

- electron $\rightarrow$ energy deposition $\rightarrow$ scintillation light

- light amplification via photomultiplier tubes (PMT)

- signal (output) ~ light level ~ γ-energy

- cutting a single crystal into smaller detector units (6 mm x 6 mm or 4 mm x 4 mm)
- read-out with 4 PMT
- length of cuts determine distribution of scintillation light onto PMT (weighing principle)
  (allows assignment to detector units)
- advantage: more dense packing than with many small crystals; requires lower number of PMT;
        size of smaller detector units determines spatial resolution

Positron Emission Tomography (PET)

crystal identification (weighing principle; cf. Anger camera)
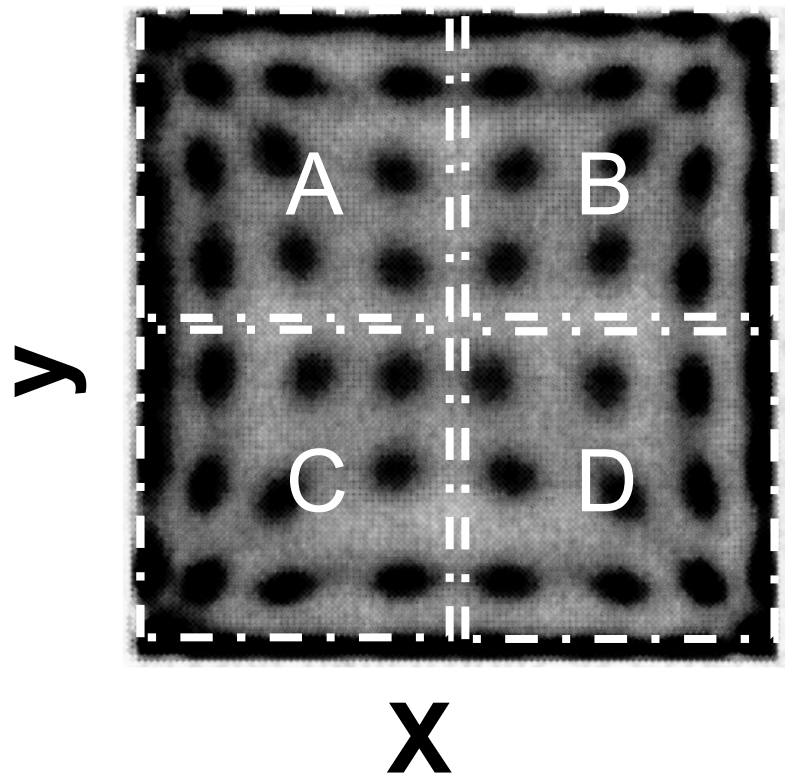
$$X = \frac{(B+D) - (A+C)}{(A+B+C+D)}$$

$$y = \frac{(A+B) - (C+D)}{(A+B+C+D)}$$

Positron Emission Tomography (PET)
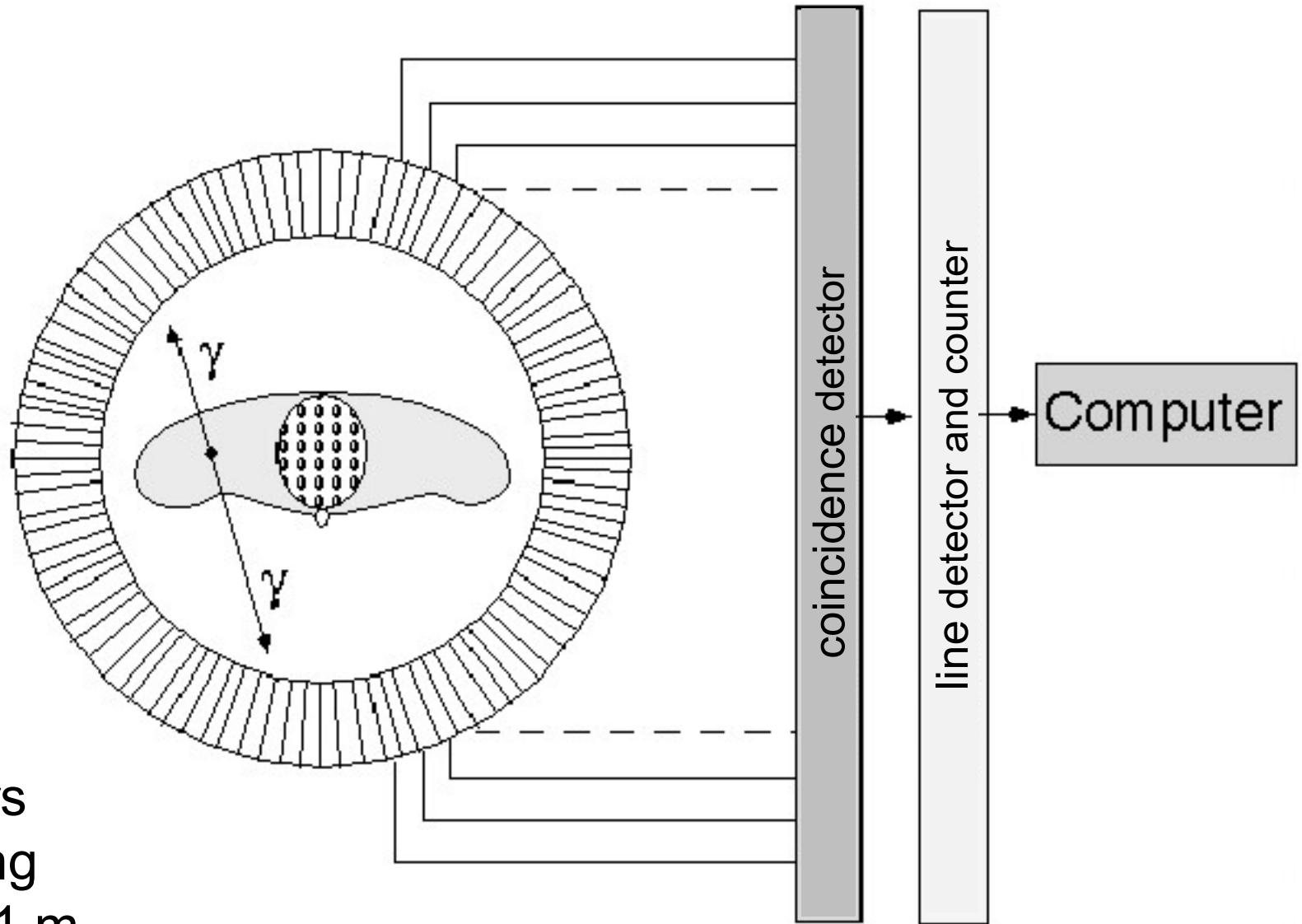
~ 600 detectors
placed on a ring
with diameter 1 m

Positron Emission Tomography   **2D acquisition mode**
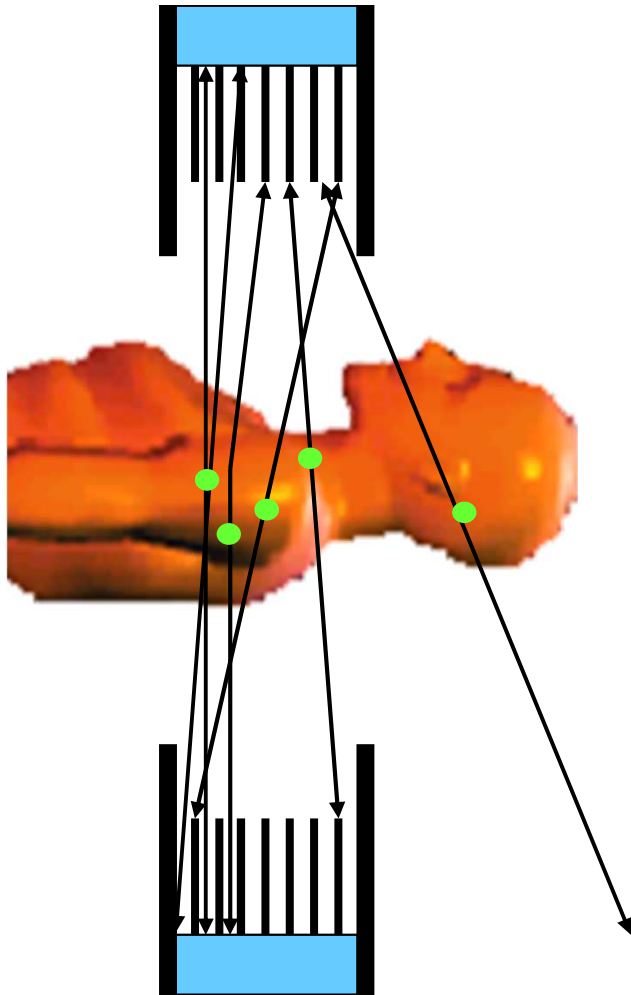
septa (tungsten) allow to separate
different detector planes:

- geometric collimation

- allows for coincidences only within
  a single detector planes and between
  directly neighbored planes

- low amount of scattering

- low sensitivity

Positron Emission Tomography 3D acquisition mode
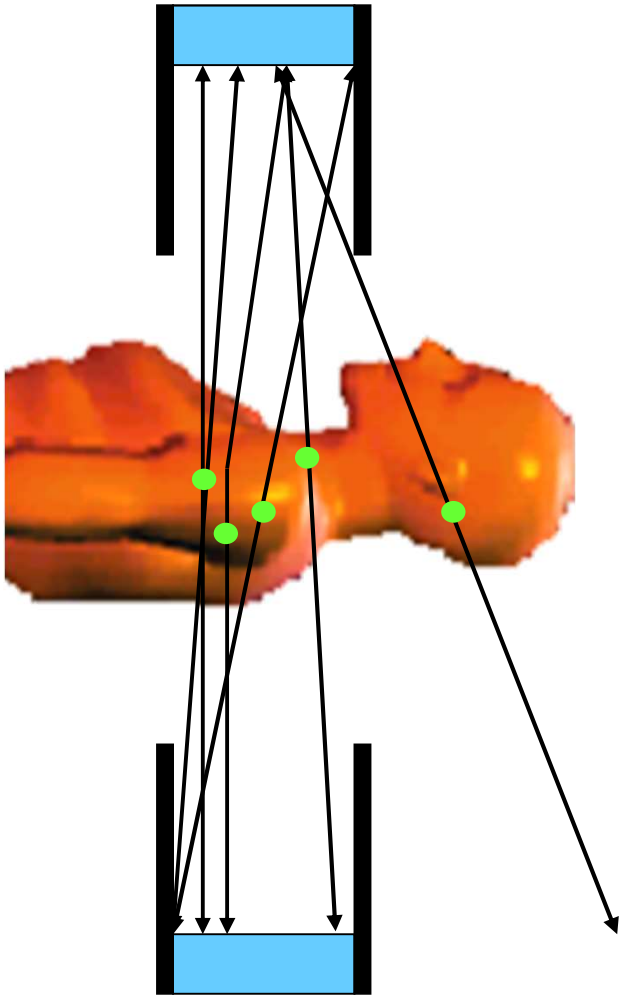
optional removal of septa:

- 2-3 times higher amount of scattering than with 2D mode

- 5 times higher sensitivity than with 2D mode

- requires specific image reconstruction algorithms (allow for different angles for coincidence detection)

Positron Emission Tomography

background due to "external" sources

3D acquisition mode

shielding

crystal

crystal
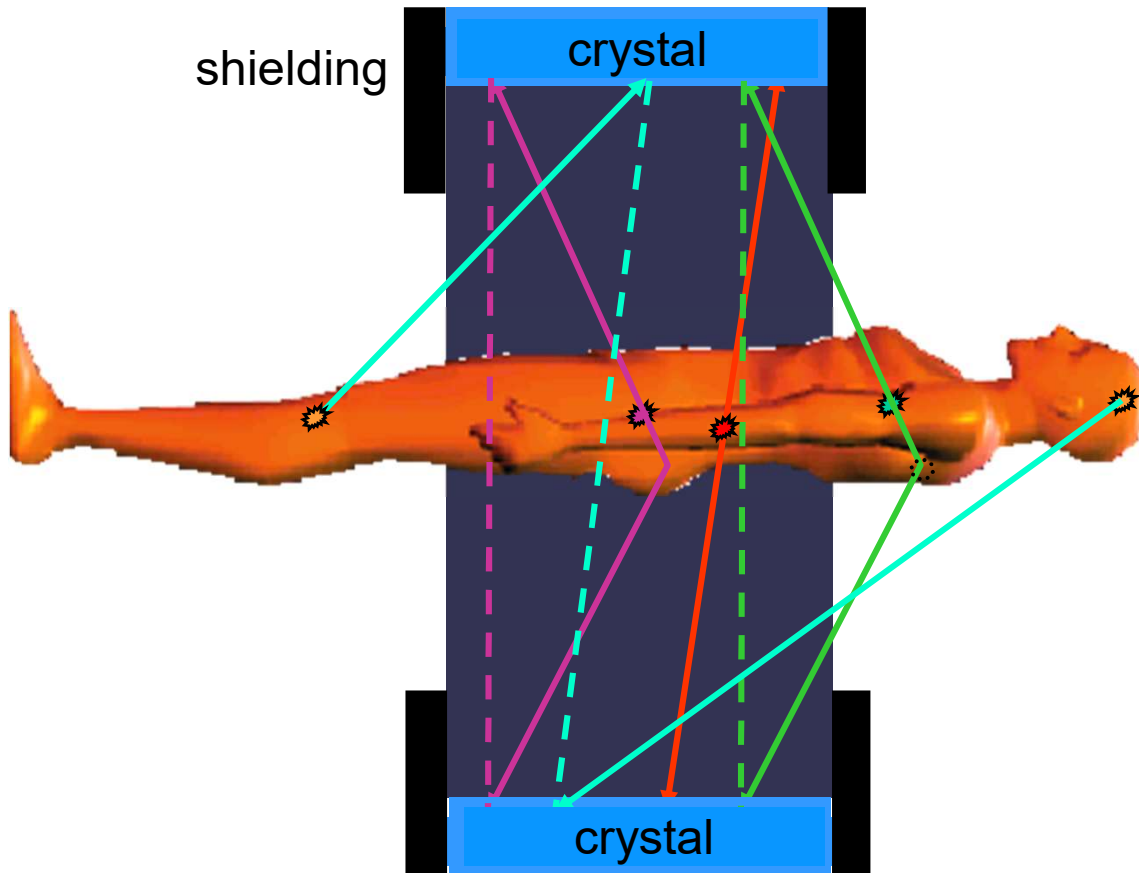
true
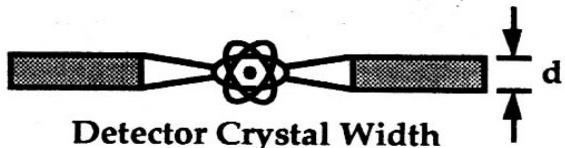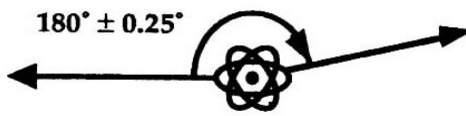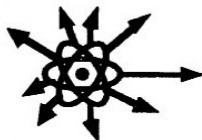
scattered from "within"

scattered from "outside"

random from "outside"

Positron Emission Tomography (PET)

Resolution Factors

Factor	Shape	FWHM
Detector Crystal Width		$d/2$
Anger Logic		0 (individual coupling) 2.2 mm (Anger logic)* *empirically determined from published data
Photon Noncolinearity		1.3 mm (head) 2.1 mm (heart)
Positron Range		0.5 mm (^{18}F) 4.5 mm (^{82}Rb)
Reconstruction Algorithm	multiplicative factor	1.25 (in-plane) 1.0 (axial)

180° ± 0.25°

110

Positron Emission Tomography (PET)
image reconstruction

projections:
recording of pairs of photons under different angles
(e.g.: 0 - 256°)

projection values (primary PET data):
sum of counts of coincident events in detectors
(along the line-of-response) within a given sampling interval
(sec - min)

$\Rightarrow$ filtered back projection or iterative reconstruction schemes

Positron Emission Tomography (PET)
image reconstruction

let $P(r,\Theta)$ denote projection value (where Θ = projection angle and r = tangential cylindrical coordinate perpendicular to direction of projection) and let $A(x,y)$ denote distribution of radioactivity of interest inside the body

$$P(r,\Theta) = \int_{L(r,\Theta)} A(x,y)d\ell \cdot e^{-\int_{L(r,\Theta)} \mu(x,y)d\ell'}$$

$$P(r,\Theta) = \int_{L(r,\Theta)} A(x,y)d\ell \cdot M$$

$$P^{corr}(r,\Theta) = P(r,\Theta)/M = \int_{L(r,\Theta)} A(x,y)d\ell$$

Positron Emission Tomography (PET)
estimation of attenuation factor M
transmission measurement with positron emitter rotating around patient

coincidence approach
^{68}Ge rod-like source
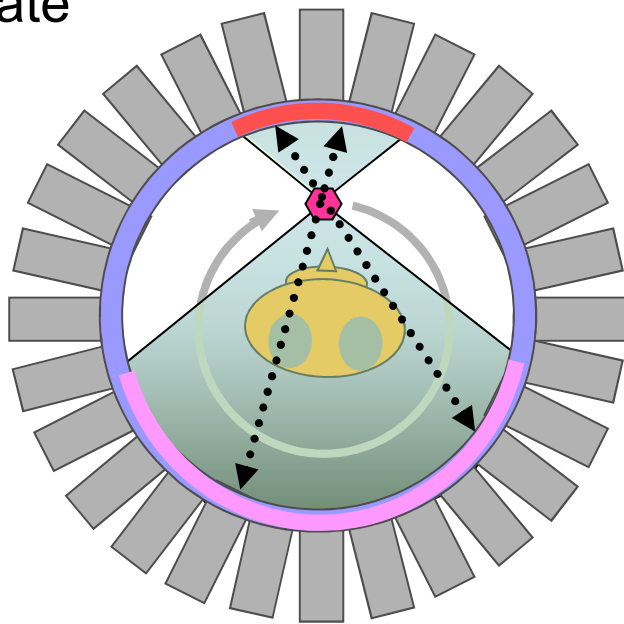
single photon approach
^{137}Cs point-like source (662 keV)

high rate

shielded
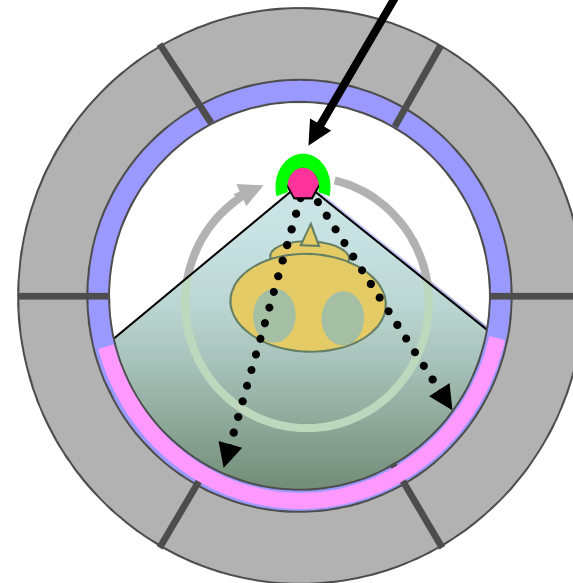
both approaches require reference measurement without patient

Positron Emission Tomography (PET)
image reconstruction — choice of filter for reconstruction
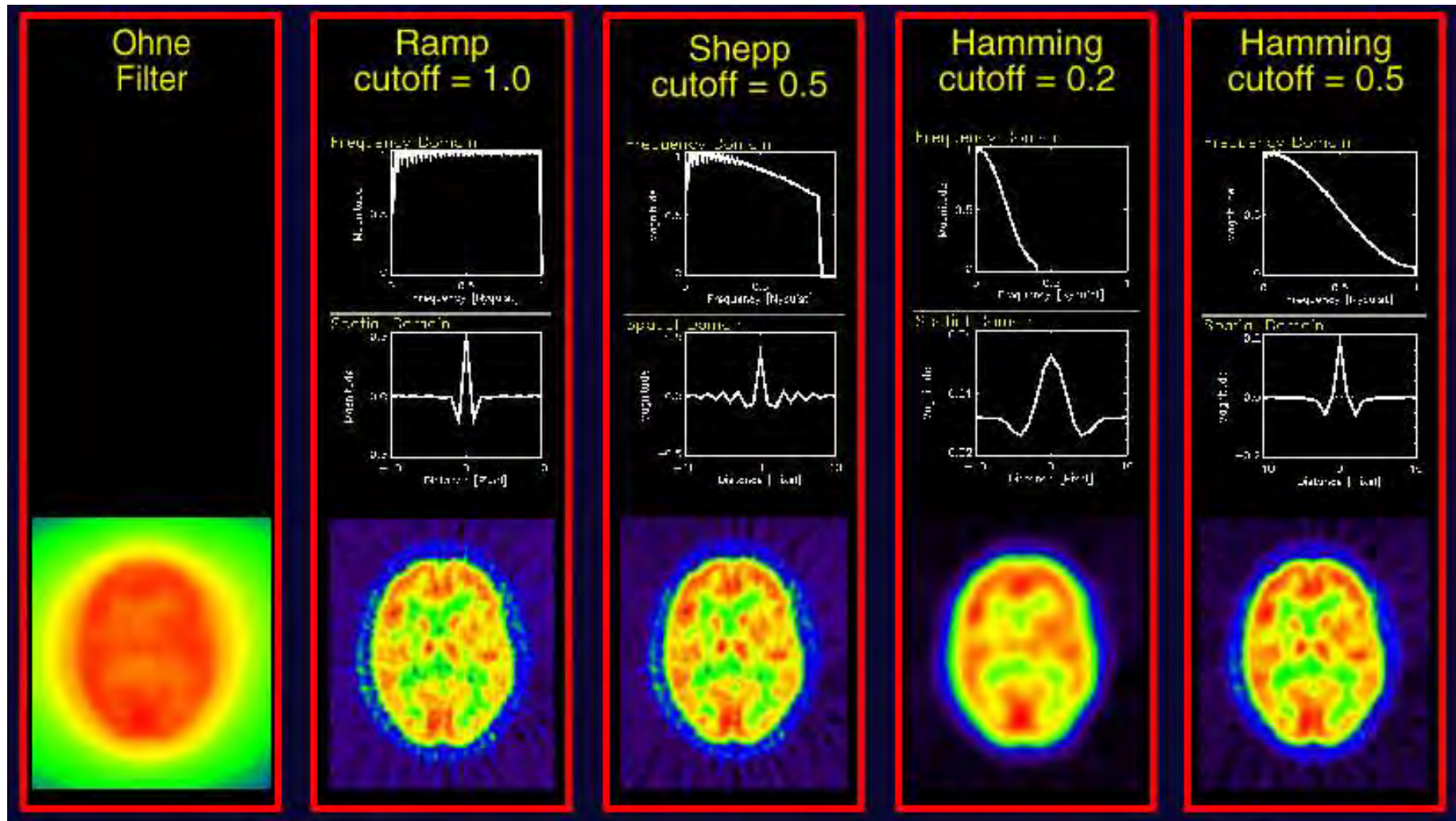
Positron Emission Tomography (PET)

resolution:

- mean free path of positrons (few mm)

- FWHM of angular distribution (180° ± 0,3°)

- accuracy of localizing a γ-quant in detector ring

typical values: 3 mm - 5 mm

Positron Emission Tomography (PET)

imaging errors

- line integrals of events that do not pass through
  the center of the system are broadened

- absorption

- random coincidences

- contribution (detectability) of scattered quanta

Positron Emission Tomography (PET)

advantages

- high sensitivity (pmol)

- high specificity (molecular targeting)

- biologically active substances (F-18, C-11)

- no interference with process(es) of interest

- no toxicity

Positron Emission Tomography (PET)

preparation of isotopes

- cyclotron
  (typical energy of protons: 10 MeV)

- nuclear reaction:

$$^{11}B(p,n)^{11}C$$

$$^{16}O(p,\alpha)^{13}N$$

$$^{15}N(p,n)^{15}O$$

$$^{18}O(p,n)^{18}F$$
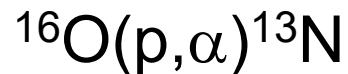
- short half life requires short distance to scanner

Positron Emission Tomography (PET)

frequently used tracer in neurology

[O-15] water	blood flow	
[O-15] butanol	blood flow	dementia, ischemia, stroke
[F-18] FDG	glucose metabolism	
[F-18] FDOPA	presynaptic dopaminergic function	Parkinson's disease
[C-11] methionine	amino acid transport and metabolism	brain tumors
[C-11] flumazenil	benzodiazepine-receptor-imaging	epilepsy

Positron Emission Tomography (PET)

frequently used tracer in cardiology

[N-13] ammonia	blood flow	
[F-18] FDG	glucose metabolism	ischemia, vitality
[C-11] acetate	oxygen consumption	
[C-11] hydroxy-ephedrine (HED)	sympathic nerve endings	infarct, diabetes transplantation
[C-11] CGP-12177	postsynaptic β-receptors	cardio-myopathy

Positron Emission Tomography (PET)

frequently used tracer in oncology

[F-18] fluoro-deoxyglucose (FDG)	glucose metabolism
[O-15] water	blood flow
[F-18] fluoroethyl-tyrosine (FET)	amino acid transport
[C-11] methionine	amino acid transport and metabolism
[F-18] deoxy-fluoro-thymidine (FLT)	proliferation
[F-18] fluoromisonidazol (FMISO)	hypoxia

Positron Emission Tomography (PET)

fields of application

oncology	tumor identification tumor growth rates metastasis follow-up at therapy
neurology	diagnosis of epilepsy diagnosis of Alzheimer's disease stroke, ischemia
cardiology	perfusion and metabolism of myocardium ischemia, diagnosis of infarct, vitality
drug discovery	identification of mechanism of action of drugs development of new drugs

Positron Emission Tomography (PET)
whole-body scan   **healthy person**

brain ➡

kidney ➡

bladder ➡
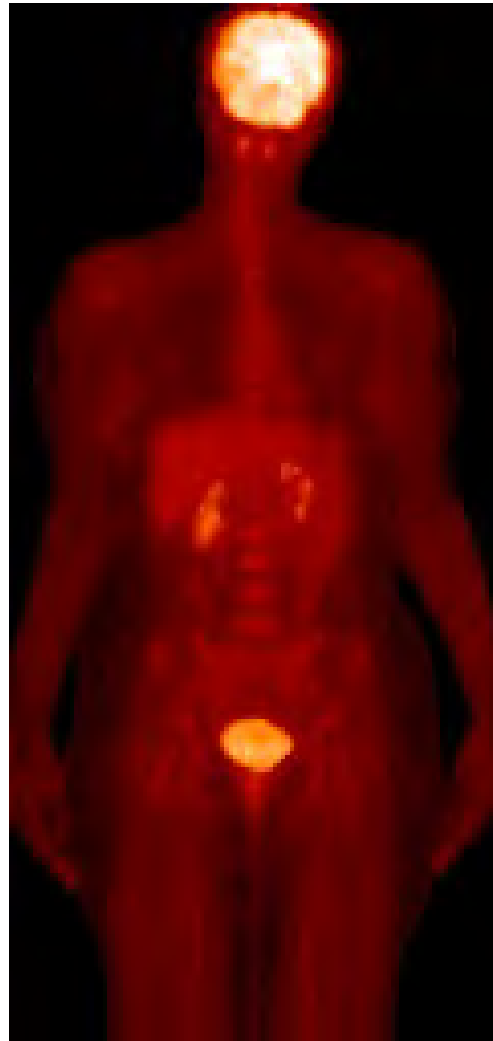
nuclear medical imaging techniques
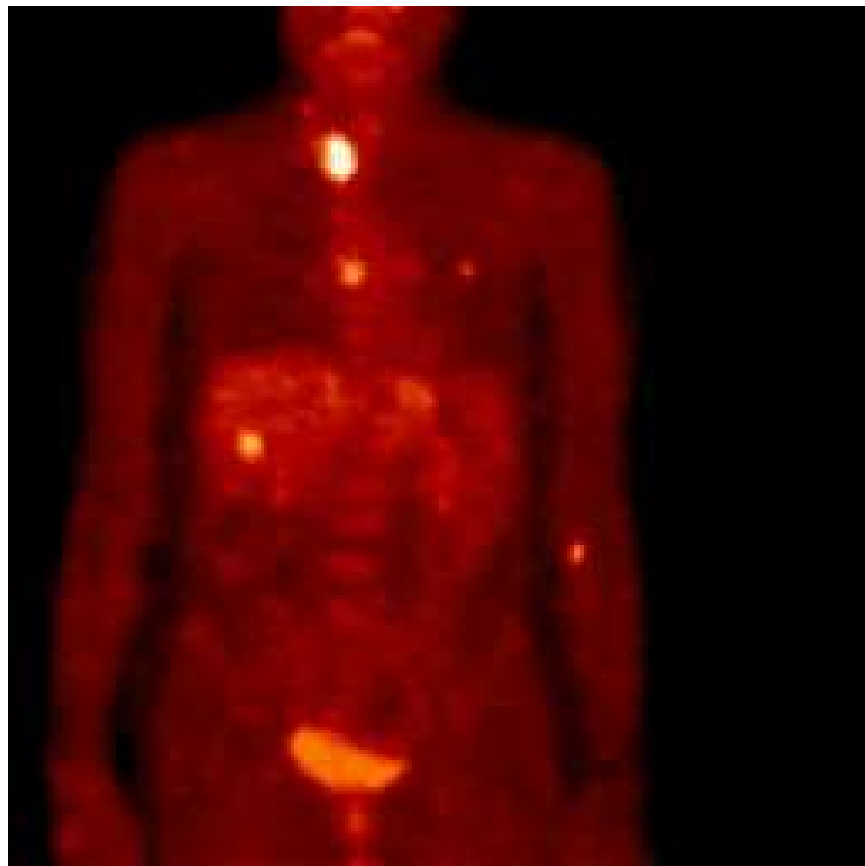
Positron Emission Tomography (PET)
whole-body scan   **colon cancer + metastases**
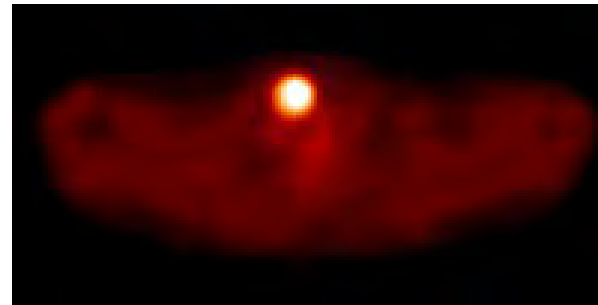
thyroid gland
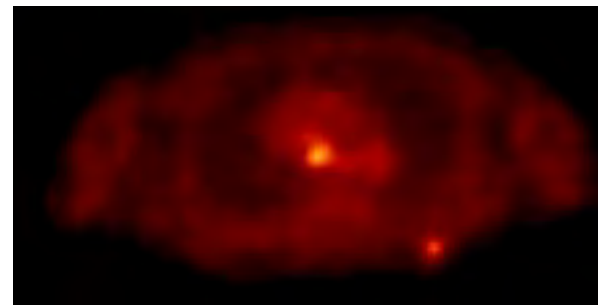
mediastinum

scapula
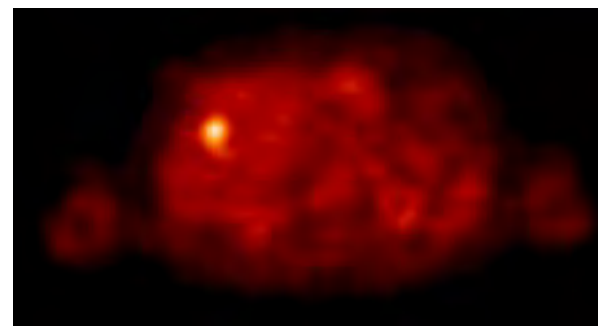
liver

projection   axial slices

nuclear medical imaging techniques

Positron Emission Tomography (PET)
neurology   **amino acid metabolism**
relapse of astrocytoma WHO-grade III
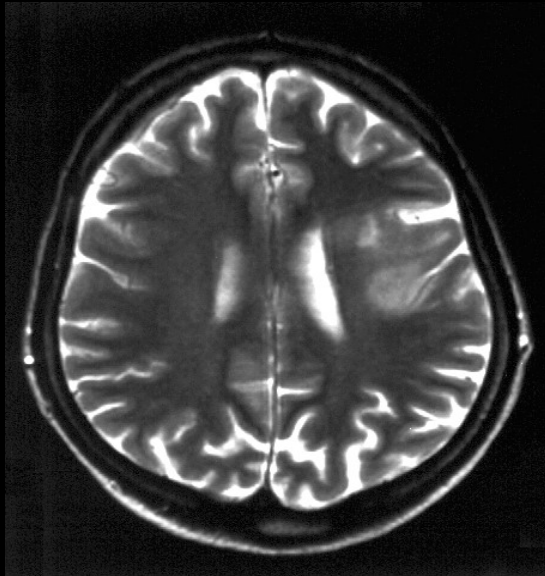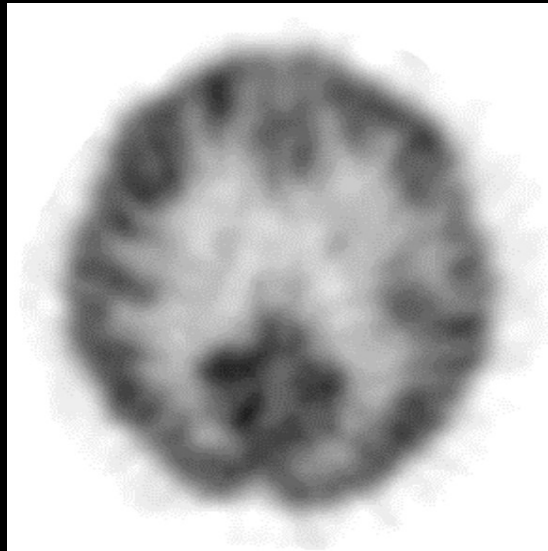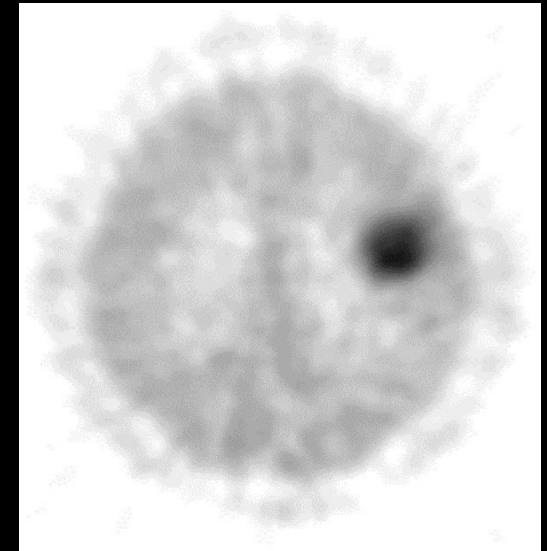
MRT (T2)   FDG-PET   Methionin-PET
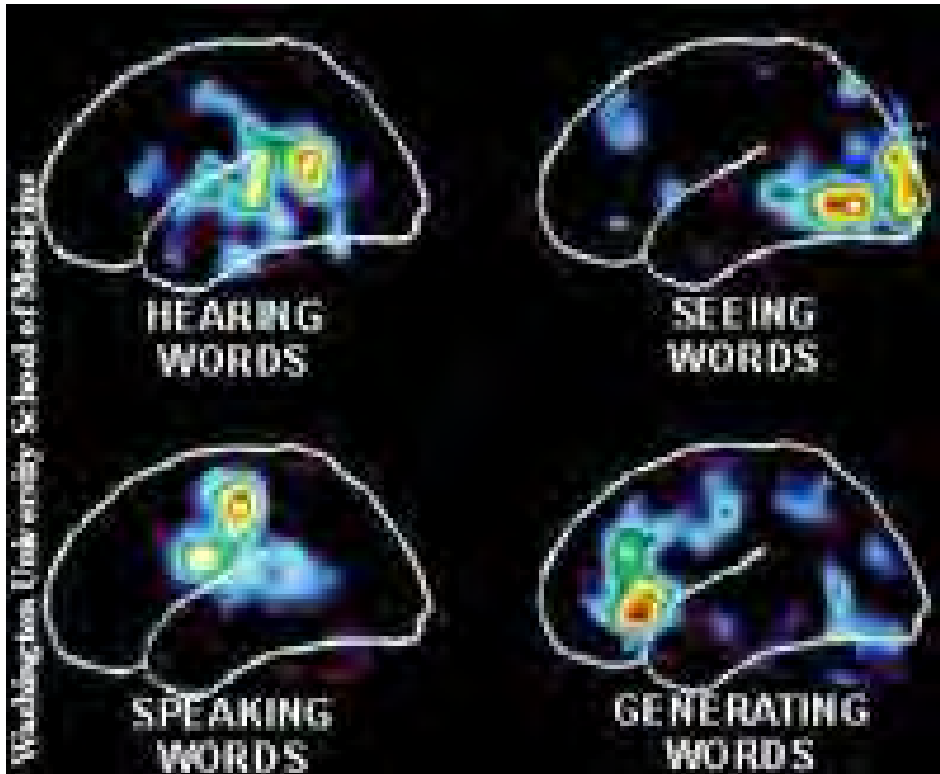
Positron Emission Tomography (PET)
functional imaging

Positron Emission Tomography (PET)
functional imaging
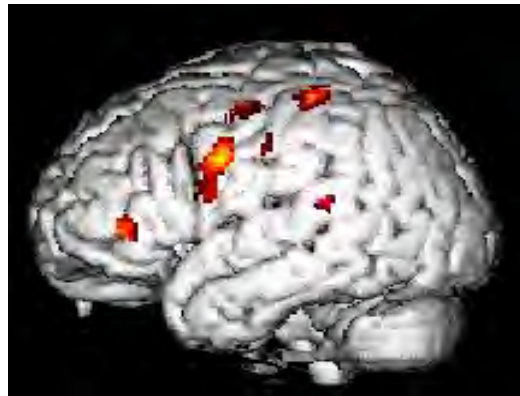
blood flow (O-15)   **activation due to itching**
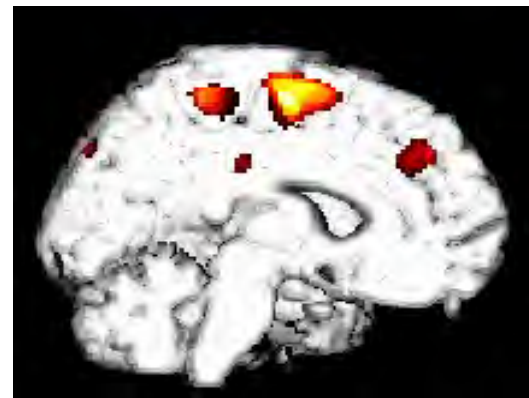
Positron Emission Tomography (PET)   epilepsy
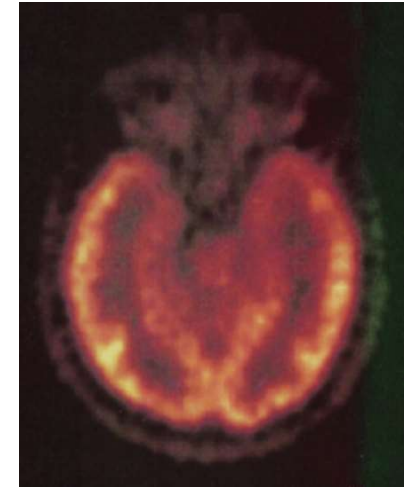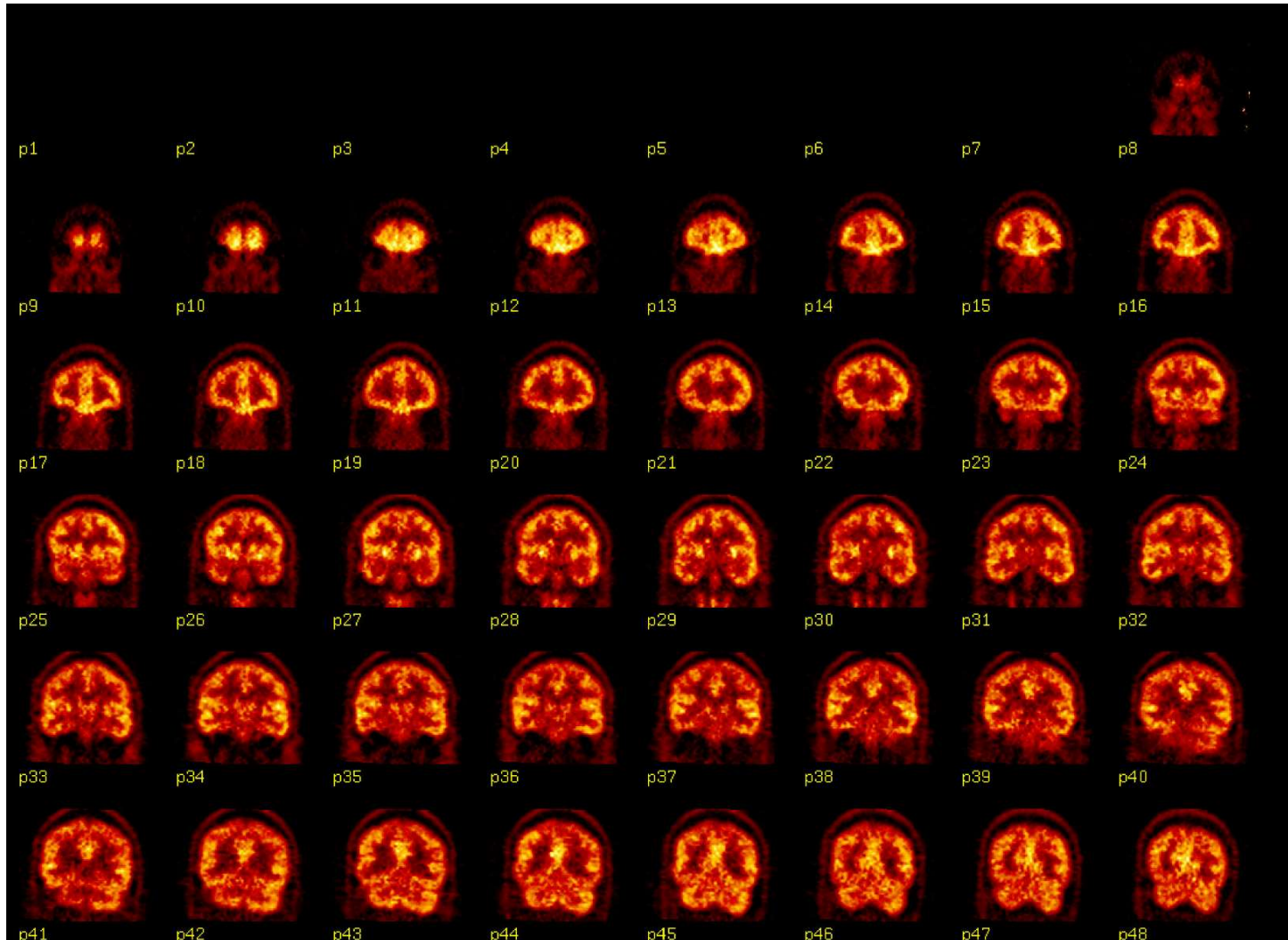
Positron Emission Tomography (PET)   Parkinson
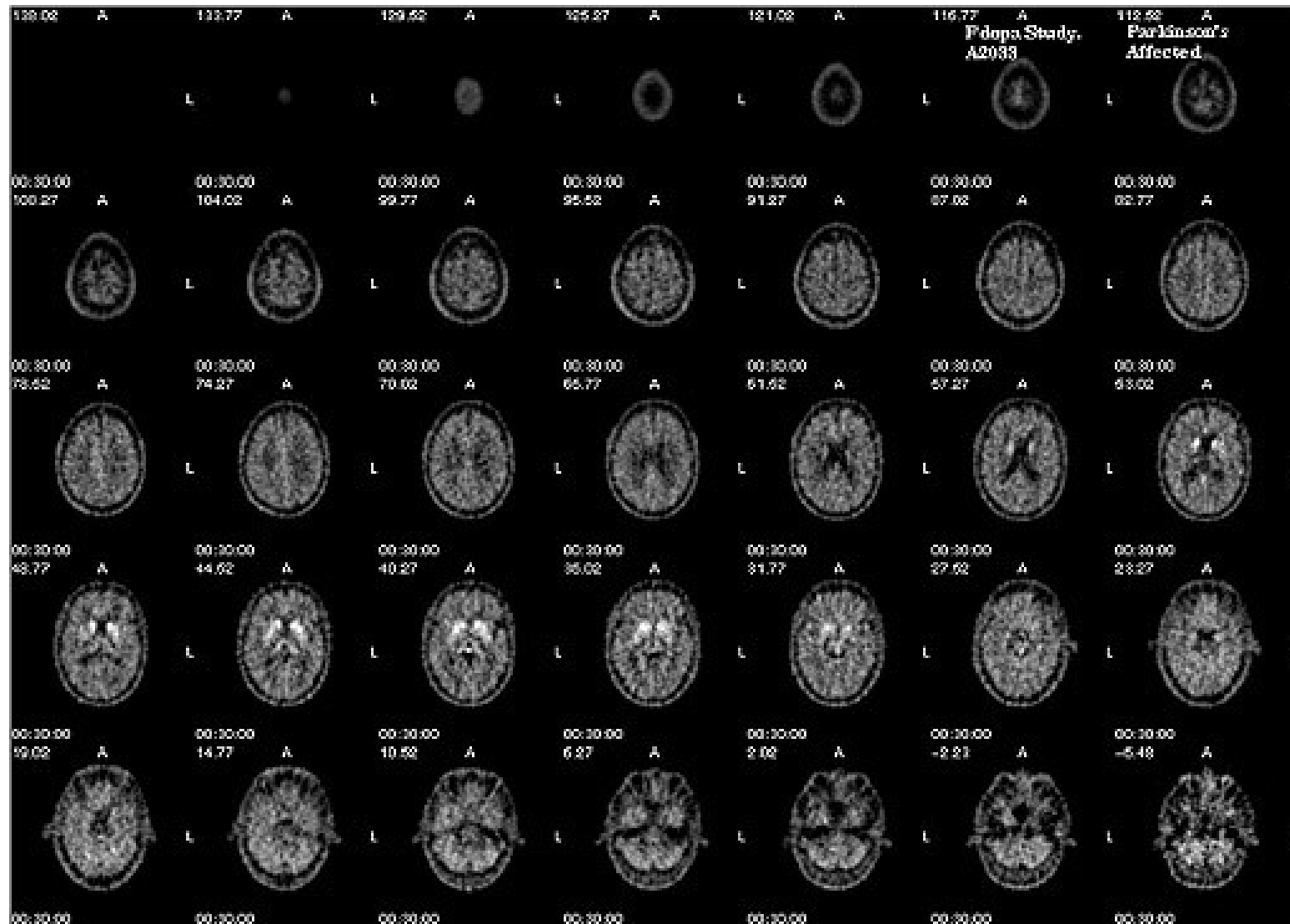
Positron Emission Tomography (PET) **Alzheimer**
brain metabolism

healthy person

right   left

100%

0%
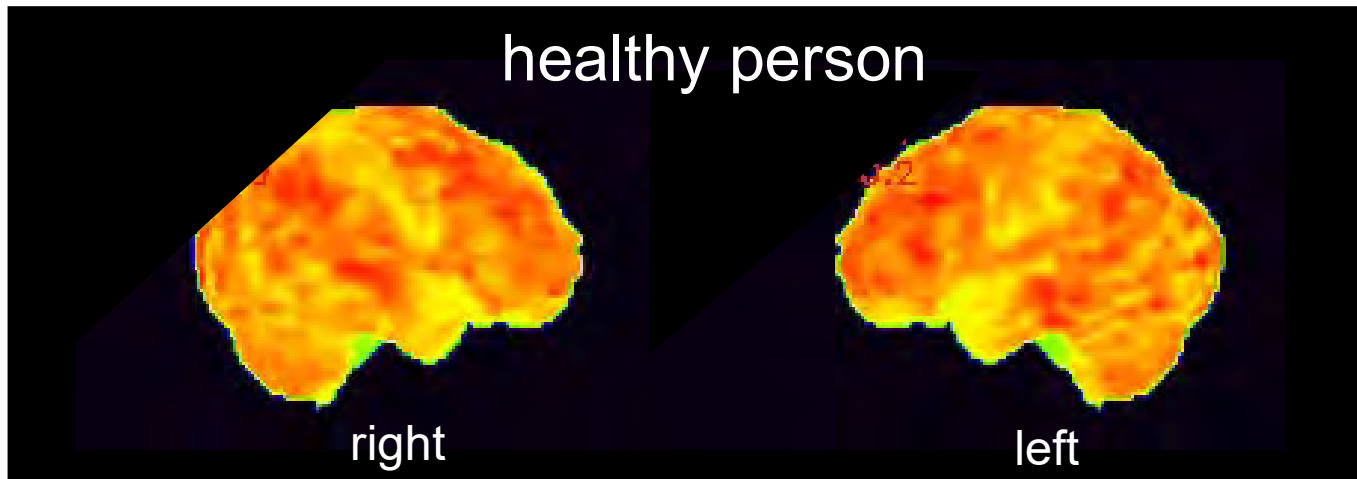
early stage Alzheimer's disease
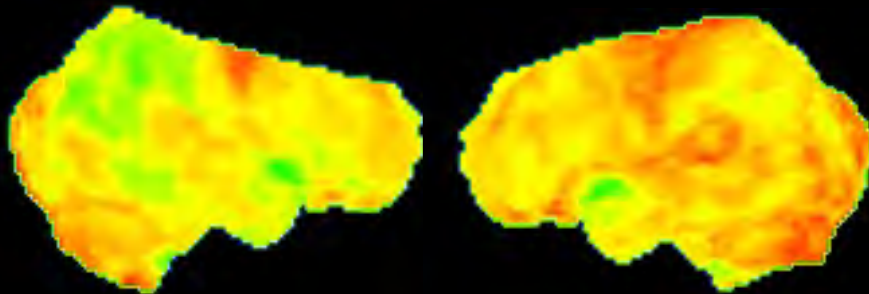
late stage Alzheimer's disease
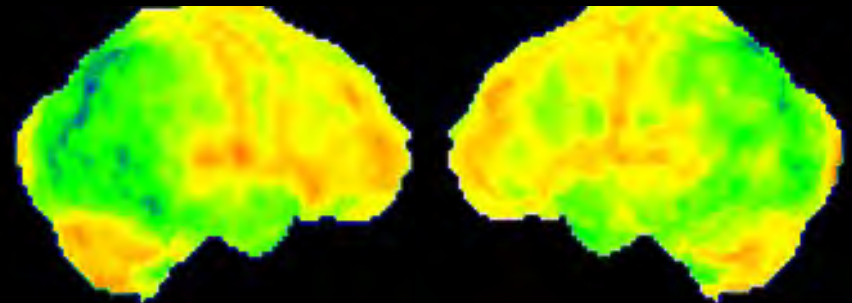
Positron Emission Tomography (PET)   **heart**
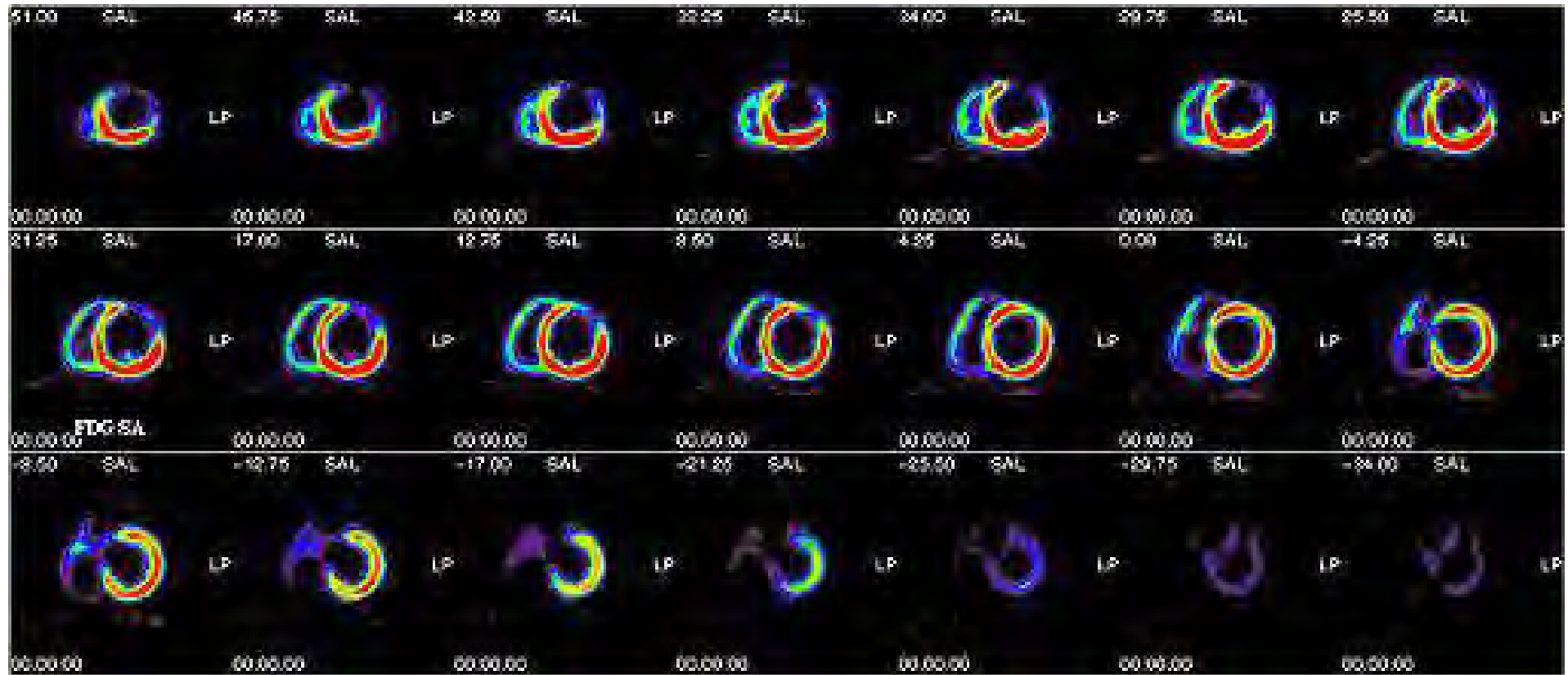
Positron Emission Tomography (PET)
advancements   light sensors
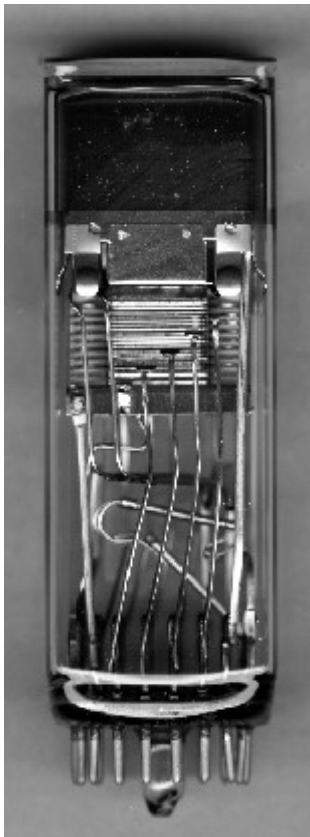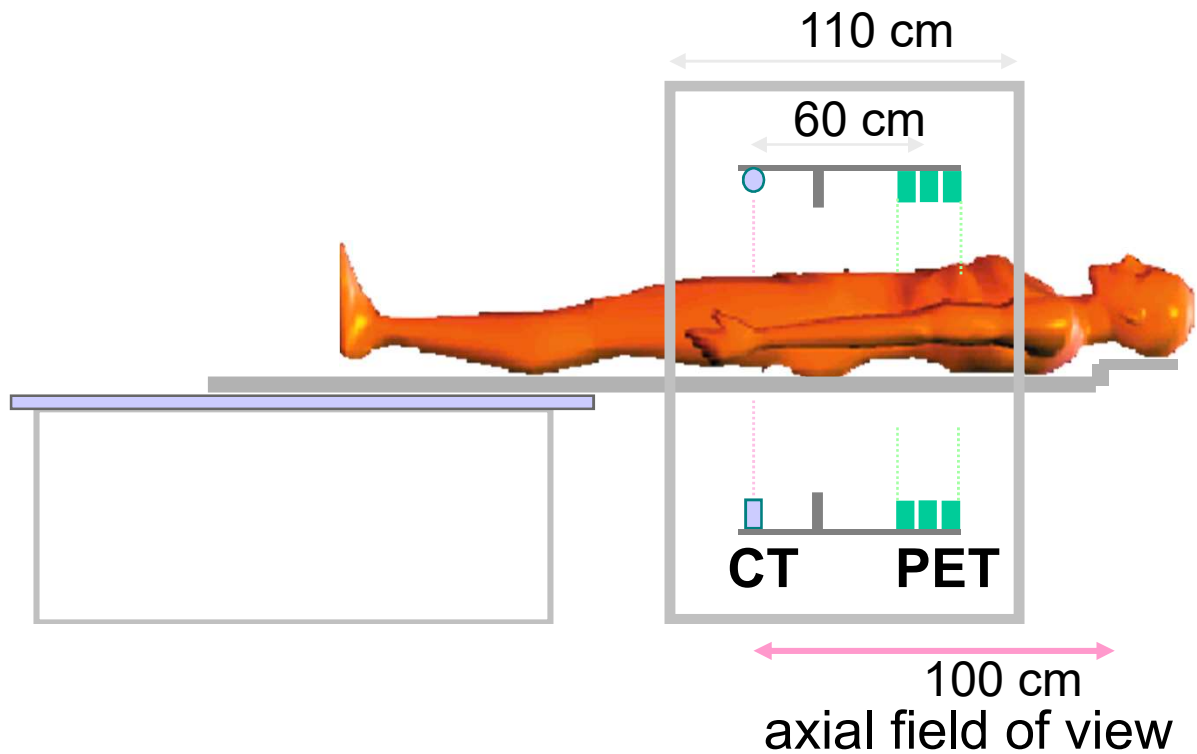
photomultiplier   avalanche photodiodes
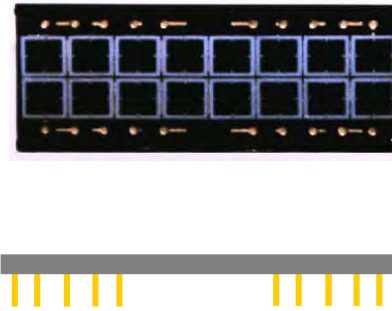
Hamamatsu Photonics

1 cm

Positron Emission Tomography (PET)
advancements   combined PET-CT

Positron Emission Tomography (PET)

advancements   **combined PET-CT**

advantages:

- functional (PET) and anatomical (CT) information
- high accuracy of co-registration
- CT-based correction of attenuation
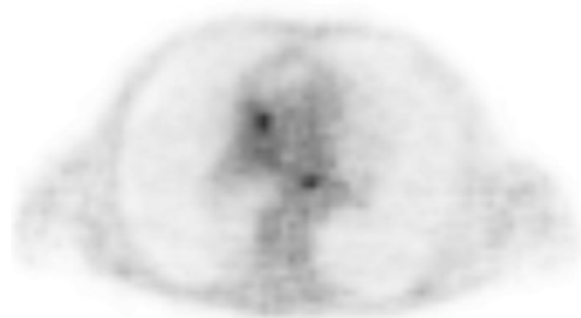   - *rescale HU with μ (511keV)*

problems:
- breathing movements,
  heart movements   co-registration?

- field of view of CT   artifacts

- beam hardening   true attenuation value?

- contrast agent   variable attenuation

Positron Emission Tomography (PET)
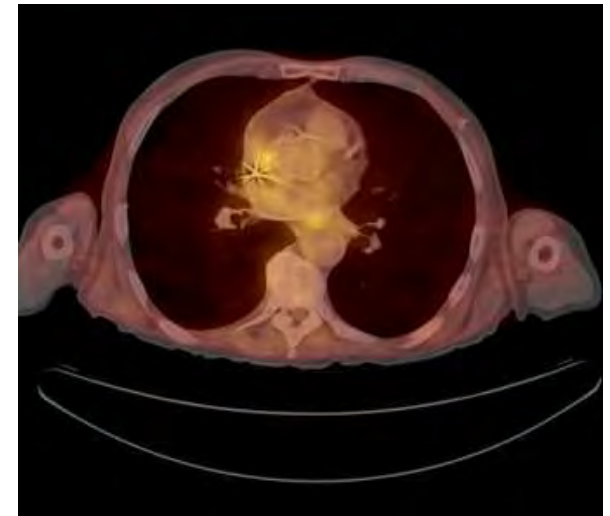## advancements   combined PET-CT
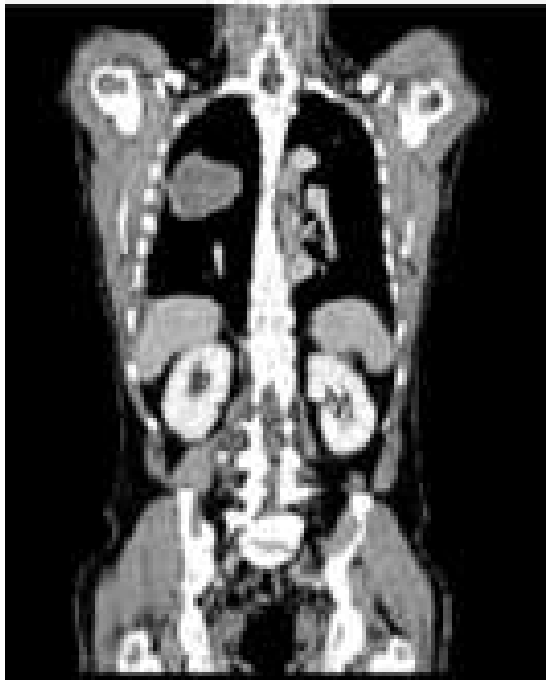

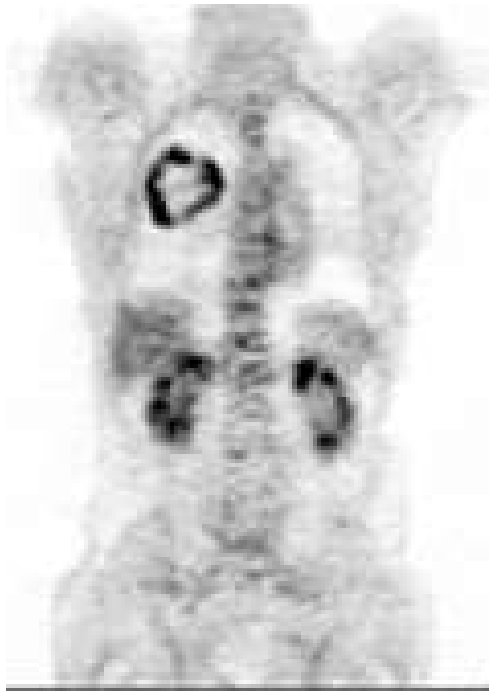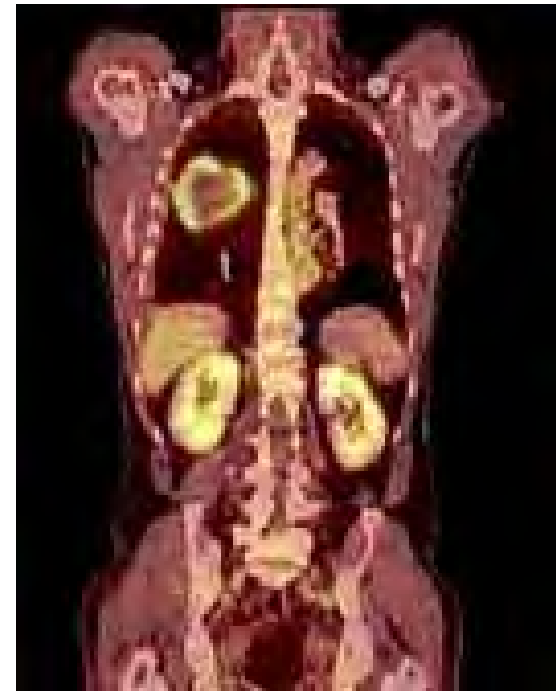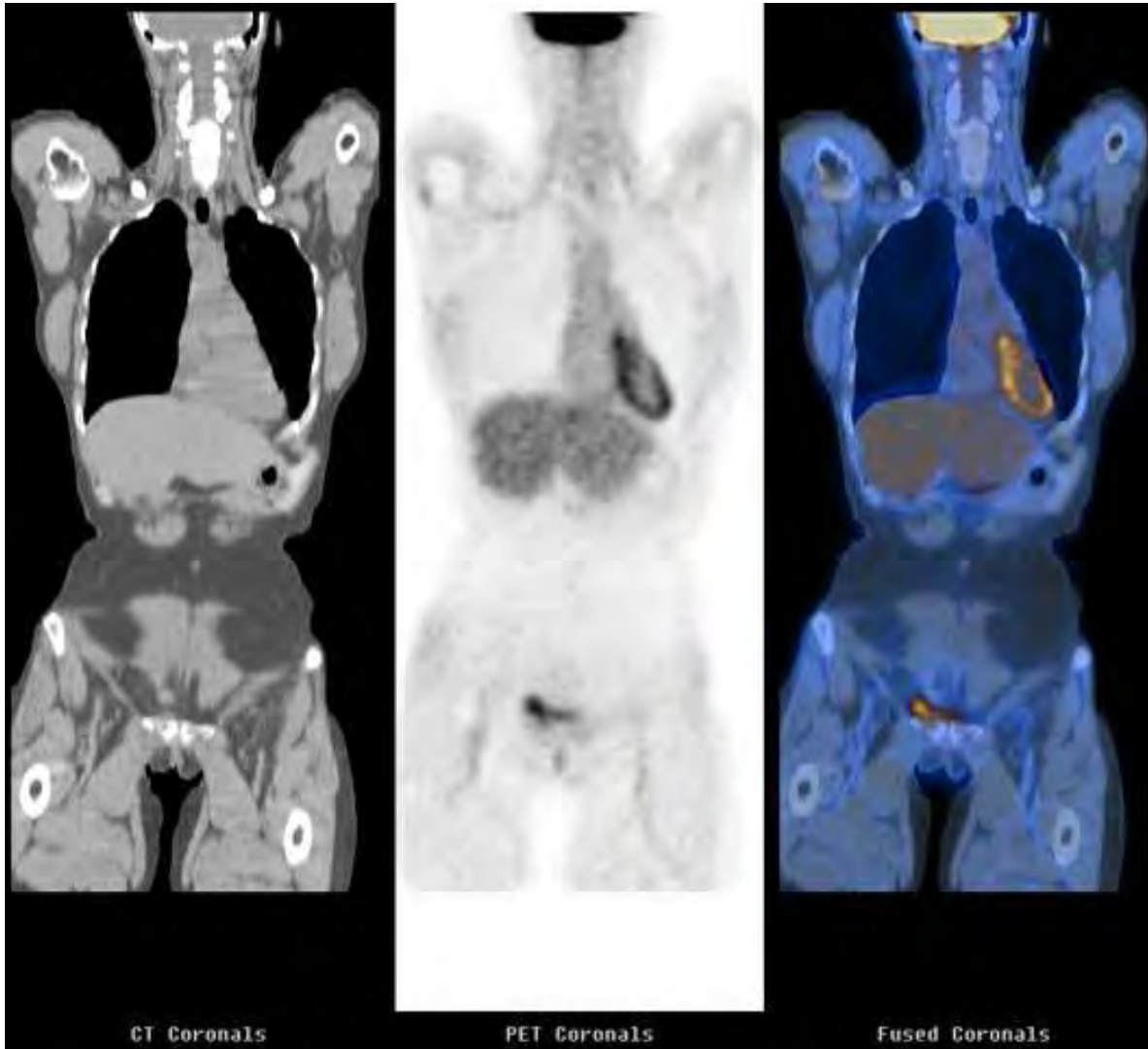CT   PET   PET-CT

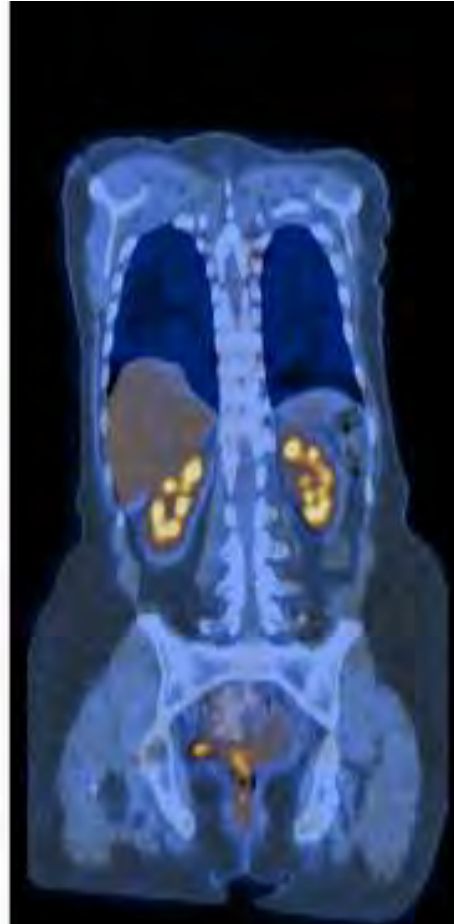**Positron Emission Tomography (PET) advancements**   **combined PET-CT**

CT   PET   PET-CT

Positron Emission Tomography (PET)
advancements   **combined PET-CT**

liver

Positron Emission Tomography (PET)
advancements   combined PET-CT

kidneys

CT Coronals   PET Coronals   Fused Coronals

138

Positron Emission Tomography (PET)
advancements   **combined PET-CT**

heart

Positron Emission Tomography (PET)
advancements   combined PET-CT
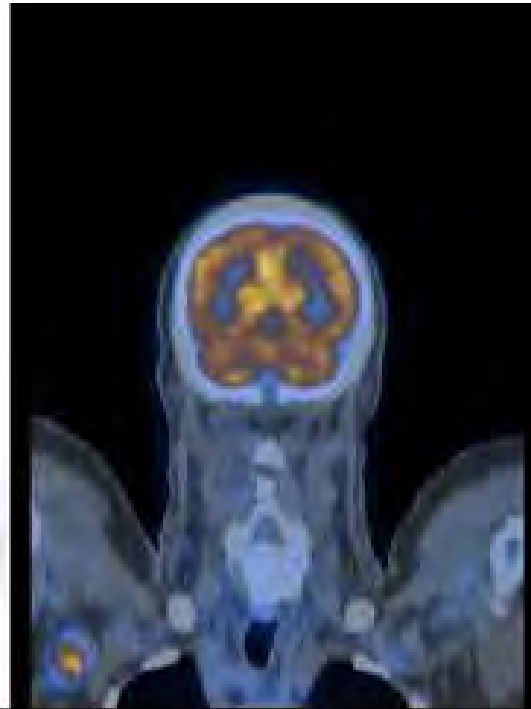

CT Coronals   PET Coronals   Fused Coronals

brain
normal finding

Positron Emission Tomography (PET)
advancements   combined PET-CT

CT Coronals   PET Coronals   Fused Coronals
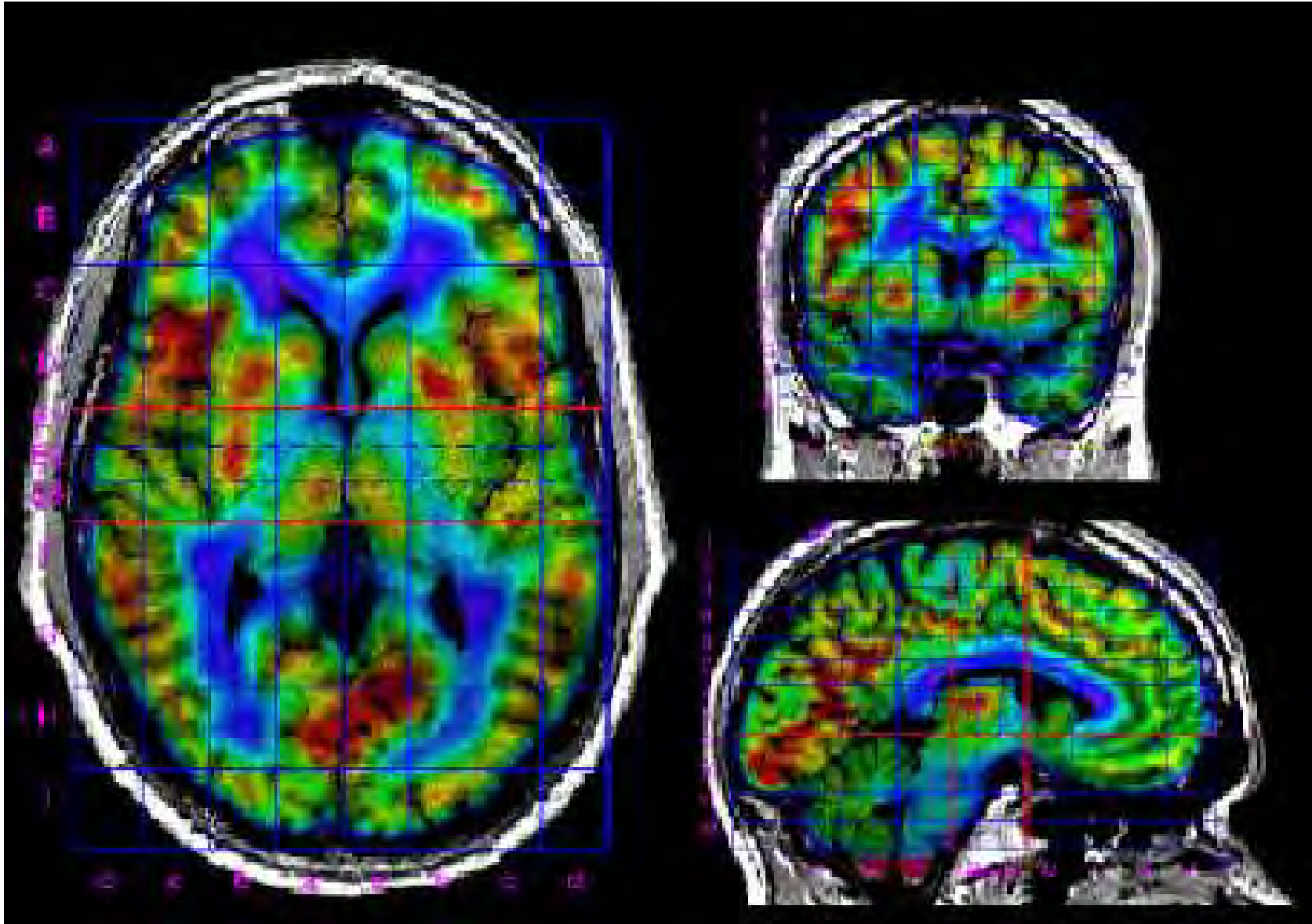
brain
normal finding

movement
artifact

Positron Emission Tomography (PET)
advancements   combined PET-CT

artifact due to cardiac pacemaker

PET-MRI fusion

comparison SPECT - PET

	PET	**SPECT**
radionuclide	$^{11}C, ^{18}F, ^{15}O$	$^{99m}Tc, ^{123}I, ^{111}In$
generation	cyclotron	on-site
emitted photons	2 X 512 keV	1 x ca. 140 keV
T$_{\frac{1}{2}}$	2 - 100 min.	hrs. - days
resolution (spatial)	3 - 7 mm	7 - 10 mm
resolution (temporal)	~ 5 sec – 1 min	> 1 min
sensitivity	x1000 (w.r.t. SPECT)	
req. computing power	high	comparably low
costs/examination	1200 - 1500 €	300 - 500 €

comparison Röntgen/CT – SPECT/PET